UC Santa Cruz

UC Santa Cruz Electronic Theses and Dissertations

Title

How chemotaxis and endogenous microbiota alter the disease outcome of Helicobacter pylori infection

Permalink

https://escholarship.org/uc/item/13d1t961

Author

Rolig, Annah Sharp

Publication Date

2012

Supplemental Material

https://escholarship.org/uc/item/13d1t961#supplemental

Peer reviewed|Thesis/dissertation

eScholarship.org Powered by the California Digital Library
University of California

UNIVERSITY OF CALIFORNIA

SANTA CRUZ

HOW CHEMOTAXIS AND ENDOGENOUS MICROBIOTA ALTER THE DISEASE OUTCOME OF *HELICOBACTER PYLORI* INFECTION

A dissertation submitted in partial satisfaction
of the requirements for the degree of

DOCTOR OF PHILOSOPHY

in

MOLECULAR, CELL AND DEVELOPMENTAL BIOLOGY

by

Annah S. Rolig

March 2012

The Dissertation of Annah S. Rolig
is approved:

_____
Professor Karen M. Ottemann

_____
Professor Fitnat H. Yildiz

_____
Professor Victoria Auerbuch Stone

_____
Professor Martha C. Zuniga

_____
Tyrus Miller
Vice Provost and Dean of Graduate Studies

Copyright © by

Annah S. Rolig

2012

TABLE OF CONTENTS

CHAPTER 1: The role of chemotaxis in mucosal infections 1

1.1. Flagellar motility promotes infection by many bacterial species 1

1.2. Chemotaxis systems in mucosal pathogens 1

1.2.1. The paradigm of chemotactic signaling drawn from *Escherichia coli*, *S.* Typhimurium and *Bacillus subtilis* 1

1.2.2. *H. pylori* chemotactic signaling 4

1.2.3. *V. cholerae* chemotactic signaling 5

1.2.4. *C. jejuni* chemotactic signaling 6

1.3. Chemotaxis and host colonization 6

1.3.1. *H. pylori* 6

1.3.2. *V. cholerae* 8

1.3.3. *S.* Typhimurium 9

1.3.4. *C. jejuni* 10

1.4. The role of chemotaxis in bacterial organ localization 11

1.4.1. *H. pylori* 11

1.4.2. *V. cholerae* 14

1.4.3. *C. jejuni* 15

1.5. The role of chemotaxis in host cell invasion 16

1.5.1. *S.* Typhimurium 16

1.5.2. *C. jejuni* 16

1.6. Chemotaxis and host responses 16

1.6.1. *H. pylori* 16

1.6.2. *V. cholerae* 18

1.6.3. *S.* Typhimurium 20

1.6.4. *C. jejuni* 21

1.7. The role of chemoreceptors in infection 22

1.7.1. *H. pylori* 22

1.7.2. *V. Cholerae* 24

1.7.3. *C. jejuni* 25

1.8. Conclusion 26

1.9. References 28

CHAPTER 2: *Helicobacter pylori* requires TlpD-driven chemotaxis for survival and growth in the antrum 44

2.1. Abstract 44

2.2. Introduction 46

2.3. Experimental procedures 49

2.3.1. *H. pylori* strains and growth conditions 49

2.3.2. Animal infections 50

2.3.3. Histology and pathology 51

2.4. Results 52

2.4.1. Chemotaxis is necessary for *H. pylori* to remain in the antrum after infection has established 52

2.4.2. Competition with wild-type *H. pylori* exacerbates the Che$^-$ *H. pylori* survival defect in the antrum 57

2.4.3. Enhanced inflammatory responses may contribute to Che$^-$ antral localization defects 58

2.4.4. The chemoreceptor TlpD is required for growth and/or survival in the antrum 59

2.5. Discussion 61

2.6. Acknowledgements 68

2.7. References 69

CHAPTER 3: Bacterial chemotaxis modulates host cell apoptosis to establish a Th17-dominant immune response in *Helicobacter pylori* infection 77

3.1. Abstract 77

3.2. Introduction 79

3.3. Experimental procedures 81

3.3.1. *H. pylori* strains and growth conditions 81

3.3.2. Animal infections 81

3.3.3. Immunohistochemistry/immunofluorescence 82

3.3.4. Gastric tissue observation 83

3.3.4.1. Pathology 83

3.3.4.2. Specific cellular infiltrates 84

3.3.5. Flow cytometry 85

3.3.6. Intracellular cytokine staining 86

3.3.7. Quantitative reverse transcriptase PCR 86

3.3.8. TUNEL assay 87

3.4. Results and Discussion 87

3.4.1. *H. pylori* chemotaxis increases inflammation two months after inoculation 87

3.4.2. Che$^-$ *H. pylori* inefficiently recruit CD4$^+$ T cells 89

3.4.3. *H. pylori* chemotaxis affects gastric cytokine profiles 92

3.4.4. Chemotactic *H. pylori* induces a Th17 response 95

3.4.5. Chemotaxis promotes apoptosis in *H. pylori* infection. 99

3.5. Acknowledgements 105

3.6. References 106

CHAPTER 4: The degree of *Helicobacter pylori* inflammation is manipulated by the pre-infection host microbiota 113

4.1. Abstract 113

4.2. Introduction 114

4.3. Experimental procedures 115

4.3.1. *H. pylori* strains and growth conditions 116

4.3.2. Animal infections 116
4.3.3. Flow cytometry 117
4.3.4. Quantitative PCR 119
4.3.5. Pathology 120
4.3.6. PhyloChip analysis 120
4.4. Results and Discussion 121
4.4.1. Mice from Taconic and Charles River have different inflammatory responses to *H. pylori* 121
4.4.2. The murine stomach microbiota is refractory to *H. pylori*-triggered perturbations and similar to the human stomach microbiota 123
4.4.3. Fewer $CD4^+$ T cells infiltrate into the stomach in response to *H. pylori* when mice have been pre-treated with antibiotics 128
4.5. Acknowledgements 139
4.6. References 140
CHAPTER 5: Conclusions and future directions 147
5.1. Summary 147
5.2. Future directions 148
5.2.1. Does TlpD promote growth or survival in the antrum? 148
5.2.2. Chemotaxis driven interactions that promote specific immune responses 150

5.2.3. Which endogenous microbiota affect the immune response to *H. pylori*? 151

5.3. Conclusions 153

5.4. References 155

APPENDIX 1: Table of primers for Chapter 3 158

References 159

APPENDIX 2: List of supplementary files 160

LIST OF FIGURES

Figure 2.1. A cartoon representation of the different physiological regions of the stomach 52

Figure 2.2. Chemotaxis is required for antral colonization at time points after 14 hours post-inoculation 54

Figure 2.3. Chemotaxis allows *H. pylori* to grow more quickly in the antrum and provides and advantage in a competition infection 56

Figure 2.4. The antrum harbors worse inflammation and reduced *H. pylori* colonization 58

Figure 2.5. The chemoreceptor TlpD is necessary for antral colonization 60

Figure 3.1. *H. pylori* chemotaxis promotes inflammation 88

Figure 3.2. Chemotaxis is required for the initial infiltration of $CD4^+$ lymphocytes 90

Figure 3.3. *H. pylori* chemotaxis is not necessary for the presence of $CD4^+$ lymphocytes two months post-inoculation 92

Figure 3.4. *H. pylori* chemotaxis is necessary to induce an inflammatory response associated with Rorγt expression 94

Figure 3.5. *H. pylori* chemotaxis promotes a Th17 response 96

Figure 3.6. IL-17A producing LTi cells do not contribute to differences in IL-17 expression seen in wild-type *H. pylori* infected mice 98

Figure 3.7. IL-17A that is not produced by CD4+ cells is not significantly elevated in wild-type *H. pylori* infected mouse stomachs 99

Figure 3.8. *H. pylori* chemotaxis correlates with increased gastric cell apoptosis. 100

Figure 3.9. Fas/FasL induced cell death does not contribute to increased apoptotic cells in wild-type *H. pylori* infected gastric tissue 101

Figure 3.10. Differential expression of VacA may contribute to reduced apoptosis in Che$^-$ infections 103

Figure 4.1. C57Bl/6N mice from different vendors mount different inflammatory responses to *H. pylori* and posses varying amounts of key *Lactobacillus* spp… 121

Figure 4.2. The murine stomach microbiota is refractory to *H. pylori*-triggered perturbations and similar to the human stomach microbiota 123

Figure 4.3. A phylogenetic tree displaying the 109 families present in all five of the uninfected mice demonstrates the diversity of the microbiota in the mouse stomach..... 125

Figure 4.4. *H. pylori* infection for four weeks does not alter the gastric microbiota 128

Figure 4.5. Components of the microbiota change overtime after *H. pylori* infection..... 129

Figure 4.6. Fewer CD4+ T cells infiltrate the stomach in response to *H. pylori* when mice have been pre-treated with antibiotics..... 130

Figure 4.7. Antibiotic treatment does not significantly change the numbers of total bacteria or *H. pylori* present in the stomach..... 131

Figure 4.8. The antibiotic-treated mice are dominated by *Clostridiales,* yet all *H. pylori* infections have increased *Foxp3* and *Il10* transcripts..... 133

Figure 4.9. *Clostridium* increased in the antibiotic treated mice all map to clusters IV and XIVa 138

LIST OF TABLES

Table 1.1. Outcome of infection for mucosal pathogens and their nonchemotactic mutants 11

Table 1.2. Known chemoreceptor genes and ligands 26

Table 2.1. Colonization levels and doubling times for *H. pylori* SS1 or its isogenic Che$^-$ (ΔCheY) mutant early after infection 55

Table 2.2. Ratio of CFU/g in the corpus (C) to antrum (A) 61

Table 4.1. The top ten most enriched OTUs in the antibiotic treated mice within two clusters of species within this genus, clusters IV and XIVa 137

Table A1.1. Primers used for qRT-PCR in Chapter 3 158

ABSTRACT

How chemotaxis and endogenous microbiota alter the disease outcome of *Helicobacter pylori* infection

By

Annah S. Rolig

The gastric pathogen *Helicobacter pylori* infects 50% of the world's population. Infection can lead to a range of diseases from asymptomatic gastritis to gastric or duodenal ulcers to gastric cancer. The reason for this disparity in disease development is an outstanding question in *H. pylori* pathogenesis. This thesis examines three components affecting disease outcome: *H. pylori* stomach localization, the immune response to *H. pylori,* and the host endogenous microbiota.

Some *H. pylori* strains preferentially colonize in the antrum, the distal region of the stomach. Inflammation in the antrum leads to duodenal ulcers—one of the most common disease outcomes of *H. pylori* infection. This suggests that *H. pylori* stomach localization may contribute to disease progression. *H. pylori* antral localization is affected by chemotaxis, or movement in response to chemical cues. Using standard microbiological techniques and *H. pylori* chemotaxis mutants (Che^-) we found that chemotaxis, and specifically the chemoreceptor TlpD, is necessary for bacterial survival and/or growth in the increased inflammatory environment of the antrum.

Che$^-$ mutants also cause less overall stomach inflammation than wild-type *H. pylori,* which makes Che$^-$ infections a good model for asymptomatic *H. pylori* infections. Thus we compared immune responses in Che$^-$ mutant versus wild-type *H. pylori* infected mouse stomachs using immunohistochemistry, flow cytometry, and quantitative PCR. Increased virulence factor expression, host cell apoptosis, and T-helper type 17 (Th17) cells characterized the inflammatory wild-type *H. pylori* infection. We concluded that chemotaxis drives *H. pylori* to interact with the host and induce pathological Th17 immune responses that promote chronic inflammation.

Lastly, one previously unappreciated parameter influencing *H. pylori* disease outcome is variation in pre-infection host microbiota. We altered the gut microbiota in mice by antibiotic treatment and found that microbiota alterations resulted in significantly reduced CD4$^+$ T-helper cells and *Ifnγ* transcript in gastric tissue after *H. pylori* infection. The altered bacterial communities had significantly more cluster IV and XIVa *Clostridium* spp., bacteria known to increase regulatory T cell populations. Our findings suggest that microbiota composition contributes to the variable disease outcome of *H. pylori* infection by promoting specific immune cell recruitment or differentiation.

ACKNOWLEDGEMENTS

This dissertation would not have been possible without the expertise, guidance, and support of many individuals who contributed their valuable time and energy during the preparation and completion of this study.

First and foremost, I owe my deepest gratitude to my advisor, Dr. Karen Ottemann, who has supported me throughout my thesis with her patience and knowledge while also allowing me to follow my scientific passions. I attribute the level of my scientific achievement to her effort and encouragement. I could not have asked for a better supervisor. Thank you.

Drs. Fitnat Yildiz, Victoria Auerbuch Stone, and Martha Zuniga, thank you for serving on my committee. I owe each of you a debt of gratitude for advice, insight, and input to various manuscripts and discussions regarding my thesis project. I have learned so much from you.

I would like to express my deepest appreciation for Dr. Susan Williams, for her vast knowledge, her patience for endless questions, and lastly for her continuing interest in immunology, which has indeed helped me keep going when times were tough!

To Dr. Elliot Carter, for his patience and expertise in pathology.

To Bari Holm Nazario, for her expertise with flow cytometry and FACS sorting. Her insights in to setting up flow cytometry experiments and her generosity for sharing resources were invaluable to this project.

To Drs. David Feldheim and Barry Bowman, for serving on my orals committee.

In my daily work I have been lucky to be surrounded by a friendly and entertaining group of students. Pam Lertsethtakarn provided great support and plenty of disco music, dry humor, and baked goods. Will Sause (pronounced: Sauce) has impressed me in his development from a wee undergrad to an excellent Ph. D grad student. We have enjoyed many discussions of pathogenesis and life. I feel confident leaving the Ottemann Lab in his capable hands. Eva Rose Murdock Balog has been there from the start! I'm so happy and thankful to have shared this experience with her. Walter Adams never failed to provide entertainment and distraction in the form of drink. Go Immuno! I know he and Miles Duncan will continue to lead IgM with pride. Ottemann Lab members, Jenny Draper, Lisa Collison, Juan Castellon, and Andrea Castillo have all contributed to my education and made the Ottemann Lab a great place to work.

I would like to thank all the students and faculty in the METX (METX United!), and MCDB departments, who have at various times provided reagents, advice, knowledge, and companionship.

Finally, it is a pleasure for me to thank those outside of science who made this thesis possible. Spencer Spetnagel, my partner and companion, who has helped me keep balance in my life, ensuring my life contained equal parts fun and work. Thank you for your comfort during the hard times and your

exuberance for my triumphs. Thank you for helping me seize the day and teaching me that everyday can be a day for champagne!

Julia Thaxton, my big sissy, will always be my number one fan and for her conviction, I will be forever grateful.

Dr. Steven and Ellen Rolig, Mom and Dad, truly deserve the credit for my passion for science. Thank you for never failing to ask me about my research, and for being interested in the answer. Thank you for instilling in me a curiosity for the world and how it works. This is for you.

The text of this dissertation includes a reprint of the following previously published material: Annah S. Rolig, J. Elliot Carter, and Karen M. Ottemann; *Bacterial chemotaxis modulates host cell apoptosis to establish a T-helper cell, type 17 (Th17)-dominant immune response in* Helicobacter pylori *infection,* published in Proceedings of the National Academy of Sciences of the United States of America, 2011, volume 108, number 49, pages 19749-19754. Karen M. Ottemann directed and supervised the research. This publication is presented in Chapter 3 with permission from Proceedings of the National Academy of Sciences of the United States of America.

CHAPTER 1

The role of chemotaxis in mucosal infections

1.1. Flagellar motility promotes infection by many bacterial species

Many bacterial species use flagellar motility for mammalian host colonization (37). Flagellar motility is almost always controlled by a chemotaxis signal transduction system that allows bacteria to detect and migrate towards favorable niches or away from deleterious environments. Therefore, it is likely that chemotaxis works in conjunction with motility to promote colonization and increase virulence. Here we focus on our current understanding of how chemotaxis contributes to bacterial virulence. This connection has been studied in several microbes, but most thoroughly in *Helicobacter pylori*, *Vibrio cholerae*, *Salmonella enterica* serovar Typhimurium (*S.* Typhimurium*)* and *Campylobacter jejuni*. Because of this depth of literature, we focus on these microbes here.

1.2. Chemotaxis systems in mucosal pathogens

1.2.1. The paradigm of chemotactic signaling drawn from *Escherichia coli*, *S.* Typhimurium and *Bacillus subtilis*

Chemotaxis systems have been most extensively studied in model bacteria including *E. coli, S.* Typhimurium and *B. subtilis* (11, 59, 86). These and other microbes have allowed us to discern that all chemotactic bacteria have a

core set of chemotaxis signaling proteins that consist of chemoreceptors, the coupling protein CheW, the kinase CheA, and the response regulator CheY (90). Each of these is discussed below.

Chemotaxis initiates when chemoreceptors detect specific environmental characteristics. The majority of chemoreceptors reside in the cytoplasmic membrane, although some are soluble in the cytoplasm. They detect ligands by direct binding or via protein-protein interactions. Chemoreceptors participate in a three-part signaling complex with the coupling protein CheW and the histidine kinase CheA. Chemoreceptor binding to a chemoattractant or repellent ligand regulates CheA, and in turn the amount of phosphorylated CheY (CheY-P). CheY-P binds to the flagellar motor switch and controls flagellar rotational direction. In *E. coli*, when a chemoattractant ligand binds the chemoreceptors, the CheA histidine kinase is inactivated. Thus, CheY-P populations are reduced and replaced with nonphosphorylated CheY. Nonphosporylated CheY does not interact with the flagellar motor, thus the flagellar motor rotates counterclockwise, the default direction, and the bacteria swim straight. Accordingly, mutants lacking *cheW, cheA* or *cheY* do not produce CheY-P and therefore predominantly swim straight.

Several additional chemotaxis proteins are variably present in bacteria. For example, a recent study showed that there are 17 known variations in the protein components that make up a microbe's chemotaxis system (90). These

variable proteins are less ubiquitous than the core proteins, but still play key roles in optimizing chemotaxis behavior. One such type of protein is a CheY-P phosphatase that accelerates the intrinsic auto-dephosphorylation activity of CheY. This activity can be performed by various proteins, including CheZ, FliY, CheC or CheZ. Many microbes also have a protein called CheV. This protein has a CheW domain fused to a phosphorylation domain (REC) that is found in two component response regulators. CheV proteins appear to act as regulatable coupling domains that control the connection between chemoreceptors and CheA (2). The final relatively common chemotaxis components are the enzymes CheR and CheB. They control adaptation to sustained ligand levels by reversibly methylating specific amino acids on the chemoreceptor. These proteins allow bacteria to adjust, or adapt, to a concentration of ligand that previously triggered a chemotactic response and thus allows navigation through a broad range of ligand concentrations.

E. coli encodes five transmembrane chemoreceptors. Chemoreceptors share a highly conserved cytoplasmic domain, termed MA, that interacts with CheW. The ligand-binding region is highly variable. In *E. coli*, the Tar, Tsr, Tap and Trg chemoreceptors have substantial periplasmic domains that have been shown to sense ligands such as amino acids, sugars, pyrimidines (52), toxic metals, and the quorum-sensing molecule AI-2 (31). The fifth receptor, Aer, is membrane bound but lacks a significant periplasmic domain. This receptor,

together with Tsr, mediates *E. coli's* response to oxygen (64), temperature, and pH (83).

The *S.* Typhimurium chemotaxis system is fairly similar to that of *E. coli*, with exceptions being the presence of a CheV and four additional chemoreceptors (28); we do not yet know what these receptors respond to. One of them, McpA, was recently reported to share similarity with *H. pylori* TlpD in a putative sensing domain (19). Another well-understood difference is that *S.* Typhimurium lacks Tap, and instead encodes a metal-citrate sensing receptor called Tcp (91).

1.2.2. *H. pylori* chemotactic signaling

H. pylori is a gastric pathogen that chronically colonizes the epithelial surface of the human stomach. The chemotaxis system of *H. pylori* shares many similarities with that of *E. coli,* but also has some distinctive proteins (50). Experiments have shown that the core signaling proteins CheW, CheA, and CheY, function as expected in *H. pylori*. Specifically, disruption of any of these core proteins renders *H. pylori* nonchemotactic *in vitro* with swimming behavior that is predominantly straight-biased (23, 78). *H. pylori* has several chemotaxis accessory proteins that each have a modest impact on chemotactic abilities. These accessory proteins include a CheZ phosphatase (49), three CheV proteins (50), and a newly identified chemotaxis protein, ChePep (35). One of the most

unusual aspects of the *H. pylori* chemotaxis system is that the bacterium lacks the adaptation proteins, CheB and CheR. It is not yet known whether *H. pylori* relies on the CheV proteins for adaptation, as seen in *B. subtilis*, or whether *H. pylori* does not have an adaptation mechanism.

H. pylori possesses three membrane bound chemoreceptors, TlpA, TlpB, TlpC, and one cytoplasmic chemoreceptor, TlpD. TlpA senses arginine and bicarbonate (14), and TlpB senses acidic pH (17) and the quorum-sensing molecule autoinducer-2 (AI-2) (63). TlpD is thought to be involved in energy taxis (70), and the ligands for TlpC are unknown.

1.2.3. *V. cholerae* chemotactic signaling

V. cholerae colonizes the human small intestine, residing at the epithelial surface in infections that are usually short in duration. Its complement of chemotactic signaling proteins is much more complex than that of *E. coli, Salmonella* or *H. pylori.* The *V. cholerae* genome has three different operons containing chemotaxis genes, although only one of these, operon 2, has been shown to be important for chemotaxis *in vitro* (10). Each operon encodes at least one of each of the core signaling proteins, plus several chemoreceptors and accessory signaling proteins (10, 29). In total, the *V. cholerae* genome encodes 46 proteins with homology to chemoreceptors (10), indicating a vast potential for chemosensory detection, yet relatively little is known about the signals that

promote tactic behavior in *V. cholerae*. Thus far chemotactic responses have been reported for 20 L-amino acids, for a pepsin digest of rabbit mucosal scrapings (25), for chitin oligosaccharides (51), and for bile and intestinal mucin (81).

1.2.4. *C. jejuni* chemotactic signaling

C. jejuni colonizes the intestinal mucosa (44) and worldwide is the leading cause of diarrheal diseases (85). The chemotaxis system of *C. jejuni* shares many of its protein components with *E. coli*, including the core chemotaxis proteins and the adaptation proteins CheR and CheB. However, while CheR and CheB function as expected to methylate/demethylate, in *C. jejuni* they do not perform that function on all the chemoreceptors (39). Like *H. pylori, C. jejuni* also has the accessory proteins CheV and CheZ (50). *C. jejuni* have seven integral membrane chemoreceptors and three soluble chemoreceptors (32); the known ligands for these receptors include pyruvate, fumerate (21), formate, and aspartate (50).

1.3. Chemotaxis and host colonization

1.3.1. *H. pylori*

Chemotaxis is important for *H. pylori's* ability to colonize a variety of animal models, as demonstrated by non-chemotactic mutants (Che^-) that lacked *cheW*, *cheA* or *cheY* as the sole infection strain. The results of these studies differ

in the magnitude of the effect of loss of chemotaxis. Some studies report complete lack of colonization by Che$^-$ mutant *H. pylori* (23, 57), while others found a more modest 5-10-fold decrease in bacterial load (78). This discrepancy can be explained by the finding that Che$^-$ mutants have a 100-fold increased 50% infectious dose (ID_{50}) compared to that of wild type (78). Thus in studies that employed doses below the ID_{50}, Che$^-$ mutants would not be expected to establish colonization. These results suggest that the chemotactic ability to sense and respond to the environment enhances the ability to establish infection; the need for chemotaxis, however, can be partially overcome by high bacterial doses.

When Che$^-$ *H. pylori* establish an infection, they display attenuated colonization for the first three weeks of infection compared to wild-type *H. pylori* (78). Long term, however, the colonization level of Che$^-$ and wild type equalize after ~ one month of infection, and both strains can persist and maintain matched colonization levels for at least six months post-inoculation (78). These findings are consistent with chemotaxis playing an early role in maximizing bacterial numbers, but a less critical role after infection is well established. However, the animal infection scenario in these experiments is somewhat artificial, in that the animals receive one *H. pylori* dose with no subsequent *H. pylori* challenge. In normal human infections it is likely that newly arriving *H. pylori* constantly challenge existing *H. pylori* infections. To model the role of chemotaxis in this scenario, Terry and colleagues established Che$^-$ infections in

the mouse stomach, then after one week of infection, challenged the animals with wild-type *H. pylori* (78). The wild-type *H. pylori* displaced a significant amount of the endogenous Che$^-$ strain, suggesting that chemotaxis benefits wild-type *H. pylori* in a chronic infection setting.

Consistent with a major role for chemotaxis in establishing infection, competition of Che$^-$ mutants with wild type results in a severe out-competition of the Che$^-$ mutants (78). This phenotype is true for mutants that have either a straight swimming bias, such as *cheW*, *cheA*, *cheY* or *cheV1* (54, 78), or a frequent direction change bias such as those in *cheV3* and *chepep* (35, 54), indicating that for *H. pylori* different chemotactic biases do not result in differential infection ability.

1.3.2. *V. cholerae*

Early work on *V. cholerae* chemotaxis and host colonization was confounded by seemingly incongruent results. Initial *in vivo* studies using the rabbit ileal loop model showed that wild-type *V. cholerae* had an increased growth rate compared to a nongenetically defined Che$^-$ mutant and also severely outcompeted the Che$^-$ mutants in a competition infection (24, 27). However, contrasting results were reported in two more recent studies. One was performed in the infant mouse model of cholera, where Che$^-$ mutants survived better than wild type (26). The second study showed that defined non-polar

mutations in *cheA-2* and *cheY-3* resulted in Che$^-$ bacteria that had increased colonization levels and a lower infectious dose compared to the isogenic wild type (48). The contrasting results were rectified when additional work demonstrated that swim-bias Che$^-$ mutants fare better than wild type, while those with a tumble-bias fare less well than wild type (13). The swim-bias Che$^-$ mutants may fare better than wild type because they colonize a broader range of the gastrointestinal tract, while the wild-type bacteria colonize a more restricted area (48). The authors speculated that swim-bias mutants might cover more distance than those with a tumble bias and therefore expand their niche beyond the middle small intestine. Interestingly, *V. cholerae* isolated from rice-water stool down regulate cheW and cheR and therefore move with a swim-bias, and they also have increased infectivity compared to normal *V. cholerae* (58). These data suggest either repression of chemotaxis or a straight swim bias increases infectivity. Indeed, Butler *et al.* showed that the ID_{50} of swim-bias Che$^-$ mutants is an order of magnitude lower than wild type, indicating that a straight swim bias increases *V. cholerae* infectivity (13).

1.3.3. *S.* Typhimurium

Unlike *H. pylori* and *V. cholerae* motility mutants (*Mot$^-$*), *Mot$^-$* mutants of *S.* Typhimurium colonize their normal target organ, the cecum, to wild-type levels (55, 74); likewise, *Mot$^-$* mutants are found at wild-type levels in the mesenteric

lymph nodes (MLN), the liver, and the spleen (74), suggesting they can initiate a systemic infection. It follows that a Che$^-$ mutant can also colonize the cecum and initiate a systemic infection (74). However, the necessity for chemotaxis in a *S.* Typhimurium infection is apparent in a competition infection, where Che$^-$ mutants are severely outcompeted (73, 74). Wild-type *S.* Typhimurium outcompetes Che$^-$ by inducing inflammation in which chemotaxis is required for survival; Che$^-$ single infections do not induce an inflammatory response, and thus colonize well (73). Chemotaxis does not appear to provide a competitive advantage in the MLN, spleen or the liver, suggesting that chemotaxis is not beneficial beyond the intestinal tract (74).

1.3.4. *C. jejuni*

Colonization of the small and large intestine by *C. jejuni* requires chemotaxis, as demonstrated by several studies of Che$^-$ mutants lacking either CheY or CheA (15, 77, 92). However, similar to *H. pylori,* the Che$^-$ *C. jejuni* colonization deficit can be overcome with larger inoculation doses, suggesting that the Che$^-$ mutants have a higher ID_{50} than wild type (77, 92). When concentrations below the ID_{50} for Che$^-$ *C. jejuni* are used for infection, some Che$^-$ *C. jejuni* can be isolated from the large intestine 10 hours post-inoculation, but not at 48 hours post-inoculation, perhaps suggesting that Che$^-$ bacteria colonize briefly but do not grow or are quickly washed out of the intestinal tract (77).

	Animal Model	Che +/-	Outcome	Ref.
H. pylori	Mouse	+	Colonization/Gastritis	Terry 2004, Williams 2007
		Che-	High ID_{50}/reduced gastritis	
	Gerbil	+	Colonization/Gastritis	McGee, 2005
		Che-	No colonization	
	Gnotobiotic pig	+	Colonization	Foynes, 2000
		Che-	No colonization	
V. cholerae	Infant mouse	+	Colonization	Butler, 2004
		Che-	swim-biased, increased colonization; tumble-biased, attenuated colonization in competition	
S. Typhimurium	Mouse ligated loop tissue	+	Invade Peyer's patches	Jones, 1992
		Che-	swim-biased, increased invasion of Peyer's patches; tumble-biased, attenuated Peyer's patch invasion	
	Mouse colitis (strep pretreated)	+	Colonization, colitis	Stecher, 2004
		Che-	Colonization, reduced colitis	
C. jejuni	Mouse ($CHNaO_3$ pretreated)	+	Colonization	Yao, 1997
		Che-	Colonies absent from stool by 6 days	
	Chick	+	Caecal Colonization	Hendrixson, 2004
		Che-	100-fold reduced caecal colonization	
	Ferret	+	Diarrheal symptoms	Yao, 1997
		Che-	Reduced diarrheal symptoms	

Table 1.1. Outcome of infection for mucosal pathogens and their nonchemotactic mutants.

1.4. The role of chemotaxis in bacterial organ localization

1.4.1. *H. pylori*

The mouse stomach is composed of four physiologically different areas. The proximal third is the forestomach, which is not found in human stomachs, thus this region is typically not analyzed in *H. pylori* mouse experiments (1). The remaining two thirds of the stomach is covered with glandular epithelium that is subdivided into three distinct regions based on dominant cell types: the corpus,

the antrum, and the corpus-antrum transition zone (C-A transition zone). The corpus, also called the body or zymogenic region, contains mucus-producing pit cells, acid-secreting parietal cells, and chief/zymogenic cells, which secrete digestive enzymes. The most distal region, the antrum, has only mucus-producing pit cells and some chief cells. The C-A transition zone is the only region where mucus glands contain some parietal cells (47, 76) and severe pathology develops there in response to *H. pylori* infection (93). *H. pylori* preferentially colonizes the C-A transition zone in some mouse strains (45, 79) (A. S. Rolig and K. M. Ottemann, Chapter 2). In concordance with that observation, Syder *et al.* used a transgenic mouse line with fewer acid secreting parietal cells to demonstrate that *H. pylori* has a tropism for areas with fewer parietal cells and are likely less acidic (76), like the C-A transition zone. However, they did not demonstrate that this preference depends on chemotaxis.

Interestingly, sub-organ localization to the C-A transition zone, corpus, or antrum differs not only between different mouse strains (45, 79), it also differs between *H. pylori* strains—*H. pylori* strain SS1 preferentially colonizes the antrum while strain X47 prefers the corpus (1). The mechanism for the difference in distribution between these strains is unknown, however sub-organ preference has been linked to two *H. pylori* virulence properties: chemotaxis and the cytotoxin-associated gene-pathogenicity island (*cag*-PAI). The presence of an intact *cag*-PAI has been shown to promote corpus colonization (65) and

supporting this, antral-dominant strain SS1 has an inactive *cag*-PAI (20). However, the antral colonization phenotype in SS1 is also at least partially dependent on chemotaxis, as the *cheW* mutant (78) and the *chePep* mutant (35) have significantly decreased colonization in the antrum compared to wild type. Furthermore, the decrease in antral colonization does not occur until 30 hours post-inoculation, suggesting that chemotaxis promotes *H. pylori* survival and growth in the antrum (A. S. Rolig and K. M. Ottemann, Chapter 2).

To begin to understand which chemotactic signals drive survival and growth in the antrum, the stomach distribution of each individual chemoreceptor mutant has been examined. The *tlpA*, *tlpB*, and *tlpC* mutants each have an intermediate antral colonization phenotype. The *tlpD* mutant, on the other hand, phenocopies the nonchemotactic mutant in reduced antrum colonization, suggesting that the chemoreceptor TlpD is responsible for SS1's antral-dominant localization phenotype (A. S. Rolig and K. M. Ottemann, Chapter 2).

In addition to motivating sub-organ localization, chemotaxis is also important for localizing *H. pylori* within the mucus above the gastric epithelial cell layer (69, 87). The mucus is frequently and rapidly turned over, yet *H. pylori* manages to live within the 15 μm of mucus closest to the epithelium by following a pH gradient (69). Chemotaxis was not directly shown to be responsible for localizing *H. pylori* in the pH gradient, however, chemotaxis is required to keep

H. pylori close to the epithelial layer (87) and deep in the gastric glands (35). Williams *et al.* reported that when examining the relative position of *H. pylori* to the gastric epithelial cells, 88% of the wild-type *H. pylori* were touching the epithelium. All of the mutants examined, *cheW, cheY, tlpA*, and *tlpB,* displayed a different distribution from the wild type, with only 53%, 71%, 74%, and 63% touching, respectively (87). Since the chemoreceptor TlpB senses protons (17) it is tempting to speculate that signals received by TlpB direct intra-mucus localization.

1.4.2. *V. cholerae*

Wild-type *V. cholerae* colonizes and replicates in the jejunum (4, 8), but the ability to do so varies among different strains. For example, in a suckling mouse wild-type *V. cholerae* El Tor strain experiences a rapid loss of CFU from the entire intestine after inoculation, while the classical strain 0395 does not have a loss of CFU after inoculation (4). Che^- mutant *V. cholerae* do not have a colonization defect in the jejunum, however they mis-localize to additionally colonize the duodenum and the stomach (48). The increased habitat occupied by the Che^- mutant likely explains their out-growth phenotype (13). These data suggest that chemorepellent signals direct *V. cholerae* away from the stomach and the duodenum or another hypothesis envisions an antibacterial mechanism in the duodenum that attracts *V. cholerae* thus reducing their numbers in that

location (26, 48). It is unknown if there are differences in distribution within the mucosa specifically in the duodenum between wild-type and Che$^-$ *V. cholerae,* although *V. cholerae* chemotaxis is known to be important for penetration of the bacteria into the mucous (25). Experiments testing the penetration of vibrios into mucous gel in rabbit and mouse intestinal loops demonstrated that significantly more wild-type vibrios access the basal half of the intestinal villi than Che$^-$ mutants (24, 27). However, while the Che$^-$ vibrios were either above the villi or on the luminal half of the villi, this positioning did not affect the rate at which they were washed from the villi (24). These data suggest that chemotaxis drives *V. cholerae* to the base of the intestinal villi, however that penetration does not protect *V. cholerae* from being washed out *in vitro*.

1.4.3. *C. jejuni*

Wild-type *C. jejuni* colonizes the entire length of the small and large intestine; Che$^-$ mutants have a more limited distribution, as they only colonize the lower third of the mouse small intestine and the large intestine (77). Wild-type *C. jejuni* continues to colonize until at least one week post-inoculation while Che$^-$ mutants are unable to maintain colonization past one day of infection (77). It is unknown if the lack of upper small intestine colonization contributes to the inability of Che$^-$ *C. jejuni* to maintain colonization.

1.5. The role of chemotaxis in host cell invasion

1.5.1. *S.* Typhimurium

In an *S.* Typhimurium infection chemotaxis directs the bacteria closer to the epithelial layer *in vivo* (73, 74). *In vitro* host cell attachment and invasion are affected by motility (43, 53, 80) and by the direction of flagellar rotation (46). Che$^-$ mutants with a straight swim-bias have increased invasiveness into HEp-2 cells and into Peyer's patches from a mouse intestinal ligated loop model. Che$^-$ mutants with a tumble-bias have reduced HEp-2 cell and Peyer's patch invasion (36). Thus, the direction of flagellar rotation in *S.* Typhimurium chemotaxis mutants dictates their ability to invade host cells.

1.5.2. *C. jejuni*

Chemotaxis appears to play a role in *C. jejuni* eukaryotic cell invasion *in vitro* but it is not yet known whether chemotaxis plays a similar role during infection (39, 60, 92).

1.6. Chemotaxis and host responses

1.6.1. *H. pylori*

All people infected with *H. pylori* develop an inflammatory response known as gastritis. The inflammatory response begins when resident monocytes and epithelial cells detect a pathogen such as *H. pylori* and secrete chemokines to

recruit antigen presenting cells (APCs) that will prime T cells (72). The APCs define the type of immune response directed against *H. pylori* based on the nature of their contact with the pathogen. APCs interacting with *H. pylori* fuel the proliferation of T-helper type 1 (Th1) cells (88), $CD25^{+}FoxP3^{+}$ T regulatory cells (T regs) (40, 88), and T-helper type 17 (Th17) cells (42).

H. pylori chemotaxis promotes inflammation in a mouse model, as shown by a reduced inflammatory score in Che^{-} mutant infections compared to wild-type infections two, three and six months post-inoculation (57, 66, 87). To understand the differences in the immune responses that may be driven by reduced interactions with the host, we examined host cell apoptosis and specific immune cells present in wild-type and Che^{-} *H. pylori* infections. We demonstrated that wild-type *H. pylori* infection induced more host cell apoptosis (66). It is known that detection of both apoptosis and bacterial products leads to the recruitment of Th17 cells (12, 82), and indeed wild-type *H. pylori* recruited proinflammatory Th17 cells two months post-inoculation, while the *cheY* infection did not (66). We suggest that chemotaxis driven localization in the mucous puts *H. pylori* in an environment that allows up regulation of apoptosis-causing virulence factors, such as VacA (66). Also, the chemotaxis-driven proximity of *H. pylori* to the gastric epithelial cells allows for efficient delivery of those virulence factors; the presence of both signals drives the recruitment of proinflammatory Th17 cells.

1.6.2. *V. cholerae*

V. cholerae is the causative agent of the disease cholera, an epidemic acute diarrheal disease. The diarrheal disease is primarily caused by the enterotoxin, cholera toxin (CT), which is a main virulence determinant (41). CT and another prominent virulence factor, the toxin coregulated pilis (TCP), are coordinately regulated by the ToxR regulon. The ToxR regulon culminates in the expression of ToxT, a regulatory protein that directly activates transcription of the CT and TCP genes (18). While disease resulting from *V. cholerae* infection was traditionally classified as noninflammatory, reports now suggest that inflammation contributes to pathogenesis (6, 67, 71). Specifically, biopsy specimens show lymphocytes and mononuclear cells present in the intestinal lamina propria (61), CT induces the proinflammatory cytokine IL-6 in rat epithelial cells (56), and *V. cholerae* culture supernatant induces IL-6, MCP-1, IL-1α, and GM-CSF through NF-κB activation (6).

Mutants in each of the *cheY* genes, *cheY-1, cheY-2, cheY-3,* and *cheY-4,* are motile, nonchemotactic, and adhere less well to an intestinal epithelial cell monolayer (5, 7). Each of these chemotaxis mutants were examined *in vitro* for deficiencies in inflammatory cytokine production in INT407 cells. Results showed that the induction of the proinflammatory cytokines, IL-8 (68), IL-6, MCP-1, IL-1α, and TNFα (5) requires chemotaxis mediated by *cheY-3* and *cheY-4*

but not *cheY-1* and *cheY-2.* The *cheY-3* and *cheY-4* mutants were slightly more defective in motility and adherence and had a delayed activation of NF-κB. Interestingly, all *cheY* mutants produced similar levels of *ctxA* and CT, but *cheY-3* and *cheY-4* had more significantly reduced levels of *toxR* and *toxT* than *cheY-1* and *cheY-2* (5). These results suggest that either reduced motility, adherence, or *toxT* production in *cheY-3* and *cheY-4* leads to delayed activation of NF-κB and reduced production of inflammatory cytokines *in vitro*.

The observation that some of the *cheY* mutants produce less virulence genes (5, 7) was later confirmed in a RIVET screen looking for *in vivo* regulators of *V. cholerae* virulence factors (48). In their screen, Lee *et al* found four chemotaxis related genes that regulated *ctxA* or *toxT: cheA-2, cheY-3, cheZ,* and *mcpX.* Furthermore, the chemotaxis gene mutations affected *toxT* production *in vivo,* where *toxT* expression was delayed by 1-3 hours and *toxT* production was reduced 45%-75%; no effect was observed *in vitro* (48). In a similar way to *H. pylori* (66), these data combined with *in vitro* data suggest that chemotaxis steers *V. cholerae* to a location in the small intestine that promotes virulence factor expression (48). However, later experiments demonstrated that 7 hours post-inoculation, induction of *tcpA* and *ctxA* was not different in the Che^- mutant compared to the wild type (13). This suggests that at this time point chemotaxis does not affect virulence gene expression and that increased virulence of wild-type *V. cholerae* may depend on the timing of virulence factor expression, which

may be influenced by the location of the bacteria within the intestine or within the intestinal mucosa.

1.6.3. *S.* Typhimurium

S. Typhimurium causes enterocolitis in humans and livestock. Multiple virulence factors contribute to the induction of inflammation, including two type three sections systems, TTSS-1 and TTSS-2, which are encoded on the *Salmonella* Pathogenicity Island 1 (SPI-1) and SPI-2 (38). Che$^-$ mutants induce less colitis than wild type (74). Since Che$^-$ mutants locate further away from the epithelial cell layer (73), the reduced colitis induced by Che$^-$ mutants might suggest that Che$^-$ mutants are less efficient at translocating SPI-1 effecter proteins, similar to hypotheses made for both *H. pylori* and *V. cholerae.*

Interestingly, wild-type *S.* Typhimurium benefit from the inflammation they induce. Normally, the microbiota can protect against colonization by *S.* Typhimurium, however in an inflammatory environment *S.* Typhimurium has an increased growth rate that allows them to out-compete the microbiota (73, 75). The increased growth rate requires chemotaxis (73). One hypothesis suggests that acute colitis is accompanied by increased mucous production, which provides high energy nutrients that chemotaxis allows the bacteria to access (73). However, gut inflammation also results in the generation of a respiratory electron acceptor, tetrathionate, that specifically promotes *S.* Typhimurium

growth (89). It is unknown at this time if chemotaxis directs *S.* Typhimurium to locate tertathionate.

1.6.4. *C. jejuni*

C. jejuni is one of the most common causes of bacterial diarrhea and inflammation is an important component of disease pathology (9). The influence of chemotaxis on inflammation has been examined both *in vitro* and *in vivo.* Incubation of *C. jejuni* with INT407 cells results in the secretion of the inflammatory cytokine, IL-8. The *cheY* mutants induced significantly more IL-8 secretion than wild type (34), in agreement with their hyperadhesive and hyperinvasive phenotype (92). One hypothesis is that chemotaxis modulates expression of virulence factors that promote adhesion and invasion, thus inducing IL-8 production. Virulence gene expression has not been examined for the Che^- mutants; however, chemoreceptor mutants that have reduced invasion do not have altered virulence gene expression when examining *cadF,* a fibronectin binding protein, *ciaB,* a host cell internalization protein or *csrA,* a putative global regulator (84). Thus, attenuated invasion of chemoreceptor mutants *in vitro* is not due to the down-regulation of these three virulence genes.

In vivo, the Che^- mutants cause less disease in a ferret model, as examined by ferrets displaying the symptoms of mucous diarrhea, dehydration, bacteraemia, and a lack of weight gain (92). These data indicate that the ability

to chemotax affects *C. jejuni* virulence, but further exploration of the differences in wild-type and Che$^-$ *C. jejuni* virulence factor expression *in vivo* and of the immune responses to wild-type and Che$^-$ *C. jejuni* is necessary.

1.7. The role of chemoreceptors in infection

Movement driven by chemotaxis requires specific signals, chemoattractants or chemorepellents, to be detected by the chemoreceptors. For *E. coli, S.* Typhimurium*, H. pylori, V. cholerae,* and *C. jejuni* some chemoattractants and chemorepellents are known (Table 1.2). Specific chemoreceptors are known to detect some of these signals, for example, in *H. pylori* TlpB senses acid and AI-2 (17, 63), however some signals are not attached to specific chemoreceptors, and likewise, some chemoreceptors do not have defined ligands. To study how sensing by individual chemoreceptors impacts mucosal colonization, bacterial mutants in single chemoreceptors have been examined.

1.7.1. *H. pylori*

Three of the four *H. pylori* chemoreceptors play roles in colonization. The TlpD receptor is important both in early single strain infections and in competition, where it displays a similar phenotype to that of Che$^-$ (87)(S. M. Williams and K. M. Ottemann, unpublished data). The TlpA and TlpC chemoreceptors are less important: *tlpA* and *tlpC* mutants do not have a

colonization defect in single infections, but are modestly outcompeted by wild type in competition infections (3).

The contribution of the TlpB chemoreceptor, which senses pH (17) and AI-2 (63), to colonization is not straight forward. A study carried out in C57BL/6 $p40^{-/-}$ mice, which do not produce the proinflammatory cytokines IL-12 and IL-23, demonstrated that TlpB was necessary for colonization (17). However, two other studies showed that *tlpB* mutants colonized both gerbils (57) and mice (87), and moreover, unlike the *tlpA, tlpC*, and *tlpD* mutants, *tlpB* mutants did not have a competitive defect (57, 87). These results suggest that TlpB is not required for bacterial growth during infection of wild-type mice. It is not yet known why TlpB is necessary for colonization in the C57BL/6 $p40^{-/-}$ mice. One possibility is that alterations in the type of inflammatory environments change the necessity for sensing by TlpB.

To understand the signal necessary for inducing host-pathogen interactions that promote inflammation, inflammatory phenotypes have been examined in individual chemoreceptor mutant infections. At three and six months post-inoculation, *tlpC and tlpD* mutant infections had similar inflammatory scores to wild-type *H. pylori*, suggesting that chemotaxis driven by TlpC and TlpD does not affect the inflammatory response to *H. pylori*. On the other hand, early post-inoculation the *tlpB* mutant causes reduced inflammation in a gerbil model (57) and both *tlpA* and *tlpB* mutant infected mice display

reduced inflammation in a mouse model (87). These results suggest that host interactions driven by TlpA and TlpB increase inflammation within three months of infection. However, by six months post-inoculation both *tlpA* and *tlpB* mutants had a significantly increased inflammatory score compared to the wild-type infection (87), suggesting that TlpA and TlpB driven interactions decrease inflammation in later stages of infection. *tlpA* and *tlpB* mutants are both further away from the epithelial cells than wild-type (87); thus, we speculate that distance from the epithelial cell layer or reduced interaction with specific cell types alters the immune response to *H. pylori*.

1.7.2. *V. Cholerae*

There are 46 chemoreceptors annotated in the *V. cholerae* genome (10); of these, only the McpX (48), AcfB (16, 22, 62), and TcpI (16) chemoreceptors have been examined for their contributions to colonization. Strains lacking either *mcpX* or *tcpI* have normal colonization in competition with wild type, suggesting they are not important in this setting or that there are chemoreceptors with redundant function (16, 48). Different studies have determined that with an inoculation concentration of 10^4 CFU *acfB* mutants do (62) or with an inoculating concentration of 10^5 CFU do not (16) have defects *in vivo* competition assays, suggesting that defects can be overcome with high inoculation concentrations. Lastly, a double mutant in *acfB* and *tcpI* did have a

significant colonization defect when in competition with wild type, suggesting that these two chemoreceptors have redundant functions in *V. cholerae* colonization (16).

1.7.3. *C. jejuni*

C. jejuni has ten chemoreceptors, seven membrane bound and three soluble (50). Individual mutants in all of the ten receptors have been examined for colonization defects in the chick intestine, and DocB, Cj0262c (33), and Tlp1 (30) displayed reduced colonization. Additionally, examination of five chemoreceptor genes, *tlp1, tlp2, tlp3, docB*, and *docC*, for their affects on *C. jejuni's* ability to invade human epithelial and chick embryo cells have showed that *tlp1, tlp3, docB* and *docC* are involved in *in vitro* eukaryotic cell invasion (84).

Bacteria	# MCP genes	Known ligands
E. coli	5	Amino acids, sugars, pyrimidines, toxic metals, AI-2, oxygen, temperature, pH
S. Typhimurium	9	Metal-citrate, citrate, phenol
V. cholerae	43	Chitin oligosaccharides, L-amino acids, bile, intestinal mucin
C. jejuni	10	Fucose, pyruvate, fumarate, aspartate, formate
H. pylori	4	Acid, AI-2, urea, bicarbonate, arginine and several other amino acids, cholesterol, $NiCl_2$

Table 1.2. Known chemoreceptor genes and ligands

1.8. Conclusion

Chemotaxis plays an important role in pathogenesis and mucosal colonization, one that goes beyond being necessary for colonization. While chemotaxis is required for colonization at low inoculation concentrations, performing experiments with increased inoculation concentrations has allowed researchers to examine the more intricate roles that chemotaxis plays in infections by *S.* Typhimurium*, H. pylori, V. cholerae,* and *C. jejuni.*

From those experiments, a few trends have emerged. First, chemotaxis directs interaction with the host by localizing bacteria to specific organ sub-regions, driving host-pathogen interaction, and increasing host cell invasion. These interactions may promote inflammatory immune responses, as infections with Che^- mutants in *S.* Typhimurium*, H. pylori, V. cholerae,* and *C. jejuni* all resulted in reduced inflammatory responses. In fact, in *H. pylori* infection,

chemotaxis drives interactions that result in an increased presence of proinflammatory Th17 cells. This increased inflammatory response may be a result of increased virulence factor expression. This is a hypothesis that has proven true for early *V. cholerae* infection, and has not been examined in detail in *C. jejuni* and *S.* Typhimurium. Interestingly, chemotaxis in *S.* Typhimurium promotes growth in inflammatory environments, which allows *S.* Typhimurium to out compete normal microbiota. Based on these studies, it is clear that chemotaxis plays a critical yet varied role in virulence of mucosal pathogens.

1.9. References

1. **Akada J. K.** 2003. Helicobacter pylori tissue tropism: mouse-colonizing strains can target different gastric niches. Microbiology **149**:1901-1909.

2. **Alexander R. P., A. C. Lowenthal, R. M. Harshey, and K. M. Ottemann**. 2010. CheV: CheW-like coupling proteins at the core of the chemotaxis signaling network. Trends in Microbiology **18**:494-503.

3. **Andermann T. M., Y.-T. Chen, and K. M. Ottemann**. 2002. Two Predicted Chemoreceptors of Helicobacter pylori Promote Stomach Infection. Infection and Immunity **70**:5877-5881.

4. **Angelichio M. J., J. Spector, M. K. Waldor, and A. Camilli**. 1999. Vibrio cholerae Intestinal Population Dynamics in the Suckling Mouse Model of Infection. Infection and Immunity **67**:3733-3739.

5. **Bandyopadhaya A., and K. Chaudhuri**. 2009. Differential modulation of NF-kappaB-mediated pro-inflammatory response in human intestinal epithelial cells by cheY homologues of Vibrio cholerae. Innate Immunity **15**:131-42.

6. **Bandyopadhaya A., M. Sarkar, and K. Chaudhuri**. 2007. Transcriptional upregulation of inflammatory cytokines in human intestinal epithelial cells following Vibrio cholerae infection. The FEBS Journal **274**:4631-42.

7. **Banerjee R., S. Das, K. Mukhopadhyay, S. Nag, A. Chakrabortty, and K. Chaudhuri**. 2002. Involvement of in vivo induced cheY-4 gene of Vibrio cholerae

in motility, early adherence to intestinal epithelial cells and regulation of virulence factors. FEBS Letters **532**:221-226.

8. **Baselski V. S., and C. D. Parker**. 1978. Intestinal Distribution of Vibrio cholerae in Orally Infected Infant Mice: Kinetics of Recovery of Radiolabel and Viable Cells. Infection and Immunity **21**:518-525.

9. **Black R. E., M. M. Levine, M. L. Clements, T. P. Hughes, and M. J. Blaser**. 1988. Experimental Campylobacter jejuni infection in humans. The Journal of Infectious Diseases **157**:472-9.

10. **Boin M. a, M. J. Austin, and C. C. Häse**. 2004. Chemotaxis in Vibrio cholerae. FEMS Microbiology Letters **239**:1-8.

11. **Bren A., and M. Eisenbach**. 2000. How Signals Are Heard during Bacterial Chemotaxis : Protein-Protein Interactions in Sensory Signal Propagation. Journal of Bacteriology **182**:6865-6873.

12. **Brereton C. F., and J. M. Blander**. 2011. The unexpected link between infection-induced apoptosis and a Th17 immune response. J Leukoc Biol **89**:565-576.

13. **Butler S. M., and A. Camilli**. 2004. Both chemotaxis and net motility greatly influence the infectivity of Vibrio cholerae. Proceedings of the National Academy of Sciences of the United States of America **101**:5018-23.

14. **Cerda O., A. Rivas, and H. Toledo**. 2003. Helicobacter pylori strain ATCC700392 encodes a methyl-accepting chemotaxis receptor protein (MCP) for arginine and sodium bicarbonate. FEMS Microbiology Letters **224**:175-181.

15. **Chang C., and J. F. Miller**. 2006. Campylobacter jejuni colonization of mice with limited enteric flora. Infection and Immunity **74**:5261-71.

16. **Chaparro A. P., S. K. Ali, and K. E. Klose**. 2010. The ToxT-dependent methyl-accepting chemoreceptors AcfB and TcpI contribute to Vibrio cholerae intestinal colonization. FEMS Microbiology Letters **302**:99-105.

17. **Croxen M. A., G. Sisson, R. Melano, and P. S. Hoffman**. 2006. The Helicobacter pylori chemotaxis receptor TlpB (HP0103) is required for pH taxis and for colonization of the gastric mucosa. Journal of Bacteriology **188**:2656-65.

18. **DiRita V. J., C. Parsott, G. Jander, and J. J. Mekalanos**. 1991. Regulatory cascade controls virulence in Vibrio cholerae. Proceedings of the National Academy of Sciences **88**:5403-5407.

19. **Draper J., K. Karplus, and K. M. Ottemann**. 2011. Identification of a chemoreceptor zinc-binding domain common to cytoplasmic bacterial chemoreceptors. Journal of Bacteriology **193**:4338-45.

20. **Eaton K. A., D. Kersulyte, M. Mefford, S. J. Danon, S. Krakowka, and D. E. Berg**. 2001. Role of Helicobacter pylori cag region genes in colonization and gastritis in two animal models. Infection and Immunity. Am Soc Microbiol **69**:2902.

21. **Elliott K. T., and V. J. Dirita**. 2008. Characterization of CetA and CetB, a bipartite energy taxis system in Campylobacter jejuni. Molecular Microbiology **69**:1091-103.

22. **Everiss K. D., K. J. Hughes, M. E. Kovach, and K. M. Peterson**. 1994. The Vibrio cholerae acfB colonization determinant encodes an inner membrane protein that is related to a family of signal-transducing proteins. Infection and Immunity **62**:3289-98.

23. **Foynes S., N. Dorrell, S. J. Ward, R. A. Stabler, A. A. M. C. Colm, A. N. Rycroft, and B. W. Wren**. 2000. Helicobacter pylori Possesses Two CheY Response Regulators and a Histidine Kinase Sensor, CheA, Which Are Essential for Chemotaxis and Colonization of the Gastric Mucosa. Infection and Immunity **64**:2016-2023.

24. **Freter R., B. Allweiss, P. O'Brien, S. Halstead, and M. Macsai**. 1981. Role of chemotaxis in the association of motile bacteria with intestinal mucosa: in vitro studies. Infection and Immunity **34**:241-249.

25. **Freter R., and P. O'Brien**. 1981. Role of chemotaxis in the association of motile bacteria with intestinal mucosa: chemotactic responses of Vibrio cholerae and description of motile nonchemotactic mutants. Infection and Immunity **34**:215-221.

26. **Freter R., and P. O'Brien**. 1981. Role of chemotaxis in the association of motile bacteria with intestinal mucosa: fitness and virulence of nonchemotactic Vibrio cholerae mutants in infant mice. Infection and Immunity **34**:222-233.

27. **Freter R., P. O'Brien, and M. Macsai**. 1981. Role of chemotaxis in the association of motile bacteria with intestinal mucosa: in vivo studies. Infection and Immunity **34**:234-240.

28. **Frye J., J. E. Karlinsey, H. R. Felise, B. Marzolf, N. Dowidar, M. Mcclelland, and K. T. Hughes**. 2006. Identification of New Flagellar Genes of Salmonella enterica Serovar Typhimurium. Journal of Bacteriology **188**:2233-2243.

29. **Gosink K. K., R. Kobayashi, I. Kawagishi, and C. C. Häse**. 2002. Analyses of the Roles of the Three cheA Homologs in Chemotaxis of Vibrio cholerae. Journal of Bacteriology **184**:1767-1771.

30. **Hartley-Tassell L. E., L. K. Shewell, C. J. Day, J. C. Wilson, R. Sandhu, J. M. Ketley, and V. Korolik**. 2010. Identification and characterization of the aspartate chemosensory receptor of Campylobacter jejuni. Molecular Microbiology **75**:710-30.

31. **Hegde M., D. L. Englert, S. Schrock, W. B. Cohn, C. Vogt, T. K. Wood, M. D. Manson, and A. Jayaraman**. 2011. Chemotaxis to the quorum-sensing signal AI-2 requires the Tsr chemoreceptor and the periplasmic LsrB AI-2-binding protein. Journal of Bacteriology **193**:768-73.

32. **Hendrixson D. R., B. J. Akerley, and V. J. DiRita**. 2001. Transposon mutagenesis of Campylobacter jejuni identifies a bipartite energy taxis system required for motility. Molecular Microbiology **40**:214-24.

33. **Hendrixson D. R., and V. J. DiRita**. 2004. Identification of Campylobacter jejuni genes involved in commensal colonization of the chick gastrointestinal tract. Molecular Microbiology **52**:471-84.

34. **Hickey T. E., S. Baqar, A. L. Bourgeois, C. P. Ewing, and P. Guerry**. 1999. Campylobacter jejuni-Stimulated Secretion of Interleukin-8 by INT407 Cells. Infection and Immunity **67**:88-93.

35. **Howitt M. R., J. Y. Lee, P. Lertsethtakarn, R. Vogelmann, L.-M. Joubert, K. M. Ottemann, and M. R. Amieva**. 2011. ChePep Controls Helicobacter pylori Infection of the Gastric Glands and Chemotaxis in the Epsilonproteobacteria. mBio **2**:1-10.

36. **Jones B. D., C. A. Lee, and S. Falkow**. 1992. Invasion by Salmonella typhimurium is affected by the direction of flagellar rotation. Infection and Immunity **60**:2475-2480.

37. **Josenhans C., and S. Suerbaum**. 2002. The role of motility as a virulence factor in bacteria. International Journal of Medical Microbiology **291**:605-614.

38. **Kaiser P., M. Diard, B. Stecher, and W.-D. Hardt**. 2012. The streptomycin mouse model for Salmonella diarrhea: functional analysis of the microbiota, the

pathogen's virulence factors, and the host's mucosal immune response. Immunological Reviews **245**:56-83.

39. **Kanungpean D., T. Kakuda, and S. Takai**. 2011. Participation of CheR and CheB in the chemosensory response of Campylobacter jejuni. Microbiology **157**:1279-89.

40. **Kao J. Y., M. Zhang, M. J. Miller, J. C. Mills, B. Wang, M. Liu, K. a Eaton, W. Zou, B. E. Berndt, T. S. Cole, T. Takeuchi, S. Y. Owyang, and J. Luther**. 2010. Helicobacter pylori immune escape is mediated by dendritic cell-induced Treg skewing and Th17 suppression in mice. Gastroenterology. Elsevier Inc. **138**:1046-54.

41. **Kaper J. B., J. G. Morris, and M. M. Levine**. 1995. Cholera. Clinical Microbiology Reviews **8**:48-86.

42. **Khamri W., M. M. Walker, P. Clark, J. C. Atherton, M. R. Thursz, K. B. Bamford, R. I. Lechler, and G. Lombardi**. 2010. Helicobacter pylori stimulates dendritic cells to induce interleukin-17 expression from CD4+ T lymphocytes. Infection and Immunity **78**:845-53.

43. **Khoramian-Falsafi T., S. Harayama, K. Kutsukake, and J. C. Pechère**. 1990. Effect of motility and chemotaxis on the invasion of Salmonella typhimurium into HeLa cells. Microbial Pathogenesis **9**:47-53.

44. **Lee A., J. L. O'Rourke, P. J. Barrington, and T. J. Trust**. 1986. Mucus colonization as a determinant of pathogenicity in intestinal infection by Campylobacter jejuni: a mouse cecal model. Infection and Immunity **51**:536-46.

45. **Lee A., J. O'Rourke, M. C. De Ungria, B. Robertson, G. Daskalopoulos, and M. F. Dixon**. 1997. A standardized mouse model of Helicobacter pylori infection: introducing the Sydney strain. Gastroenterology **112**:1386-97.

46. **Lee C. a, B. D. Jones, and S. Falkow**. 1992. Identification of a Salmonella typhimurium invasion locus by selection for hyperinvasive mutants. Proceedings of the National Academy of Sciences of the United States of America **89**:1847-51.

47. **Lee E., J. Trasler, S. Dwivedi, and C. Leblond**. 1982. Division of the mouse gastric mucosa into zymogenic and mucous regions on the basis of gland features. The American Journal of Anatomy **164**:187-207.

48. **Lee S., S. Butler, and A. Camilli**. 2001. Selection for in vivo regulators of bacterial virulence. Proceedings of the National Academy of Sciences **98**:6889-6894.

49. **Lertsethtakarn P., and K. M. Ottemann**. 2010. A remote CheZ ortholog retains phosphatase function. Molecular Microbiology **77**:225-235.

50. **Lertsethtakarn P., K. M. Ottemann, and D. R. Hendrixson**. 2011. Motility and Chemotaxis in Campylobacter and Helicobacter. Annual Review of Microbiology **65**:389-410.

51. **Li X., and S. Roseman**. 2004. The chitinolytic cascade in Vibrios is regulated by chitin oligosaccharides and a two-component chitin catabolic sensor/kinase. Proceedings of the National Academy of Sciences of the United States of America **101**:627-31.

52. **Liu X., and R. E. Parales**. 2008. Chemotaxis of Escherichia coli to pyrimidines: a new role for the signal transducer tap. Journal of Bacteriology **190**:972-9.

53. **Lockman H. a, and R. Curtiss**. 1990. Salmonella typhimurium mutants lacking flagella or motility remain virulent in BALB/c mice. Infection and Immunity **58**:137-43.

54. **Lowenthal A. C., C. Simon, A. S. Fair, K. Mehmood, K. Terry, S. Anastasia, and K. M. Ottemann**. 2009. A fixed-time diffusion analysis method determines that the three cheV genes of Helicobacter pylori differentially affect motility. Microbiology **155**:1181-91.

55. **McCormick B., B. Stocker, D. Laux, and P. Cohen**. 1988. Roles of motility, chemotaxis, and penetration through and growth in intestinal mucus in the ability of an avirulent strain of Salmonella typhimurium to colonize the large intestine of streptomycin-treated mice. Infection and Immunity **56**:2209-17.

56. **McGee D. W., C. O. Elson, and J. R. McGhee**. 1993. Enhancing effect of cholera toxin on interleukin-6 secretion by IEC-6 intestinal epithelial cells: mode

of action and augmenting effect of inflammatory cytokines. Infection and Immunity **61**:4637-44.

57. **McGee D., M. Langford, E. Watson, and JE**. 2005. Colonization and inflammation deficiencies in Mongolian gerbils infected by Helicobacter pylori chemotaxis mutants. Infection and Immunity **73**:1820-1827.

58. **Merrell D. S., S. M. Butler, F. Qadri, N. a Dolganov, A. Alam, M. B. Cohen, S. B. Calderwood, G. K. Schoolnik, and A. Camilli**. 2002. Host-induced epidemic spread of the cholera bacterium. Nature **417**:642-5.

59. **Miller L. D., M. H. Russell, and G. Alexandre**. 2009. Diversity in Bacterial Chemotactic Responses and Niche Adaptation. Advances in Applied Microbiology **66**:53-75.

60. **Novik V., D. Hofreuter, and J. E. Galán**. 2010. Identification of Campylobacter jejuni genes involved in its interaction with epithelial cells. Infection and Immunity **78**:3540-53.

61. **Pastore G., G. Schiraldi, G. Fera, E. Sforza, and O. Schiraldi**. 1976. A bioptic study of gastrointestinal mucosa in cholera patients during an epidemic in southern Italy. The American Journal of Digestive Diseases **21**:613-7.

62. **Peterson K., and J. Mekalanos**. 1988. Characterization of the Vibrio cholerae ToxR regulon: identification of novel genes involved in intestinal colonization. Infection and Immunity **56**:2822-2829.

63. **Rader B. A., C. Wreden, K. G. Hicks, E. G. Sweeney, K. M. Ottemann, and K. Guillemin**. 2011. Helicobacter pylori perceives the quorum-sensing molecule AI-2 as a chemorepellent via the chemoreceptor TlpB. Microbiology **157**:2445-2455.

64. **Rebbapragada A., M. S. Johnson, G. P. Harding, A. J. Zuccarelli, H. M. Fletcher, I. B. Zhulin, and B. L. Taylor**. 1997. The Aer protein and the serine chemoreceptor Tsr independently sense intracellular energy levels and transduce oxygen, redox, and energy signals for Escherichia coli behavior. Proceedings of the National Academy of Sciences of the United States of America **94**:10541-6.

65. **Rieder G., J. L. Merchant, and R. Haas**. 2005. Helicobacter pylori cag-Type IV Secretion System Facilitates Corpus Colonization to Induce Precancerous Conditions in Mongolian Gerbils. Gastroenterology **128**:1229-1242.

66. **Rolig A. S., J. E. Carter, and K. M. Ottemann**. 2011. Bacterial chemotaxis modulates host cell apoptosis to establish a T-helper cell, type 17 (Th17)-dominant immune response in Helicobacter pylori infection. Proceedings of the National Academy of Sciences of the United States of America **108**:19749-19754.

67. **Saha D., S. Niyogi, G. Nair, B. Manna, and B. SK**. 2000. Detection of faecal leucocytes & erythrocytes from stools of cholera patients suggesting an evidence of an inflammatory response in cholera. Indian Journal of Medical Research **112**:5-8.

68. **Sarkar M., and K. Chaudhuri**. 2004. Association of adherence and motility in interleukin 8 induction in human intestinal epithelial cells by Vibrio cholerae. Microbes and Infection **6**:676-85.

69. **Schreiber S., M. Konradt, C. Groll, P. Scheid, G. Hanauer, H. O. Werling, C. Josenhans, and S. Suerbaum**. 2004. The spatial orientation of Helicobacter pylori in the gastric mucus. Proceedings of the National Academy of Sciences of the United States of America. National Acad Sciences **101**:5024.

70. **Schweinitzer T., T. Mizote, N. Ishikawa, A. Dudnik, S. Inatsu, S. Schreiber, S. Suerbaum, S.-ichi Aizawa, and C. Josenhans**. 2008. Functional characterization and mutagenesis of the proposed behavioral sensor TlpD of Helicobacter pylori. Journal of Bacteriology **190**:3244-55.

71. **Silva T. M. J., M. A. Schleupner, C. O. Tacket, T. Steiner, J. B. Kaper, R. Edelman, and R. L. Guerrant**. 1996. New evidence for an inflammatory component in diarrhea caused by selected new, live attenuated cholera vaccines and by El Tor and Q139 Vibrio cholerae. Infectiona and Immunity **64**:2362-2364.

72. **Soehnlein O., and L. Lindbom**. 2010. Phagocyte partnership during the onset and resolution of inflammation. Nature Reviews Immunology. Nature Publishing Group **10**:427-439.

73. **Stecher B., M. Barthel, M. C. Schlumberger, L. Haberli, W. Rabsch, M. Kremer, and W.-D. Hardt**. 2008. Motility allows S. Typhimurium to benefit from the mucosal defence. Cellular Microbiology **10**:1166-80.

74. **Stecher B., S. Hapfelmeier, C. Müller, M. Kremer, T. Stallmach, and W. Hardt-Dietrich**. 2004. Flagella and Chemotaxis Are Required for Efficient Induction of Salmonella enterica Serovar Typhimurium Colitis in Streptomycin-Pretreated Mice. Infection and Immunity **72**:4138-4150.

75. **Stecher B., R. Robbiani, A. W. Walker, A. M. Westendorf, M. Barthel, M. Kremer, S. Chaffron, A. J. Macpherson, J. Buer, J. Parkhill, G. Dougan, C. von Mering, and W.-D. Hardt**. 2007. Salmonella enterica serovar typhimurium exploits inflammation to compete with the intestinal microbiota. PLoS biology **5**:2177-89.

76. **Syder A. J., J. D. Oh, J. L. Guruge, D. O'Donnell, M. Karlsson, J. C. Mills, B. M. Björkholm, and J. I. Gordon**. 2003. The impact of parietal cells on Helicobacter pylori tropism and host pathology: an analysis using gnotobiotic normal and transgenic mice. Proceedings of the National Academy of Sciences of the United States of America **100**:3467-72.

77. **Takata T., S. Fujimoto, and K. Amako**. 1992. Isolation of Nonchemotactic Mutants of Campylobacter jejuni and Their Colonization of the Mouse Intestinal Tract. Infection and Immunity **60**:3596-3600.

78. **Terry K., S. M. Williams, L. Connolly, and K. M. Ottemann**. 2005. Chemotaxis Plays Multiple Roles during Helicobacter pylori Animal Infection. Infection and Immunity **73**:803-811.

79. **Thompson L., S. Danon, J. Wilson, J. O'Rourke, N. Salama, S. Falkow, H. Mitchell, and A. Lee**. 2004. Chronic Helicobacter pylori infection with Sydney strain 1 and a newly identified mouse-adapted strain (Sydney strain 2000) in C57BL/6 and BALB/c mice. Infection and Immunity **72**:4668-4679.

80. **Tomita T., and S. Kanegasaki**. 1982. Enhanced phagocytic response of macrophages to bacteria by physical impact caused by bacterial motility or centrifugation. Infection and Immunity **38**:865-870.

81. **Toole R. O., S. Lundberg, S.-åke Fredriksson, A. Jansson, B. Nilsson, and H. Wolf-watz**. 1999. The Chemotactic Response of Vibrio anguillarum to Fish Intestinal Mucus Is Mediated by a Combination of Multiple Mucus Components. Journal of Bacteriology **181**:4308-4317.

82. **Torchinsky M. B., J. Garaude, A. P. Martin, and J. M. Blander**. 2009. Innate immune recognition of infected apoptotic cells directs T(H)17 cell differentiation. Nature. Nature Publishing Group **458**:78-82.

83. **Umemura T., Y. Matsumoto, K. Ohnishi, M. Homma, and I. Kawagishi**. 2002. Sensing of cytoplasmic pH by bacterial chemoreceptors involves the linker region that connects the membrane-spanning and the signal-modulating helices. The Journal of Biological Chemistry **277**:1593-8.

84. **Vegge C. S., L. Brøndsted, Y.-P. Li, D. D. Bang, and H. Ingmer**. 2009. Energy taxis drives Campylobacter jejuni toward the most favorable conditions for growth. Applied and Environmental Microbiology **75**:5308-14.

85. **Vliet a H. van, and J. M. Ketley**. 2001. Pathogenesis of enteric Campylobacter infection. Journal for Applied Microbiology **90**:45S-56S.

86. **Wadhams G. H., and J. P. Armitage**. 2004. Making sense of it all: bacterial chemotaxis. Nature Reviews Molecular Cell Biology **5**:1024-37.

87. **Williams S. M., Y.-ting Chen, T. M. Andermann, J. E. Carter, D. J. Mcgee, and K. M. Ottemann**. 2007. Helicobacter pylori Chemotaxis Modulates Inflammation and Bacterium-Gastric Epithelium Interactions in Infected Mice. Infection and Immunity **75**:3747-3757.

88. **Wilson K. T., and J. E. Crabtree**. 2007. Immunology of Helicobacter pylori: insights into the failure of the immune response and perspectives on vaccine studies. Gastroenterology **133**:288-308.

89. **Winter S. E., P. Thiennimitr, M. G. Winter, B. P. Butler, D. L. Huseby, R. W. Crawford, J. M. Russell, C. L. Bevins, L. G. Adams, R. M. Tsolis, J. R. Roth, and A. J. Bäumler**. 2010. Gut inflammation provides a respiratory electron acceptor for Salmonella. Nature **467**:426-429.

90. **Wuichet K., and I. Zhulin**. 2010. Origins and diversification of a complex signal transduction system in prokaryotes. Science Signaling **3**:ra50.

91. **Yamamoto K., and Y. Imae**. 1993. Cloning and characterization of the Salmonella typhimurium-specific chemoreceptor Tcp for taxis to citrate and from phenol. Proceedings of the National Academy of Sciences of the United States of America **90**:217-21.

92. **Yao R., D. H. Burr, and P. Guerry**. 1997. CheY-mediated modulation of Campylobacter jejuni virulence. Molecular microbiology **23**:1021-31.

93. **Zanten S. J. Van, M. F. Dixon, and A. Lee**. 1999. The gastric transitional zones: neglected links between gastroduodenal pathology and helicobacter ecology. Gastroenterology **116**:1217-29.

CHAPTER 2

Helicobacter pylori requires TlpD-driven chemotaxis for survival and growth in the antrum

2.1. Abstract

Different diseases arise when the gastric pathogen *Helicobacter pylori* localizes to the stomach corpus versus the antrum, indicating that the localization of *H. pylori* within the stomach may be an important component of disease progression. One bacterial property known to affect murine corpus-antrum localization is chemotaxis, the ability to move in response to chemical cues. In this report, we analyzed whether chemotaxis is required for initially locating a particular stomach region, or for growth after initial colonization. As anticipated from previous work, we found that non-chemotactic mutants (Che^-) did not display a growth defect in the corpus. In the antrum, however, we found that Che^- mutants initially colonize this region normally, but are unable to multiply to normal levels. Wild-type *H. pylori,* in contrast, readily colonize and multiply in the antrum. This outcome indicates that chemotaxis is not necessary to initially find the antrum, but is needed for subsequent steps of growth and/or survival. To determine which chemoreceptor is responsible for the antral phenotype, we infected mice with strains lacking each chemoreceptor. Only the *tlpD* mutant resembled the Che^- mutant in the antral colonization defect, suggesting that TlpD is the main receptor responsible for antral colonization.

Additionally, the inflammation grade of each stomach region showed that inflammation is worse in the antrum compared to the corpus in both the wild-type and the Che$^-$ infection. These results suggest that chemotaxis, specifically TlpD, is necessary for *H. pylori* to survive or grow in the increased inflammatory environment of the antrum.

2.2. Introduction

The gastric pathogen *Helicobacter pylori* chronically infects the stomachs of 50% of the world's population. Infection with *H. pylori* triggers gastric inflammation, also known as gastritis, that can lead to a wide range of disease outcomes, from mild gastritis to gastric and peptic ulcers to cancers such as gastric adenocarcinoma and mucosa-associated lymphoid tumors (MALT) (29). *H. pylori* induced gastritis primarily occurs in the antrum (3, 19, 41), one of three distinct regions in the human stomach; each region is defined by the cell types that exist in the gastric glands. The two largest regions are the corpus and the antrum, and a third region called the corpus-antrum (C-A) transition zone separates them. Multiple lines of evidence suggest that *H. pylori*-triggered inflammation in each of these regions results in distinct disease outcomes. For example, gastritis that affects predominantly the antrum correlates with *H. pylori*-triggered duodenal ulcers (3, 47), a disease state that does not develop to gastric cancer (3, 36, 41). Gastritis that affects predominantly the corpus, on the other hand, increases the risk of gastric ulcers and intestinal-type gastric cancer (3, 41), while gastritis throughout the stomach, so-called pangastritis, increases the risk for diffuse-type gastric cancer (41). These observations demonstrate that specific *H. pylori* diseases correlate with inflammation in specific stomach regions. The basis for these different patterns of inflammation is unclear, but one possible reason for the differential location of diseased tissue is that different *H.*

pylori strains preferentially colonize either the corpus or the antrum, and in turn trigger elevated inflammation in that region. Thus *H. pylori's* localization within the stomach may be important for driving disease development.

Studies have shown that different *H. pylori* strains achieve higher bacterial numbers in either the corpus or the antrum (1, 20, 24). Specifically, strain SS1 colonizes the murine corpus and antrum approximately equally while strain X47 has a strong preference for the corpus (1, 20, 39). The ability to predominate in a particular stomach region has thus far been linked to three *H. pylori* characteristics: 1) the presence of cytotoxin-associated pathogenicity island, or *cag*-PAI (31); 2) the presence of the ferric uptake regulator (Fur) (24), which is necessary for *H. pylori* adaptation to iron limitation (42), and resistance to acid and oxidative stress (6, 14); and 3) the ability to chemotax, or move in response to chemical cues (39).

Bacterial chemotaxis has been extensively studied in *Escherichia coli* (25, 43). *E. coli* has five chemoreceptors that detect environmental cues and transmit information to a histidine kinase, CheA, via the coupling protein, CheW. In the absence of chemotaxis attractants, the ligand-free chemoreceptors activate the CheA histidine kinase, which in turn phosphorylates the response regulator, CheY. Phosphorylated CheY (CheY-P) interacts with the flagellar motor, which causes the motor to rotate clockwise, and the bacteria move randomly in a tumbling behavior. Conversely, when the chemoreceptors are bound by

chemoattractant ligand, the CheA histidine kinase is inactivated, and thus CheY-P populations are reduced and replaced with nonphosphorylated CheY. Non-phosphorylated CheY does not interact with the flagellar motor, which in turn rotates in the default counterclockwise direction and the bacteria swim straight.

H. pylori's chemotaxis system is similar to that of *E. coli* (22). *H. pylori* has the core signaling complex proteins, CheW, CheA and CheY, and disruption of any of these core proteins renders *H. pylori* nonchemotactic (5, 15, 28). *H. pylori* has three membrane bound chemoreceptors, TlpA, TlpB, TlpC, and one cytoplasmic chemoreceptor, TlpD (22). TlpA has been shown to sense arginine and bicarbonate (7), and TlpB has been shown to sense pH (9) and the quorum sensing molecule, autoinducer-2 (AI-2) (30). TlpD is involved in energy taxis (35) and the ligands for TlpC are unknown.

Individual *H. pylori* strain SS1 chemoreceptor mutants are able to colonize the mouse stomach to wild-type levels (2, 27), however in co-infections with wild type *H. pylori* in mice, mutants lacking TlpA or TlpC have a colonization defect (2), while those lacking TlpB have no defect (23, 45). This phenotype is less severe than that of fully non-chemotactic *H. pylori* SS1 mutants (Che^-) that lack core-signaling components such as CheW, CheA or CheY. These Che^- mutants have colonization defects both when they are the sole infecting strain and in a co-infection model (39). In the single-strain infection, colonization of Che^- mutants is not different from wild type after three weeks

post inoculation, but defects are apparent within the first two weeks (39). In the first two weeks of infection, Che$^-$ mutants have a striking inability to colonize the antrum, while occupying the corpus at only modestly decreased levels as compared to those of wild type (39). Thus far, it is unknown why antral localization requires chemotaxis. Chemotaxis may be necessary to locate the antrum or to maintain colonization there, and one of the four chemoreceptors may be specifically responsible for the localization defects.

Since *H. pylori* infections are associated with antral gastritis (3, 19, 41) we found it interesting that bacterial chemotaxis both drives antral localization (39) and increases the inflammatory response to *H. pylori* (23, 32, 45). Therefore, we undertook this study to determine if chemotaxis is necessary for *H. pylori* to locate the antrum or to remain there after initial colonization and to determine which chemoreceptor is responsible for this localization phenotype.

2.3. Experimental procedures

2.3.1. *H. pylori* strains and growth conditions

H. pylori strain SS1 (20) and its isogenic mutants were used for all studies. SS1 was a gift of Jani O'Rourke (University of New South Wales) and was minimally lab passaged before our experiments. SS1 *ΔcheY::cat, ΔtlpA::cat, ΔtlpB::cat, ΔtlpC::cat,* and *ΔtlpD::cat* were created previously (2, 23, 39, 45) and all have most of the target gene replaced with the *Campylobacter cat* gene. *H.*

pylori was cultured on Columbia blood agar (Remel) with 5% difibrinated horse blood (Hemostat Labs, Davis, CA), 50 μg/ml cycloheximide, 10 μg/ml vancomycin, 5 μg/ml cefsulodin, 2.5 Units/ml polymyxin B, and 0.2% β-cyclodextrin. Mouse stomach samples were plated on the same medium plus 5μg/ml trimethoprim, 8 μg/ml amphotericin B, 10 μg/ml nalidixic acid and 200 μg/ml bacitracin. To prepare *H. pylori* for mouse infection, we grew the bacteria shaking in brucella broth (Becton, Dickinson and Company) with 10% fetal bovine serum (FBS, Gibco) (BB10). Cultures were incubated at 37°C with 7-10% O_2, 10% CO_2, and 80-83% N_2, with chloramphenicol at 13 μg/ml to select for the various mutants as needed. For mouse infection, we inoculated animals orally intragastrically via a 20g x 1.5 inch feeding needle with 500 μl containing ~ 1 x 10^7 CFU/mL brucella broth-grown *H. pylori*.

2.3.2. Animal infections

The University of California, Santa Cruz Institutional Animal Care and Use Committee approved all animal protocols and experiments. Female C57Bl/6N mice (*Helicobacter*-free, Taconic Labs, Germantown, NY) and female and male FVB/N (*Helicobacter*-free, Charles River Laboratories) were housed at the animal facility of the U.C. Santa Cruz. Mice were between 6-8 weeks old at the time of *H. pylori* infection and age-matched uninfected mice were included in all experiments. After the infection period, the animals were sacrificed via CO_2

narcosis, the stomach dissected, opened along the lesser curvature and divided into four parts—the corpus, the transition zone, the antrum, and the upper duodenum (Fig. 2.1.). The nonglandular forestomach was identified as a yellow, thin tissue structure; it was removed from the stomach and not included in experimental analysis. The corpus is a brownish, thick walled section of tissue, and the antrum is a paler, pinkish, thinner walled section. The transition zone is an ~ 1.0 mm wide region demarcating these two sections. These regions were identified as described in Lee *et al* (21). The tissue pieces were homogenized using the Bullet Blender (Next Advance) with 1.0 mm Zirconium Silicate beads and plated to determine the number of *H. pylori* CFU/gram of stomach.

2.3.3. Histology and pathology

Mice infected for six months had their stomachs removed and half of the stomach was placed in a histology cassette with a sponge (Fisher) and preserved Buffered formalin (Fisher). The tissue was embedded in paraffin, sectioned (5 μm), stained with hematoxylin and eosin, and evaluated blindly by a pathologist (J.E. Carter). Each stomach slice received five separate grades, one each for the cardia, antrum, and pylorus, and two for the corpus. Each slide was evaluated twice. Lymphocytic infiltration was scored as outlined by Eaton et al (12), using scores of 0, no infiltrate; 1, mild, multifocal infiltration; 2 mild, widespread infiltration; 3, mild widespread and moderate multifocal infiltration; 4,

moderate, widespread infiltration; and 5, moderate, widespread and severe multifocal infiltration. Neutrophils were noted as either present or absent. Gastric atrophy was assessed using the method of Rugge *et al* (33) but was not present in any sample.

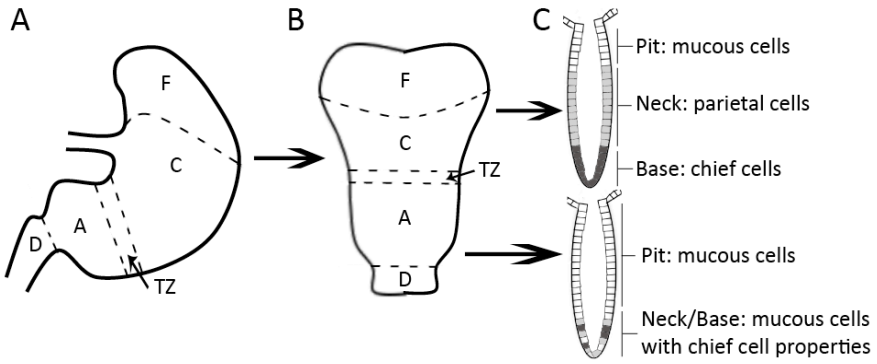

Figure 2.1. A cartoon representation of the different physiological regions of the stomach (21). **(*A*)** Side view of the stomach regions. **(*B*)** The stomach is opened up along the lesser curvature and divided down the middle along the longitudinal axis. **(*C*)** Representation of the different cell types found in the glands of the antrum and the corpus. F, forestomach; C, corpus; TZ, transition zone; A, antrum; D, duodenum.

2.4. Results

2.4.1. Chemotaxis is necessary for *H. pylori* to remain in the antrum after infection has established.

Our lab reported previously that Che$^-$ *H. pylori* are missing from the murine antrum at two weeks post-inoculation, as compared to wild-type *H. pylori* (39). This finding is consistent with chemotaxis either directing the bacteria to initially locate the antrum or for allowing the bacteria to remain in

the antrum after infection has been established. To determine at what point chemotaxis was needed in infection, we examined the numbers of wild-type and Che$^-$ *H. pylori* in the corpus, transition zone, and antrum at very early time points (14 hours) as compared to later time points post inoculation. For our first time point we only wanted to enumerate stably infecting bacteria, so we chose 14 hours post-inoculation, a time well after the three hours required for the mouse stomach to empty from one feeding (38). At 14 hours post inoculation, Che$^-$ bacteria were found in numbers that did not differ significantly from those of wild type in both the transition zone and antrum, indicating Che$^-$ mutants did not have a substantial initial colonization defect for these regions (Fig. 2.2 *A* - *C*). Interestingly, by 36 hours post inoculation, Che$^-$ *H. pylori* had undergone only a modest increase in numbers compared to the substantial increase in wild-type numbers, and thus Che$^-$ colonization levels were significantly lower in the transition zone and the antrum. We observed that this phenotype remained at one week post-inoculation (Fig. 2.2 *A* - *C*), similar to what we observed previously at two weeks (39). These results suggest that chemotaxis is modestly needed for the initial seeding of the antrum and the transition zone to a lesser degree, but is very important during the increase in *H. pylori* numbers that occurs from 14 hours to one week post inoculation in these regions.

In the corpus, Che$^-$ *H. pylori* colonization levels were somewhat lower at 14 hours and remained so at 36 hours, suggesting that chemotaxis plays a role in

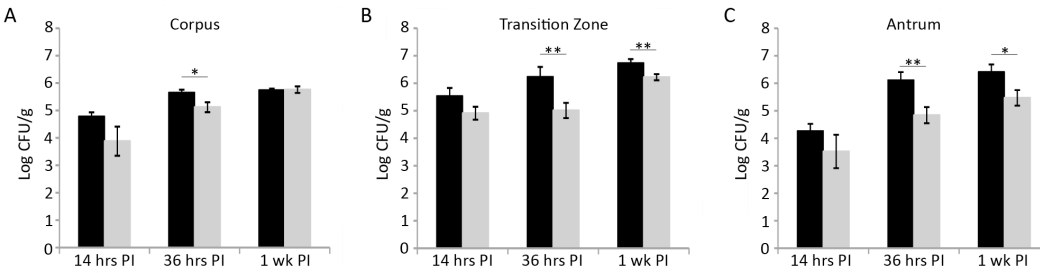

Figure 2.2. Chemotaxis is required for antral colonization at time points after 14 hours post inoculation. Female FVB/N mice were infected with SS1 wild type (black bars) or isogenic Che$^-$ (grey bars) for 14 hours, 36 hours, or 1 week. At each time point, stomachs were removed, and divided into three pieces: the corpus **(*A*)**, the transition zone **(*B*)**, and the antrum **(*C*)** and plated. *H. pylori* colonies were counted. Error bars indicate standard error of the mean. N=8 or 9 for 14 and 36 hours; derived from two independent infections. N=7 for 1 week; derived from one independent infection. *p<0.05, **p<0.01, Student T Test.

the initial seeding of this stomach region. Between 36 hours and one week, numbers of both Che$^-$ and wild-type *H. pylori* increased, such that they were nearly equal at one-week post inoculation (Fig. 2.2 *A* - *C*). Thus it seems that chemotaxis is not needed for bacterial multiplication in the corpus.

We also examined the upper duodenum to identify if bacteria were washed out of the stomach into the duodenum. However, *H. pylori* colonies rarely grew from the duodenal samples, suggesting that *H. pylori* are dead, unculturable, or present in the duodenum at numbers below our limit of detection (~200 colony forming units per gram) (data not shown).

We used the first two time points, 14 and 36 hours post inoculation, to estimate *H. pylori's* doubling time early in infection. Wild-type *H. pylori* double approximately every 6.5 or 8 hours in the corpus and the transition zone,

respectively, yet do considerably better in the antrum, doubling every 3 hours (Fig. 2.3 *A*; Table 2.1). Similar to wild type, the Che$^-$ mutant doubles approximately every 5.5 hours in the corpus; however, in the antrum Che$^-$ doubles approximately every 5 hours, which is nearly two times slower than wild type in this region. Additionally, the Che$^-$ mutant does not double in the transition zone over this time period (Fig. 2.3 *A*; Table 2.1). These data further indicate that chemotaxis is necessary for growth in the transition zone and the antrum.

			Corpus	**Transition Zone**	**Antrum**
14 hours PI[a,b]	Single	WT	4.79 ± 0.15	5.53 ± 0.30	4.26 ± 0.27
		ΔCheY	4.10 ± 0.34	4.91 ± 0.24	3.77 ± 0.40
	Competition	WT	4.85 ± 0.20	6.24 ± 0.20	5.38 ± 0.29
		ΔCheY	3.86 ± 0.19	5.21 ± 0.19	4.16 ± 0.65
36 hours PI[a,b]	Single	WT	5.65 ± 0.11	6.23 ± 0.36	6.11 ± 0.30
		ΔCheY	5.12 ± 0.18	5.01 ± 0.28	4.84 ± 0.29
	Competition	WT	6.20 ± 0.15	6.38 ± 0.24	6.05 ± 0.44
		ΔCheY	5.39 ± 0.23	4.79 ± 0.05	4.08 ± 0.24
Doubling Time[c]	Single	WT	6.46	7.87	3.00
		ΔCheY	5.47	57.29	5.20
	Competition	WT	5.28	49.49	10.55
		ΔCheY	4.63	No growth	No growth

Table 2.1. Colonization levels and doubling times for *H. pylori* SS1 or its isogenic Che$^-$ (ΔCheY) mutant early after infection. Data are also shown in Fig. 2.3 *A*.

[a] Log CFU/g stomach tissue

[b] Average ± standard error of the mean

[c] Doubling time = (22 hours)/((log CFU/g$^{36\ h}$ - log CFU/g$^{14\ h}$)/log(2))

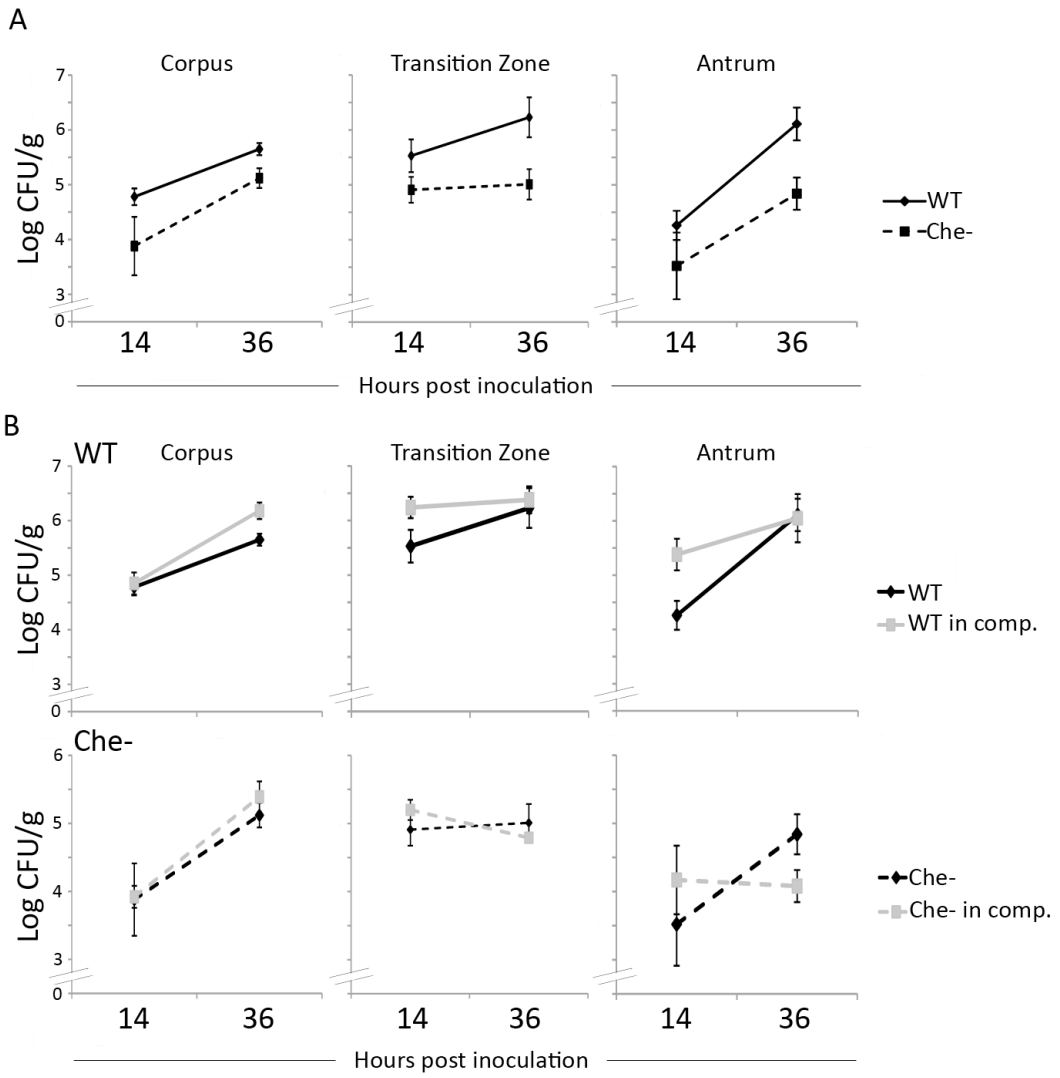

Figure 2.3. Chemotaxis allows *H. pylori* to grow more quickly in the antrum and provides and advantage in a competition infection. (*A*) Female FVB/N mice were infected with SS1 wild type (solid line) or isogenic Che- (dotted line) for 14 or 36 hours. At each time point stomachs were removed and divided into three pieces: the corpus, the transition zone, and the antrum and plated to determine the number of *H. pylori*. N= 8 or 9 for wild type and Che- for all time points, derived from two independent infections. **(*B*)** Competition experiments were carried out by infecting female FVB/N mice with a 1:1 ratio of wild type and Che- for 14 or 36 hours. At each time point, stomachs were removed, divided, and plated as in part A. Black lines represent each strain in single infection, as in part A, grey lines indicate the strains in competition. N=5 for wild type and Che- for all time points, derived from one experiment. Error bars represent standard error of the mean.

2.4.2. Competition with wild-type *H. pylori* exacerbates Che$^-$ *H. pylori* survival defect in the antrum.

We also determined how chemotaxis aids stomach region colonization under conditions where this process is more important—the competition infection—at the two earliest time points. For these experiments, we infected mice with a mixture of equal amounts of wild-type and Che$^-$ *H. pylori* and assessed numbers of each strain at 14 and 36 hours post inoculation as above. Generally speaking, the numbers of both wild type and Che$^-$ were not affected by the presence of the other in the corpus and transition zone at 14 or 36 hours (Fig. 2.3 *B*). One possibility is that the total bacterial numbers of both strains are below the threshold at which competition has an effect, or alternatively that conditions that result in a competitive defect do not exist at these early infection times. The antrum represented a different situation. In this region, numbers of Che$^-$ *H. pylori* were dramatically affected by the wild-type strain, particularly at 36 hours post inoculation (Fig. 2.3 *B*). In the antrum, the Che$^-$ mutant did not increase in numbers at all in this competition experiment (Fig. 2.3 *B*; Table 2.1), supporting the idea that chemotaxis greatly facilitates bacterial survival or growth in this region.

2.4.3. Enhanced inflammatory responses may contribute to Che- antral localization defects.

Several studies have reported that the majority of gastritis cases are antral dominant in humans (3, 19, 41). Since chemotaxis is necessary for *H. pylori* to remain in the antrum after infection has been established, we wondered whether antral immune responses make this localization unfavorable for Che- *H. pylori.* Reports on the location of gastritis in mice suggest that there is increased inflammation in the C-A transition zone and the antrum at six months post-inoculation (20), and so we sought to examine if inflammation specifically in the antrum correlates with reduced Che- colonization. Inflammation is not

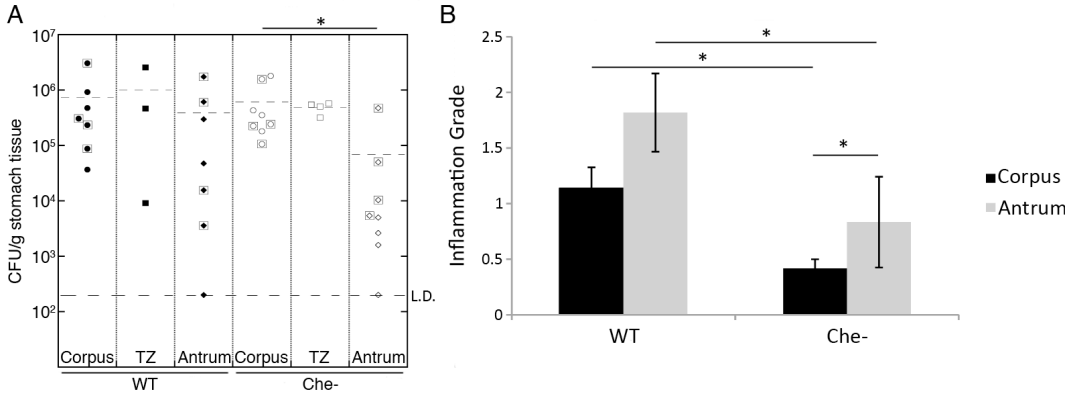

Figure 2.4. The antrum harbors worse inflammation and reduced *H. pylori* colonization. (*A*) Female C57BL/6N mice were infected for three (symbols surrounded by boxes) or six months (symbols without boxes) with *H. pylori* strain SS1 or the isogenic Che- mutant. The stomach was divided into the corpus, transition zone (6 months only), and antrum, and then plated to determine *H. pylori* colonies. N=7 for wild type, N=8 for Che-. **(*B*)** Gastric tissue was analyzed by a pathologist and graded for inflammation. Error bars indicate standard error of the mean. L.D.=Limit of detection. N=5 for wild type and Che-. *p<0.05, Student T Test.

detectable until late in mouse infection (13), so we examined inflammation and colonization levels in each physiologic region of stomachs from mice infected with wild-type or Che$^-$ *H. pylori* for three or six months. At these time points, we found that wild-type *H. pylori* induces more inflammation than Che$^-$ overall, as reported previously (Fig. 2.4 *B*) (45). Inflammation in the antrum was higher in both infection types as compared to the corpus (Fig. 2.4 *B*). Additionally, we noted that Che$^-$ strains continue to struggle to colonize the antrum (Fig. 2.4 *A*). Thus it appears that the antrum has significantly more inflammation than the corpus in infections of both strains and the antrum is significantly more challenging for Che$^-$ *H. pylori* to colonize.

2.4.4. The chemoreceptor TlpD is required for growth and/or survival in the antrum.

To help distinguish the signals required for colonization of the corpus versus the antrum, we next investigated whether individual chemoreceptor mutants had any distinct antrum or corpus colonization defects. Toward this end, we infected mice with either SS1 *ΔtlpA::cat*, SS1 *ΔtlpB::cat*, SS1 *ΔtlpC::cat*, or SS1 *ΔtlpD::cat* and examined the colonization levels of each mutant two weeks post-inoculation in the corpus and the antrum. As observed previously at this time point (39), the Che$^-$ mutant colonization levels in the antrum were significantly below that of wild type (Fig. 2.5). Loss of one receptor, TlpD, came

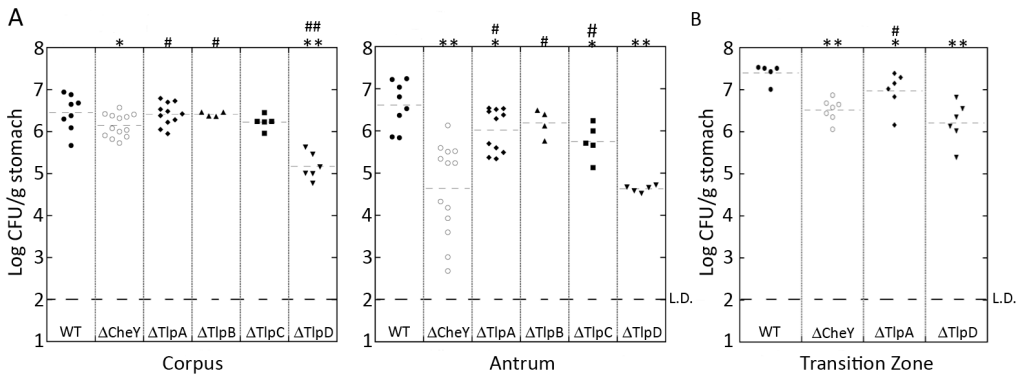

Figure 2.5. The chemoreceptor TlpD is necessary for antral colonization. FVB/N mice were infected with wild type, Che$^-$, TlpA$^-$, TlpB$^-$, TlpC$^-$, or TlpD$^-$ for 2 weeks, at which time the stomachs were removed, divided into **(*A*)** two pieces, the corpus and the antrum, or **(*B*)** three pieces including the transition zone and plated. *H. pylori* colonies were counted. N is between 4 and 13. L.D., limit of detection. *p<0.05, **p<0.0001 from wild type. #p<0.05, ##p<0.0001 from Che$^-$, Student T Test.

the closest to phenocopying the antral colonization defect observed in the Che$^-$ mutant (Fig. 2.5 *A*). In contrast, mutants lacking chemoreceptors TlpA, TlpB or TlpC had only a slight defect in antral localization (Fig. 2.5 *A*). To confirm these results we repeated the experiment and included the transition zone. In this independent infection, we again observed that the TlpD mutant had a significant antral colonization defect (Fig. 2.5 *A*) as well as a defect in colonizing the transition zone (Fig. 2.5 *B*). These findings suggest that the TlpD chemoreceptor is needed for *H. pylori* to flourish in the antrum and transition zone.

Interestingly, we also observed the *ΔtlpD* mutant had a significant colonization defect in the corpus (Fig. 2.5 *A*), which was not observed with any other chemoreceptor mutant and was more significant than the slight colonization defect of the Che$^-$ strain in the corpus (Fig. 2.5 *A*). Because of the colonization

defect in the corpus, we also compared the corpus colonization to the antral colonization to ensure that the defect of the *ΔtlpD* mutant was due to a localization defect and not an overall colonization defect (Table 2.2). This analysis showed that the TlpD mutant had a corpus:antrum ratio of 5.2, significantly higher than that of wild type (0.55) and similar to that of Che$^-$ (12) (Table 2.2). Thus, the TlpD mutant came the closest of all the receptor mutants to phenocopying Che$^-$, consistent with TlpD driving normal *H. pylori* antral localization.

Strain	Time PI	C/A Ratio	Range
WT	36 hours	0.92	0.04 - 8.08
ΔCheY	36 hours	1.05	0.29 - 18.0
WT	2 weeks	0.55	0.04 - 3.71
ΔCheY	2 weeks	12.0	2.08 - 1117.74
ΔTlpA	2 weeks	1.90	0.57 - 15.62
ΔTlpB	2 weeks	1.39	0.75 - 4.96
ΔTlpC	2 weeks	2.30	1.75 - 6.76
ΔTlpD	2 weeks	5.19	1.10 - 507.35
WT	6 months	1.88	0.13 - 437.50
ΔCheY	6 months	8.96	3.32 - 2158.27

Table 2.2. Ratio of CFU/g in the corpus (C) to the antrum (A). Data are also presented in Figures 2.3 - 2.5.

2.5. Discussion

We report here that bacterial chemotaxis promotes initial organ seeding in some stomach regions, and the ability to rapidly multiply in others. Specifically, we find that *H. pylori* chemotaxis is needed to guide *H. pylori* to the corpus, but not the antrum or transition zone, but once in the corpus, chemotaxis

is not needed for bacterial replication. Thus, despite typically starting at a lower colonization in the corpus, Che$^-$ mutants multiply to rapidly achieve near wild-type numbers. The situation is different in the antrum and transition zone, where chemotaxis is required for the bacteria to thrive. In these niches, Che$^-$ mutant numbers do not rise at the same rate as do those of wild type, and by one-week post inoculation the Che$^-$ mutants are found in significantly lower numbers. The main chemoreceptor that allows *H. pylori* to thrive in the antrum is TlpD, with the other chemoreceptors playing minor roles.

The development of *H. pylori*-induced disease depends of the sub-organ localization of inflammation: gastritis in the antrum predisposes patients to duodenal ulcer, while gastritis in the corpus predisposes patients to gastric ulcers and cancer (3, 41). While it is unknown why inflammation develops in different stomach regions, one explanation could be that different *H. pylori* strains target specific gastric regions (1). The mouse stomach has four distinct physiological regions: the forestomach, the corpus, the C-A transition zone, and the antrum (Fig. 2.1) (21). Each region is defined by the composition of its glands. The corpus is more complex than the antrum, and is made up of glands that contain mainly mucous, parietal, and chief cells, while the antrum is made up almost entirely of mucous cells, with a few cells that have chief cell properties at the base of the glands. The transition zone is a mixture of these two (Fig. 2.1) (21, 27). Mucous cells throughout the stomach secrete mucin and other peptides

with luminal protective functions. Mucous cells also spontaneously release abundant superoxide anion (O_2-), an oxygen radical (40). Interestingly, parietal cells are enriched in mRNAs encoding free radical scavengers such as peroxiredoxin, glutathione peroxidase, mitochondrial superoxide dismutase, and catalase (26). These differences suggest that the corpus may have lower levels of damaging reactive oxygen species (ROS) than the antrum. Parietal cells also secrete concentrated HCl, which may result in a lower pH in the corpus than in the antrum. Lastly, the cells in the antrum have a much higher turnover rate than those in the corpus (16). Thus the different regions of the stomach possess distinct physiological characteristics that likely present *H. pylori* with different chemotactic signals.

Our studies presented here demonstrate that chemotaxis does not help *H. pylori* locate the antrum but does help it achieve normal bacterial numbers in this region. This finding suggests that some parameter of the antrum is particularly difficult for *H. pylori* and chemotaxis helps to overcome this challenge. We report here that one potentially challenging condition is the elevated inflammation found in the antrum, which we could detect at three to six months of infection. We do not yet know if early inflammatory events in the antrum render this area difficult to grow in early in infection, but this possibility is consistent with our data.

Based on this information we envision two possibilities: 1) chemotaxis allows *H. pylori* to locate a nutrient source necessary for growth and survival in the antrum or 2) chemotaxis allows *H. pylori* to detect and move away from damaging components of the immune response. Increased inflammation could amplify the necessity for chemotaxis in either situation, as inflammation alters the nutrient status by, for example, chelating critical metals such as iron, zinc and manganese in a process known as "nutritional immunity" (8, 18), and inflammation also increases production of ROS during the host's strong oxidative stress response (4). *H. pylori* depends on many enzymes, such as SodB, catalase, AhpC, MdaB and NapA (17, 44) to protect itself against the host's oxidative stress response and concurrent production of ROS (4) suggesting that avoiding ROS is a critical part of *H. pylori* survival in the stomach.

To help us determine the nature of the chemotactic signal required for growth or survival in the antrum, we investigated which chemoreceptor was responsible for antral localization. *H. pylori* has four chemoreceptors, TlpA, TlpB, TlpC, and TlpD: TlpA senses arginine and bicarbonate (7), TlpB senses protons (9) and AI-2 (30), TlpD is involved in energy taxis (35), and the ligands for TlpC are unknown. In mouse infections, *ΔtlpA*, *ΔtlpB* and *ΔtlpC* mutants each had a moderate antral colonization defect, with colonization levels that were between those of wild type and Che$^-$ mutant. We were surprised not to detect a localization defect in the *ΔtlpB* mutant, since acid helps determine *H. pylori*

localization in the stomach (37) and TlpB senses pH (9). While pH gradients have been shown to impact *H. pylori's* orientation in the mucous (34), our results suggest that pH sensing by TlpB does not contribute to *H. pylori* localization in the antrum after infection has been established. However, we do not know if TlpB contributes to the initial seeding of the corpus.

The *ΔtlpD* mutant phenocopied the Che$^-$ mutant for reduced colonization in the antrum, suggesting that TlpD plays the dominant role in *H. pylori's* antral colonization. Also similar to the Che$^-$ mutant, the *ΔtlpD* mutant had a colonization defect in the transition zone. Interestingly, the *ΔtlpD* mutant had a colonization defect in the corpus, a phenotype that was not observed in the nonchemotactic mutant. Although we do not yet know why TlpD mutants experience such a corpus challenge, it is possible that without TlpD the bacteria move toward harmful conditions due to activity of another chemoreceptor, and so are killed.

TlpD is the only cytoplasmic chemoreceptor in *H. pylori* (35). Previous work showed that *tlpD* mutants display near wild-type mouse colonization and inflammation (45). Current evidence suggests that TlpD senses cellular energy levels (35), thus it seems plausible that to remain colonized in the antrum, *H. pylori* requires TlpD to find optimal energy-generating conditions. One possibility is that increased antral inflammation reduces the metabolically optimal area for *H. pylori* growth. Inflammation has been tied to the presence of

new respiratory electron acceptors in *Salmonella* infection. In this case, inflammation encourages wild-type *Salmonella* growth by creating new respiratory electron acceptors through the presence of ROS, which can alter thiosulphate to form tetrathionate (46). In the case of *H. pylori*, it may be that inflammation sequesters a specific nutrient. A second possibility is that TlpD-driven chemotaxis is necessary to locate increasingly limited nutrient supplies as inflammation creates a nutrient-deficient environment. For example, neutrophil-derived calprotectin chelates Mn^{2+} and Zn^{2+} to inhibit *Staphylococcus aureus* growth (8). TlpD has been shown to bind zinc (11), however, the function of zinc remains unclear.

Another possibility is that TlpD senses and directs a repellent response to a deleterious component of the immune system, allowing *H. pylori* to escape and survive. Wild-type *H. pylori,* but not *ΔtlpD,* has a repellent response to the presence of H_2O_2, a major contributor to oxidative damage (S. M. Williams and K. M. Ottemann, personal communication). In this scenario, *ΔtlpD* cannot sense the increased production of ROS in the antrum, which subjects the bacteria to ROS damage. Supporting this possibility, *H. pylori* fur mutants are predicted to be more sensitive to oxidative damage because they poorly express the SodB superoxide disumutase (10, 14) and are unable to colonize the antrum (24).

In summary, we have shown that chemotaxis plays distinct roles in colonizing specific stomach regions, suggesting there are subtle chemotactic

cues that vary across this organ. In the corpus, chemotaxis is needed for initial seeding but not for subsequent growth. In the antrum, chemotaxis is not needed for initial seeding but is necessary for *H. pylori* to flourish after infection has established. Moreover, this ability depends on the function of the cytoplasmic chemoreceptor, TlpD. We hypothesize that antral success requires detection of a limited energy source and/or movement away from deleterious immune responses.

2.6. Acknowledgements

I would like to thank James Shanks for his assistance with experiments covered in figures 2.2 and 2.3 and tables 2.1 and 2.2. I would also like to thank Dr. J. Elliot Carter for his expertise in pathology and his contribution to figure 2.4 *B*. I would also like to acknowledge Susan Williams and Marla Hill for experimental assistance. The described project was supported by Grant Number AI050000 (to K.M.O.) from the National Institutes of Allergy and Infectious Disease (NIAID) at the National Institutes of Health. Its contents are solely the responsibility of the authors and do not necessarily represent the official views of the NIH.

2.7. References

1. **Akada J. K.** 2003. Helicobacter pylori tissue tropism: mouse-colonizing strains can target different gastric niches. Microbiology **149**:1901-1909.

2. **Andermann T. M., Y.-T. Chen, and K. M. Ottemann**. 2002. Two Predicted Chemoreceptors of Helicobacter pylori Promote Stomach Infection. Infection and Immunity **70**:5877-5881.

3. **Atherton J. C.** 2006. The pathogenesis of Helicobacter pylori-induced gastro-duodenal diseases. Annual Review of Pathology **1**:63-96.

4. **Baik S.-C., H.-S. Youn, and M.-H. Chung**. 1996. Increased Oxidative DNA Damage in Helicobacter pylori -infected Human Gastric Mucosa. Cancer Res **56**:1279-1282.

5. **Beier D., G. Spohn, R. Rappuoli, and V. Scarlato**. 1997. Identification and characterization of an operon of Helicobacter pylori that is involved in motility and stress adaptation. Journal of Bacteriology. Am Soc Microbiol **179**:4676.

6. **Bijlsma J. J. E., B. Waidner, A. H. van Vliet, N. J. Hughes, S. Häg, S. Bereswill, D. J. Kelly, C. M. J. E. Vandenbroucke-grauls, M. Kist, and J. G. Kusters**. 2002. The Helicobacter pylori Homologue of the Ferric Uptake Regulator Is Involved in Acid Resistance. Infection and Immunity **70**:606-611.

7. **Cerda O., A. Rivas, and H. Toledo**. 2003. Helicobacter pylori strain ATCC700392 encodes a methyl-accepting chemotaxis receptor protein (MCP) for arginine and sodium bicarbonate. FEMS Microbiology Letters **224**:175-181.

8. **Corbin B. D., E. Seeley, A. Raab, J. Feldmann, M. R. Miller, V. Torres, K. Anderson, B. Dattilo, P. Dunman, R. Gerads, R. Caprioli, W. Nacken, W. Chazin, and E. Skaar**. 2008. Metal Chelation and Inhibition of Bacterial Growth in Tissue Abscesses. Science **319**:962-965.

9. **Croxen M. A., G. Sisson, R. Melano, and P. S. Hoffman**. 2006. The Helicobacter pylori chemotaxis receptor TlpB (HP0103) is required for pH taxis and for colonization of the gastric mucosa. Journal of Bacteriology **188**:2656-65.

10. **Delany I., G. Spohn, R. Rappuoli, and V. Scarlato**. 2001. The Fur repressor controls transcription of iron-activated and -repressed genes in Helicobacter pylori. Molecular Microbiology **42**:1297-1309.

11. **Draper J., K. Karplus, and K. M. Ottemann**. 2011. Identification of a chemoreceptor zinc-binding domain common to cytoplasmic bacterial chemoreceptors. Journal of Bacteriology **193**:4338-45.

12. **Eaton K. A., M. J. Radin, and S. Krakowka**. 1995. An Animal Model of Gastric Ulcer Due to Bacterial Gastritis in Mice. Veterinary Pathology **32**:489-497.

13. **Eaton K. A., S. J. Danon, S. Krakowka, and S. E. Weisbrode**. 2007. A Reproducible Scoring System for Quantification of Histologic Lesions of Inflammatory Disease in Mouse Gastric Epithelium. Comparative Medicine **57**:57-65.

14. **Ernst F. D., G. Homuth, J. Stoof, U. Mäder, B. Waidner, E. J. Kuipers, M. Kist, G. Kusters, S. Bereswill, and A. H. M. V. Vliet**. 2005. Iron-Responsive

Regulation of the Helicobacter pylori Iron-Cofactored Superoxide Dismutase SodB Is Mediated by Fur. Journal of Bacteriology **187**:3687-3692.

15. **Foynes S., N. Dorrell, S. J. Ward, R. A. Stabler, A. A. M. C. Colm, A. N. Rycroft, and B. W. Wren**. 2000. Helicobacter pylori Possesses Two CheY Response Regulators and a Histidine Kinase Sensor, CheA, Which Are Essential for Chemotaxis and Colonization of the Gastric Mucosa. Infection and Immunity **64**:2016-2023.

16. **Hansen O., T. Pedersen, and J. Larsen**. 1976. Cell proliferation kinetics in normal human gastric mucosa. Gastroenterology **70**:1051-1054.

17. **Harris A., J. Wilson, S. Danon, M. Dixon, K. Donegan, and S. Hazell**. 2003. Catalase (KatA) and KatA-associated protein (KapA) are essential to persistent colonization in the Helicobacter pylori SS1 mouse model. Microbiology **149**:665-672.

18. **Kehl-Fie T. E., and E. P. Skaar**. 2010. Nutritional immunity beyond iron: a role for manganese and zinc. Current Opinion in Chemical Biology. Elsevier Ltd **14**:218-224.

19. **Kuipers E. J.** 1998. Review article: relationship between Helicobacter pylori, atrophic gastritis and gastric cancer. Alimentary Pharmacology and Therapeutics **12**:25-36.

20. **Lee A., J. O'Rourke, M. C. De Ungria, B. Robertson, G. Daskalopoulos, and M. F. Dixon**. 1997. A standardized mouse model of Helicobacter pylori infection: introducing the Sydney strain. Gastroenterology **112**:1386-97.

21. **Lee E., J. Trasler, S. Dwivedi, and C. Leblond**. 1982. Division of the mouse gastric mucosa into zymogenic and mucous regions on the basis of gland features. The American Journal of Anatomy **164**:187-207.

22. **Lertsethtakarn P., K. M. Ottemann, and D. R. Hendrixson**. 2011. Motility and Chemotaxis in Campylobacter and Helicobacter. Annual Review of Microbiology **65**:389-410.

23. **McGee D., M. Langford, E. Watson, and JE**. 2005. Colonization and inflammation deficiencies in Mongolian gerbils infected by Helicobacter pylori chemotaxis mutants. Infection and Immunity **73**:1820-1827.

24. **Miles S., M. B. Piazuelo, C. Semino-Mora, M. K. Washington, A. Dubois, R. M. Peek, P. Correa, and D. S. Merrell**. 2010. Detailed In Vivo Analysis of the Role of Helicobacter pylori Fur in Colonization and Disease. Infection and Immunity **78**:3073-3082.

25. **Miller L. D., M. H. Russell, and G. Alexandre**. 2009. Diversity in Bacterial Chemotactic Responses and Niche Adaptation. Advances in Applied Microbiology **66**:53-75.

26. **Mills J. C., a J. Syder, C. V. Hong, J. L. Guruge, F. Raaii, and J. I. Gordon**. 2001. A molecular profile of the mouse gastric parietal cell with and without

exposure to Helicobacter pylori. Proceedings of the National Academy of Sciences of the United States of America **98**:13687-92.

27. **Mills J. C., and R. a Shivdasani**. 2010. Gastric Epithelial Stem Cells. Gastroenterology. Elsevier Inc. **140**:412-424.

28. **Pittman M. S., M. Goodwin, and D. J. Kelly**. 2001. Chemotaxis in the human gastric pathogen Helicobacter pylori: different roles for CheW and the three CheV paralogues, and evidence for CheV2 phosphorylation. Microbiology **147**:2493-2504.

29. **Polk D. B., and R. M. Peek**. 2010. Helicobacter pylori: gastric cancer and beyond. Nature Reviews Cancer. Nature Publishing Group **10**:403-14.

30. **Rader B. A., C. Wreden, K. G. Hicks, E. G. Sweeney, K. M. Ottemann, and K. Guillemin**. 2011. Helicobacter pylori perceives the quorum-sensing molecule AI-2 as a chemorepellent via the chemoreceptor TlpB. Microbiology **157**:2445-2455.

31. **Rieder G., J. L. Merchant, and R. Haas**. 2005. Helicobacter pylori cag-Type IV Secretion System Facilitates Corpus Colonization to Induce Precancerous Conditions in Mongolian Gerbils. Gastroenterology **128**:1229-1242.

32. **Rolig A. S., J. E. Carter, and K. M. Ottemann**. 2011. Bacterial chemotaxis modulates host cell apoptosis to establish a T-helper cell, type 17 (Th17)-dominant immune response in Helicobacter pylori infection. Proceedings of the National Academy of Sciences of the United States of America **108**:19749-19754.

33. **Rugge M., P. Correa, M. F. Dixon, R. Fiocca, T. Hattori, J. Lechago, G. Leandro, a B. Price, P. Sipponen, E. Solcia, H. Watanabe, and R. M. Genta**. 2002. Gastric mucosal atrophy: interobserver consistency using new criteria for classification and grading. Alimentary Pharmacology & Therapeutics **16**:1249-59.

34. **Schreiber S., M. Konradt, C. Groll, P. Scheid, G. Hanauer, H. O. Werling, C. Josenhans, and S. Suerbaum**. 2004. The spatial orientation of Helicobacter pylori in the gastric mucus. Proceedings of the National Academy of Sciences of the United States of America. National Acad Sciences **101**:5024.

35. **Schweinitzer T., T. Mizote, N. Ishikawa, A. Dudnik, S. Inatsu, S. Schreiber, S. Suerbaum, S.-ichi Aizawa, and C. Josenhans**. 2008. Functional characterization and mutagenesis of the proposed behavioral sensor TlpD of Helicobacter pylori. Journal of Bacteriology **190**:3244-55.

36. **Sipponen P., and H. Hyvarinen**. 1993. Role of Helicobacter pylori in the Pathogenesis of Gastritis, Peptic Ulcer and Gastric Cancer. Scand J Gastroenterol **28**:3-6.

37. **Syder A. J., J. D. Oh, J. L. Guruge, D. O'Donnell, M. Karlsson, J. C. Mills, B. M. Björkholm, and J. I. Gordon**. 2003. The impact of parietal cells on Helicobacter pylori tropism and host pathology: an analysis using gnotobiotic normal and transgenic mice. Proceedings of the National Academy of Sciences of the United States of America **100**:3467-72.

38. **Symonds E. L., R. N. Butler, and T. I. Omari**. 2000. Assessment of gastric emptying in the mouse using the [13C]-octanoic acid breath test. Clinical and Experimental Pharmacology and Physiology **27**:671-675.

39. **Terry K., S. M. Williams, L. Connolly, and K. M. Ottemann**. 2005. Chemotaxis Plays Multiple Roles during Helicobacter pylori Animal Infection. Infection and Immunity **73**:803-811.

40. **Teshima S., K. Rokutan, T. Nikawa, and K. Kishi**. 1998. Guinea pig gastric mucosal cells produce abundant superoxide anion through an NADPH oxidase-like system. Gastroenterology **115**:1186-96.

41. **Uemura N., S. Okamoto, S. Yamamoto, N. Matsumura, S. Yamaguchi, M. Yamakido, K. Taniyama, N. Sasaki, and R. J. Schlemper**. 2001. Helicobacter pylori infection and the development of gastric cancer. The New England Journal of Medicine **345**:784-789.

42. **Vliet A. H. van, J. Stoof, R. Vlasblom, S. A. Wainwright, N. J. Hughes, D. J. Kelly, S. Bereswill, J. J. E. Bijlsma, T. Hoogenboezem, M. J. E. Christina, M. Kist, E. J. Kuipers, and J. G. Kusters**. 2002. The Role of the Ferric Uptake Regulator (Fur) in Regulation of Helicobacter pylori Iron Uptake. Helicobacter **7**:237-244.

43. **Wadhams G. H., and J. P. Armitage**. 2004. Making sense of it all: bacterial chemotaxis. Nature Reviews Molecular Cell Biology **5**:1024-37.

44. **Wang G., P. Alamuri, and R. J. Maier**. 2006. The diverse antioxidant systems of Helicobacter pylori. Molecular Microbiology **61**:847-60.

45. **Williams S. M., Y.-ting Chen, T. M. Andermann, J. E. Carter, D. J. Mcgee, and K. M. Ottemann**. 2007. Helicobacter pylori Chemotaxis Modulates Inflammation and Bacterium-Gastric Epithelium Interactions in Infected Mice. Infection and Immunity **75**:3747-3757.

46. **Winter S. E., P. Thiennimitr, M. G. Winter, B. P. Butler, D. L. Huseby, R. W. Crawford, J. M. Russell, C. L. Bevins, L. G. Adams, R. M. Tsolis, J. R. Roth, and A. J. Bäumler**. 2010. Gut inflammation provides a respiratory electron acceptor for Salmonella. Nature **467**:426-429.

47. **Wroblewski L. E., R. M. Peek, and K. T. Wilson**. 2010. Helicobacter pylori and gastric cancer: factors that modulate disease risk. Clinical Microbiology Reviews **23**:713-39.

CHAPTER 3

Bacterial chemotaxis modulates host cell apoptosis to establish a Th17-dominant immune response in *Helicobacter pylori* infection

3.1. Abstract

The host inflammatory response to chronic bacterial infections often dictates the disease outcome. In the case of the gastric pathogen *Helicobacter pylori*, host inflammatory responses result in outcomes that range from moderate asymptomatic to more severe with concomitant ulcer or cancers. It was recently found that *H. pylori* chemotaxis mutants (Che^-), which lack directed motility but colonize to near wild-type levels, trigger less host inflammation. We utilized these mutants to observe host immune responses that resulted in reduced disease states. Here we report that these mutants are defective for early gastric recruitment of $CD4^+$ T cells as compared to wild-type infection. Furthermore, Che^- mutant infections lack the Th17 component of the immune response, as measured by cytokine mRNA levels in the gastric tissue, intracellular cytokine staining, and immunofluorescence. We additionally find that a Che^- mutant infection results in significantly less host cell apoptosis than does wild-type infection, in accordance with previous observations that Th17 responses in *Citrobacter rodentium* infections are driven by concomitant bacterial and apoptotic cell signals. We propose that bacterial chemotaxis allows *H. pylori* to access a particular host niche that allows the bacteria to express or

deliver pro-apoptotic host cell factors. This report is the first indicating that chemotaxis plays a role in enhancing apoptosis, suggesting bacterial chemotaxis systems might serve as therapeutic targets for infections whose symptoms arise from host cell apoptosis and tissue damage.

3.2. Introduction

Infection with the gastric pathogen *Helicobacter pylori* leads to chronic inflammation, or gastritis, in all infected individuals. This bacterium colonizes 50% of the world's population and triggers a wide range of disease severities; many infected individuals remain asymptomatic, but others develop peptic or gastric ulcers, gastric adenocarcinoma, or mucosa-associated lymphoid tumors (25).

The pathogenesis of *H. pylori*-induced inflammation is not well understood. Inflammation is promoted by both host factors (26) and *H. pylori* factors, such as the proteins CagA (25, 26) and VacA (7, 25) and bacterial chemotaxis (36). Chemotaxis is the bacterial ability to move toward beneficial environmental signals and away from harmful ones. *H. pylori* genetically altered to lack chemotaxis (Che^-) retain flagella and motility, but cannot migrate toward or away from environmental signals. In mouse models, these mutants have a marginal colonization defect (13, 33, 36) but induce less overall chronic inflammation (36). Specifically, Che^- mutants localize far from the epithelial surface and do not colonize the gastric glands robustly (13, 36), suggesting that chemotaxis-driven contact with epithelial cells, resident dendritic cells (DC), or monocytes promotes the inflammatory response to *H. pylori*.

Inflammation begins when resident monocytes and epithelial cells detect injury or a pathogen such as *H. pylori* (31). Epithelial cells secrete chemokines to recruit antigen presenting cells (APCs) such as DCs that will prime T cells (31). The newly recruited APCs define the immune response to *H. pylori* based on the nature of their contact with the pathogen, because the APCs produce cytokines that dictate the character of the adaptive immune response. DCs interacting with *H. pylori* fuel the proliferation of particular T cells, including Th1 cells (37), $CD25^{+}FoxP3^{+}$ T regulatory cells (T regs) (15, 37), and Th17 cells (16).

The inflammatory response to *H. pylori* includes all these T cell types. However, the roles of the Th17 cell and T reg cell populations during *H. pylori* infections have been debated recently. The Th17 cell is involved in promoting chronic inflammation (21, 29); the T reg cell, in contrast, regulates host immune responses. Th17 and T reg cells are developmentally related, and exist in a delicate balance (19) that can dictate the outcome of a bacterial infection (14). Evidence suggests that *H. pylori* pathogenesis primarily results from the immune response, and thus understanding how this immune response is initiated and controlled is critical. Currently it is unknown if a Th17 response (29) or a T reg response (15) underlies the ineffective immune response to *H. pylori*. Therefore we sought to better understand how *H. pylori* promotes gastritis by comparing the host immune cell and cytokine responses to wild-type *H. pylori* and a Che^{-} mutant. Our studies provide evidence that bacterially driven interactions with

host tissues alter the nature of the immune and pathological response generated during infection.

3.3. Experimental procedures

3.3.1. *H. pylori* strains and growth conditions

Helicobacter pylori strain SS1 (17) and its isogenic mutants were used for all studies. SS1 was a gift of Jani O'Rourke (University of New South Wales) and was minimally lab passaged before our experiments. SS1 *ΔcheY::cat* was created by replacing most of the *cheY* gene (HP1067) with the *Campylobacter cat* gene as described (33). *H. pylori* was cultured on Columbia blood agar (Difco) with 5% difibrinated horse blood (Hemostat Labs, Davis, CA), 50 μg/ml cycloheximide, and 0.2% β-cyclodextrin. Mouse stomach samples were plated on the same medium plus 5 μg/ml trimethoprim, 8 μg/ml amphotericin B, 10 μg/ml vancomycin, 5 μg/ml cefsulodin, 2.5 U/ml polymyxin B, 10 μg/ml nalidixic acid and 200 μg/ml bacitracin. For mouse infection, *H. pylori* was grown shaking in brucella broth (Difco) with 10% fetal bovine serum (FBS, Gibco). Cultures were incubated at 37°C with 7-10% O_2, 10% CO_2, and 80-83% N_2. To select for the *H. pylori cheY* mutant, chloramphenicol was used at 13 μg/ml.

3.3.2. Animal infections

The University of California, Santa Cruz Institutional Animal Care and Use Committee approved all animal protocols and experiments. Female C57Bl/6N mice (*Helicobacter*-free, Taconic Labs, Germantown, NY) were housed at the animal facility of U.C. Santa Cruz. Mice were between 6-8 weeks old at the time of *H. pylori* infection and age-matched uninfected mice were included in all experiments. Animals were inoculated orally intragastrically via a 20g x 1.5 inch feeding needle with 500 μl containing ~ 1 x 10^7 CFU/mL brucella broth-grown *H. pylori*. After the infection period, the animals were sacrificed via CO_2 narcosis, the stomach dissected, opened along the lesser curvature and divided into longitudinal strips for preservation and analysis. The tissue pieces were either, (1) homogenized using the Bullet Blender (Next Advance) with 1.0mm Zirconium Silicate beads and plated to determine the number of CFU/gram of stomach; (2) preserved in Optimal Cutting Temperature (OCT, Tissue Tek), snap frozen in liquid nitrogen and stored at -80°C for immunohistochemistry; (3) frozen in liquid nitrogen and stored at -80°C for quantitative RT PCR of cytokines; (4) stored in cold Hanks Balanced Salt Solution (HBSS, Lonza) to be used in flow cytometry experiments.

3.3.3. Immunohistochemistry/immunofluorescence

Immunohistochemical staining was performed on 6 μm frozen sections (Cryostat, Leica) mounted on glass slides (SuperFrost/Plus; Fisher). Sections

were fixed in 75% acetone/25% ETOH. Endogenous biotin activity was blocked using the Biotin Blocking System (DAKO) following manufacturer's protocols. Sections were incubated with monoclonal antibodies against CD4 or rat IgG2a isotype control (BD Pharmingen) for 1 hour at room temperature at a concentration of 0.625 μg/mL. Antibody staining was visualized using the Anti-Rat Ig HRP Detection Kit (BD Pharmingen) following manufactures' protocol. Sections were lightly counterstained with Gill's Hematoxylin (Fisher), dehydrated with ethanol and xylene and mounted with Permount (Fisher). For immunofluorescence, the following antibodies were used sequentially: rat anti-mouse IL-17A (BD Pharmingen), Alexa Fluor 488 goat anti-rat IgG (Invitrogen), rat anti-mouse CD4 (BD Pharmingen), and TRITC donkey anti-rat IgG (Jackson Immunoresearch Laboratories). In the immunofluorescence images (Fig. 3.5 and 3.8), the brightness and contrast were increased on the green channel.

3.3.4. Gastric tissue observation

3.3.4.1. Pathology

Gastric tissue preserved in OCT was sectioned, stained with hematoxylin and eosin and evaluated in a blind fashion by a pathologist (J.E. Carter). Each slide was evaluated twice. Lymphocytic infiltration was scored as outlined by Eaton et al (10). The scores are 0, no infiltrate; 1, mild, multifocal infiltration; 2 mild, widespread infiltration; 3, mild widespread and moderate multifocal

infiltration; 4, moderate, widespread infiltration; and 5, moderate, widespread and severe multifocal infiltration. Neutrophils were noted as either present or absent. Gastric atrophy was assessed using the method of Rugge et al (27) but was not present in any sample.

3.3.4.2. Specific cellular infiltrates

To evaluate immune cell infiltration and co-localization, sections were examined under 200x magnification (Nikon Eclipse E600 Microscope) and images of the tissue were captured with a Spot Insight 4 camera (Diagnostic Instruments, Inc). The immunohistochemistry images were subjected to analysis with Photoshop CS3 (Adobe). Photoshop identified each pixel in the image whose color matched that of positively stained cells (R: 75, G: 35, B: 46); the selection identifying the pixels was expanded to encompass the whole cell. The image was converted to a black (cells) and white (background) image and analyzed with Image J software (NIH) to count the number of positively stained cells present in using the 'Analyze Particles' function. Data are reported in numbers of cells per mm^2 of tissue. An ANOVA analysis was performed to determine that analysis of 10 images per slice, 7 stomach slices per mouse (70 images and an average of 14.1 μm^2 analyzed) provided a complete assessment of variance.

3.3.5. Flow cytometry

To prepare single cell suspensions, mouse stomachs were dissected, opened longitudinally along the lesser curvature and placed in cold HBSS (Lonza). The stomach was cut into 2 cm slices and incubated for 45 minutes at 37ºC in an HBSS solution supplemented with 10% FBS, 15mM HEPES, 5mM EDTA and 0.014% DTT. After, the tissue was rinsed with cold HBSS and incubated for 1 hour at 37ºC in 10 mL RPMI media with 10% FBS plus 1 mg/mL Dispase (Roche) and 0.25 mg/mL collagenase (Roche). The tissue was then gently massaged through a 40μm cell strainer (BD Biosciences), and the strainer was rinsed with 10mL cold HBSS. Then the cells were collected by centrifugation and incubated on ice with IgG (US Biological) to block non-specific binding. Single cell suspensions were then stained for CD3 and CD45, and CD4 or CD8. The optimal concentrations for the antibodies were determined in prior experiments to be 2 μg/mL for AlexaFlour488-CD3 (eBioscience), PeCy7-CD4 (eBioscience), APC/Cy-7-CD8 (Biolegend), and for AlexaFluor647-CD45 (Biolegend). An isotype control was included. Prior to analysis the cells were fixed in 2% paraformaldehyde. 50,000 cells were counted on a BD LSR II (BD Biosciences) and analyzed using FlowJo (BD Biosciences) software; results are presented as a percentage of the 50,000 cells counted. Mann-Whitney U test was used for statistical analysis.

3.3.6. Intracellular cytokine staining

For intracellular cytokine staining, gastric cells in a single cell suspension were stained with AlexaFluor647-CD45 and Propidium Iodide (PI), and then sorted on the BD FACSAria cell sorter (BD Biosciences) for $CD45^{+}PI^{-}$. The entire stomach from each mouse was sorted, resulting in different yields depending on infection type. After overnight incubation in DMEM (Cell Gro) plus 10% FBS (Gibco), 1x Pen Strep Glutamine (Gibco), 1M HEPES (Fisher), and 1x non-essential amino acid solution (Invitrogen) cells were stimulated for 4 hours with the Leukocyte Activation Cocktail (BD Biosciences) in a tissue culture CO_2 incubator at 37°C. Surface staining was performed with AlexaFlour488-CD3 (eBioscience), PeCy7-CD4 (eBioscience), and AlexaFluor647-CD45 (Biolegend). After surface staining, cells were resuspended in a fixation/permeablization solution kit (BD Cytofix/cytoperm, BD Biosciences) and intracellular staining was performed with PE-IL17A (BD Pharmingen) as per manufacturers' protocol.

3.3.7. Quantitative reverse transcriptase PCR

Quantitative analysis of the cytokines in the mouse stomach was performed by real-time PCR. RNA was isolated from mouse stomach samples using the TRIzol RNA isolation protocol (Gibco) and converted to cDNA using Superscript III First Strand Synthesis System (Invitrogen). The cDNA was measured in a qPCR reaction with SYBR green master mix (SAbioscience).

Primers used for qPCR are given in Table A1.1. Mammalian data were analyzed by the ΔΔ threshold cycle (Ct) method. All samples were analyzed in triplicate, along with no reverse transcriptase controls. The Mann Whitney U test was used for statistical analysis.

3.3.8. TUNEL assay

Samples used for the TUNEL assay were prepared from 14 μm thick OCT-frozen sections mounted on glass slides (SuperFrost/Plus, Fisher). Sections were fixed in 3.7% buffered formaldehyde (Fisher) then stained using the TACS 2 TdT-DAB *In Situ* Apoptosis Detection Kit (Trevigen) following the manufacturer's protocol. Tissue was counterstained with methyl green (Trevigen). To analyze apoptotic cells, numbers of positively stained cells were counted in 20 well-oriented glands in the corpus from 6 mice infected with WT, 6 mice infected with Che^-, and 3 uninfected mice. The Student T test was used for statistical analysis.

3.4. Results and Discussion

3.4.1. *H. pylori* chemotaxis increases inflammation two months after inoculation.

As stated above, Che- *H. pylori* cause milder inflammation than do wild-type infections after three to six months of colonization (36). To determine whether bacterial chemotaxis affected inflammation earlier, we examined inflammation at the earliest time inflammation was detectable, two months after inoculation. For these experiments, we orally infected mice with either wild-type *H. pylori* or an isogenic Che- mutant lacking a central chemotaxis protein, CheY. *H. pylori cheY* mutants have been characterized extensively and found to retain flagella and motility, but lack chemotaxis completely (23, 33). Che- mutants have early mouse colonization defects but achieve normal bacterial levels by one month after inoculation (3, 33). All *cheY* mutant-associated phenotypes can be complemented, indicating that loss of *cheY* is responsible for the chemotaxis and animal-colonization deficits (23, 33). Using standard inflammation

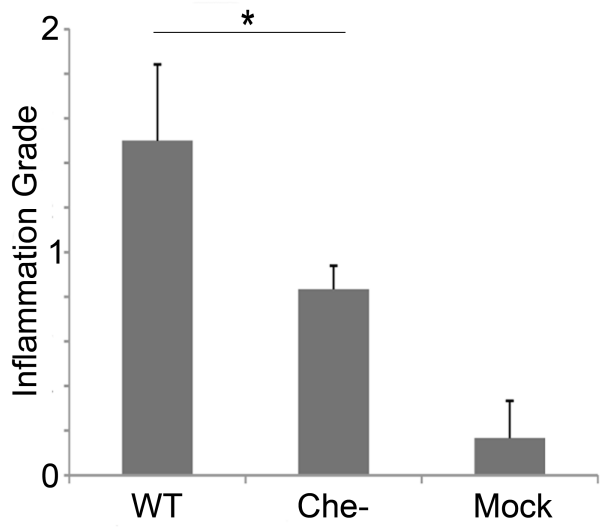

Figure 3.1. *H. pylori* chemotaxis promotes inflammation. Inflammation grade of stomach sections taken from C57Bl/6 mice infected for two months with wild-type or Che- *H. pylori* SS1. N=6 for WT and Che- infections; N=3 for mock infections. Error bars represent SEM. At two months post inoculation, there was a not a statistically significant difference between the Log CFU/g stomach tissue for WT (6.29 ± 1.1) and Che- *H. pylori* (5.72 ± 0.24).

grading that captures the number and distribution of lymphocytes, we found that inflammation was significantly lower in mice infected for two months with Che$^-$ *H. pylori* than in mice infected with wild type *H. pylori* but was greater than in the no-*H. pylori* control (Fig. 3.1). Overall scores at this time point are low, confirming that two months after inoculation is the earliest time point inflammation is pathologically identifiable. Bacterial numbers at two months after inoculation in both infection groups were ~ $1x10^6$ CFU/g and did not differ significantly from each other, similar to previous findings (33, 36), suggesting that inflammatory differences are not caused by a disparity in bacterial burden. Additionally, there was no correlation within individual mice between bacterial colonization levels and inflammation grade, as seen previously (36). This finding thus suggests that Che$^-$ inflammatory deficits arise before two months of infection.

3.4.2. Che$^-$ *H. pylori* inefficiently recruit CD4$^+$ T cells.

We were curious about the exact cell types that are reduced in the Che$^-$ infection. Numerous studies have found that T cells are the dominant lymphocyte in an *H. pylori* infection (37) so we examined T-cell subsets in detail using both flow cytometry and immunohistochemistry.

We infected mice with either wild-type or Che$^-$ *H. pylori* and allowed infections to proceed for two weeks to three months. The total T-cell populations (CD3$^+$CD45$^+$) in infected stomachs rose steadily from week two to week five and displayed a subtle trend for the wild type to recruit more T cells than the Che$^-$ mutant (Fig. 3.2 *A*). Additionally, the percentage of CD4$^+$ T cells remained at background levels in Che$^-$ infections but increased significantly above background in wild-type *H. pylori* infections (Fig. 3.2 *B*). T-cytotoxic cells (CD8$^+$CD3$^+$) never increased over the mock infection control and were not different between the wild-type and Che$^-$ infections (Fig. 3.2 *B*), in agreement with previous reports that this T cell type does not play a major role in *H. pylori*

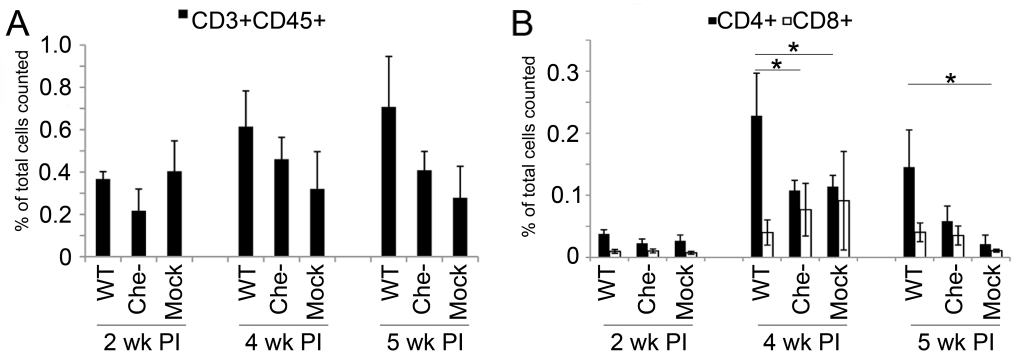

Figure 3.2. Chemotaxis is required for the initial infiltration of CD4$^+$ lymphocytes. C57Bl/6 mouse stomach single cell suspensions were stained with fluorescently labeled **(*A*)** anti-CD45 and anti-CD3, and **(*B*)** anti-CD4, and anti-CD8 and analyzed by flow cytometry. Percentages of CD4$^+$ cells are presented as the percent of CD4 positively stained cells out of 50,000 total cells counted. For the 2 week samples, N=6 for WT and Che$^-$; mock, N=3. For the 4 and 5 week samples, N=5 for WT and Che$^-$; mock, N=3 or 4. Results are representative of two independent experiments; each bar represents the mean ± SEM.

immunity (1).

When we extended our flow cytometric analysis to three months after inoculation, we observed that the percentage of $CD4^+$ T cells in the Che^- infection had risen to match those in the wild-type infection, suggesting $CD4^+$ T-cell recruitment is delayed but not abrogated in Che^- infections (Fig. 3.3 *A* and *B*). To verify our flow cytometry result, we further used immunohistochemistry at two months after inoculation and indeed confirmed that wild-type and Che^- *H. pylori* recruited similar numbers of $CD4^+$ cells at this later time (Fig. 3.3 *C* and *D*). However, we did observe slight differences in the distribution of $CD4^+$ cells between the two infection types, with wild-type infections bearing more widespread inflammatory cells (Fig. 3.3 *C*). Overall, these findings show that early Che^- infections recruit fewer $CD4^+$ T cells than do wild-type infections. This difference dissipates sometime between five and eight weeks after inoculation, but significant differences in the inflammation grading remain. The inflammation grading method examines lymphocyte density in gastric tissue, and thus our score differences suggest that Che^- inflammation is more "multifocal" in character while wild type inflammation is more "widespread" (Materials and Methods) (Fig. 3.3 *C*).

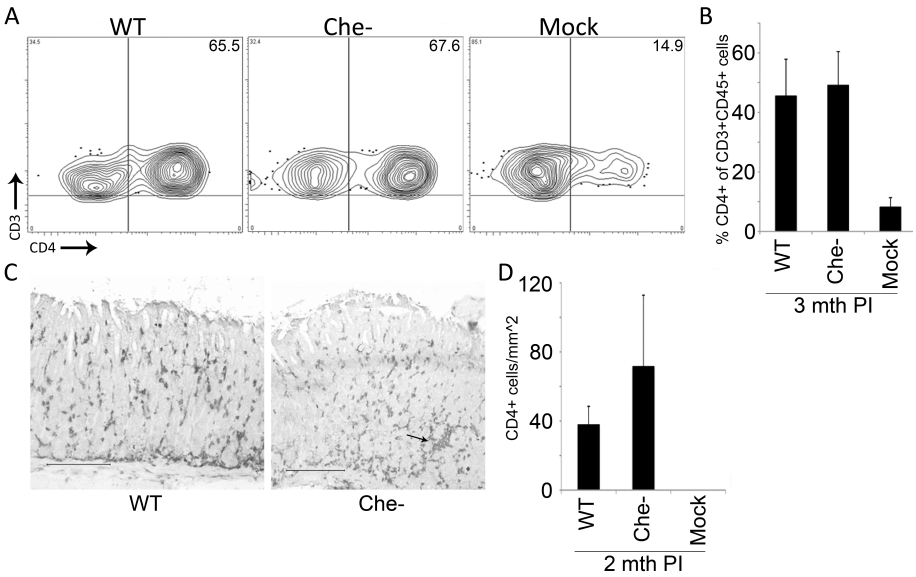

Figure 3.3. *H. pylori* chemotaxis is not necessary for the presence of CD4⁺ lymphocytes two months post-inoculation. (*A*) Representative flow cytometry plots showing the percentage of $CD3^+CD4^+$ T cells of the $CD45^+CD3^+$ gastric lymphocytes from three-month infected tissue. Numbers in quadrants indicate the percentage of positively stained cells. **(*B*)** $CD4^+$ cell percentage is presented as the percent of CD4 positively-stained cells out of $CD3^+CD45^+$ lymphocytes. In total, 50,000 cells were counted. WT and Che^-, N=6; mock, N=4. Results of flow cytometric experiments are representative of two independent experiments. Each bar represents the mean ± SEM. **(*C*)** Representative images of mouse stomach tissue stained with CD4 antibody from either WT *H. pylori* infection (left) with mild, widespread inflammation or Che^- *H. pylori* infection (right), demonstrating mild, multifocal infiltration. Arrow indicates a focus of CD4 cells. Size bar=50μm. **(*D*)** Immunohistochemical enumeration of $CD4^+$ cells in mouse stomach tissue two months post-inoculation. An average of 14.1 mm^2 of tissue was analyzed per mouse. Data are reported in number of cells per mm^2 of tissue ± SD. This data was subjected to Grubbs Statistical Outlier Test, which resulted the removal of 1 WT and 1 mock data point. WT, N=5; Che^-, N=6; mock, N=2.

3.4.3. *H. pylori* chemotaxis affects gastric cytokine profiles.

$CD4^+$ T cells comprise different subsets that play distinctive roles during infection. Therefore, we examined total gastric tissue for the types of $CD4^+$ T

cells present by monitoring transcripts of genes encoding cytokines and transcription factors associated with Th1 (IFNγ), Th2 (IL4), Th17 (IL6, IL17α, TGFβ and Rorγt), and T reg (IL10, TGFβ and Foxp3). IL6 and TGFβ are required for Th17 cell differentiation, whereas T regs require only TGFβ (19). Examining the induction of the Th17 specific transcription factor, Rorγt (19), and the production of IL17α further identifies IL17-producing cells. We additionally assessed T cell activation by monitoring IL2.

Two months post inoculation when both infection types had equal numbers of $CD4^+$ cells (Fig. 3.3), stomachs infected with wild-type *H. pylori*-displayed statistically significant increases in mRNA for *Il10* and the Rorγt-encoding gene *Rorc* as well as a strong increase in *Il17a, IL6,* and *Foxp3* compared with levels in the Che^- infected stomach, which remained at the levels occurring in mock-infected stomachs (Fig. 3.4 *A* and *B*). Rorγt, IL17α and IL6 are associated with IL17-producing cells, suggesting that the wild-type infection skews the response toward IL17 producing cells. *Tgfβ* and *Foxp3* (Fig. 3.4) were not significantly altered from the levels in mock infection, but *Il10* was up-regulated significantly in the wild-type infection, suggesting that T regs may be more active in a wild-type than in a Che^- *H. pylori* infection. The presence of T regs in *H. pylori* infection has been well established (37) but their role in the outcome of the immune response is still debated. Additionally, Th1 and Th2 cells

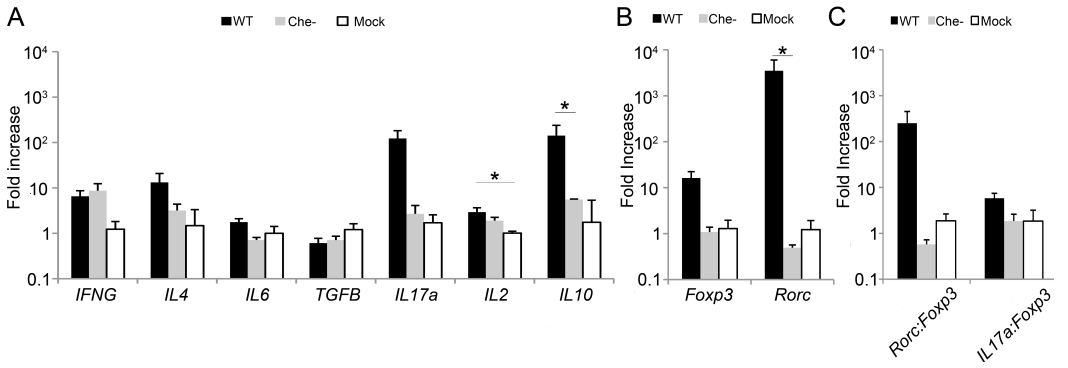

Figure 3.4. ***H. pylori*** **chemotaxis is necessary to induce an inflammatory response associated with Rorγt expression. (*A*)** Gastric mRNA expression of *Ifng, Il4, Il6, Tgfb, Il17a, Il2 and Il10* in wild-type or Che- *H. pylori*-infected mice for two months. RNA was isolated from total mouse stomach tissue and used for qRT-PCR. mRNA expression levels are presented as the fold increase over mock, as determined by the ΔΔCt method. **(*B*)** Gastric mRNA expression of the transcription factors *Foxp3* and *Rorc* (Rorγt) after two months of infection. **(*C*)** Ratio of *Rorc* or *Il17a* to *Foxp3.* Each bar represents the mean ± SEM based on experiments using 5 or 6 (WT and Che-) or 2 to 5 (mock) mice. All experiments were performed in triplicate. *p<0.05, **p<0.001, Student T Test. These mice were colonized with WT (6.29 ± 1.1 Log CFU/g) and Che- *H. pylori* (5.72 ± 0.24 Log CFU/g).

secrete IL10 as a way to control their responses (24), and Th17 cells have also been shown to produce IL10 under some circumstances (22).

Because we observed the up-regulation of *Il10*, a regulatory cytokine, we additionally determined the ratio of Rorγt-encoding gene *Rorc* to *Foxp3* to assess whether the immune response is more inflammatory or regulatory in character; higher ratios of *Rorc: Foxp3* indicate that the immune response trends toward inflammatory. This parameter has also been examined as the *Il17a: Foxp3* ratio (15). We found that both the *Rorc: Foxp3* ratio and the *Il17a: Foxp3* ratio are increased in the wild-type infection than in the Che- infection and the mock infection (Fig. 3.4 *C*). This finding is consistent with previous evidence showing

IL17 expression in *H. pylori*-infected gastric tissue (1, 15, 29). Furthermore, studies have shown that depletion of IL17 or use of $IL17^{-/-}$ mice lowers both *H. pylori* colonization levels and inflammation grade (29).

3.4.4. Chemotactic *H. pylori* induces a Th17 response.

Although the qPCR data for *IL6, IL17*, and *Rorc* suggests that key cytokines critical for the development and activation of the Th17 subset are significantly elevated in the wild-type infection, qPCR of total gastric tissue cannot specifically identify the cellular cytokine source. IL17A, for example, is secreted from Th17 cells, as well as γδ T cells (9) and lymphoid tissue inducer (LTi) cells (28). We therefore performed intracellular cytokine staining to assess which gastric tissue lymphocytes produce IL17A. To accomplish this goal, we sorted $CD45^+$ live cells from gastric tissue of *H. pylori*-infected mice, stimulated them, and subsequently stained them with the surface markers CD3, CD4 and CD45, and the cytokine IL17A. In wild-type *H. pylori* infections, IL17A producing cells were detected within the $CD4^+$ cells after gating on $CD3^+CD45^+$ populations, consistent with Th17 cells (Fig. 3.5 *A* and *B*). A smaller population of IL17A-producing cells was also detected within the $CD4^-CD3^+CD45^+$ populations,

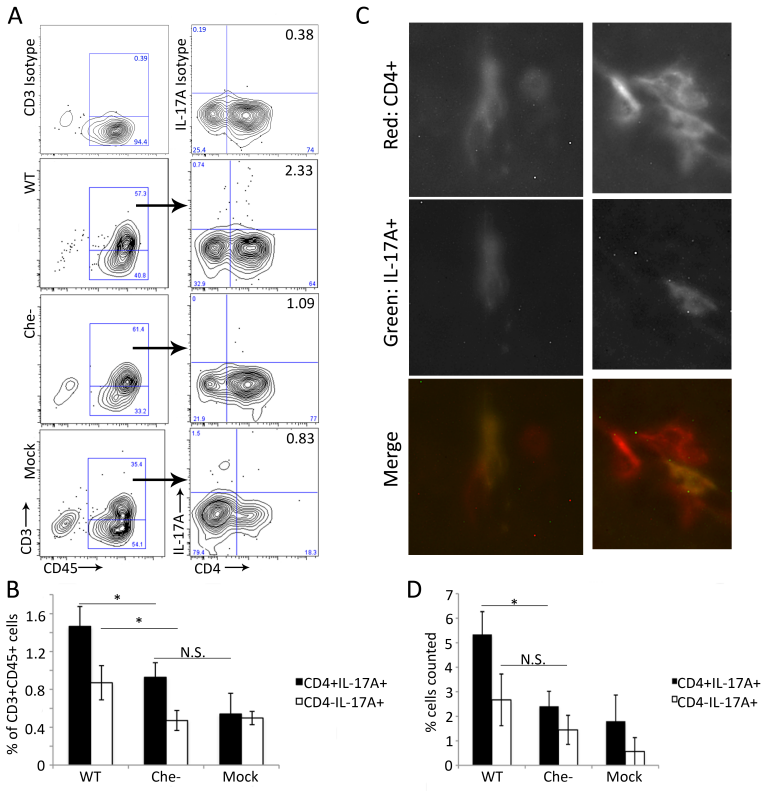

Figure 3.5. ***H. pylori*** **chemotaxis promotes a Th17 response. (*A*)** $CD45^{+}PI^{-}$ cells were sorted from the entire stomach of each mouse, which gave different yields depending on infection type and status, therefore, results are presented as percentages of parent populations. Intracellular cytokines were detected 4 h post re-stimulation with PMA/ionomycin. Flow cytometry plots were gated on $CD3^{+}CD45^{+}$ (left column) to select the $CD3^{+}CD45^{+}$ cells for additional analysis for CD4 and IL17A (right column). The top two boxes show isotype controls to demonstrate the veracity of the sorted cell populations. Numbers in quadrants indicate the percentage of positively stained cells. Data shown is one representative of an N=6 from two experiments for WT and Che^{-}, and an N=4 for mock. **(*B*)** Percentage of $CD4^{+}$ and $CD4^{-}$ $IL17A^{+}$ cells. These cells were collected two months post inoculation, when the mice were colonized with 6.91 ± 0.18 log CFU/g or 6.16 ± 0.18 log CFU/g for WT and Che^{-}, respectively. **(*C*)** Two representative examples showing co-localization of $CD4^{+}$ (Red) and IL17A (green) in stomach tissue. **(*D*)** Quantification for immunofluorescence data in 3.5C presented as percentage of total cells counted that co-localized IL17A and $CD4^{+}$ (black bars) or stained with IL17A alone (white bars). Samples from 6 (WT), 5 (Che^{-}), or 3 (mock) mice were examined, with 2029, 1531, or 145 cells examined for WT, Che^{-}, and mock, respectively. Each bar represents the mean ± SEM. *$p<0.05$, Student T Test. Two independent infections were used to generate the data for A-B and C-D.

suggesting secretion by $CD3^+$ γδ T cells, given that there are few CD8 T cells in these infections (Fig. 3.2). No IL17A production was detected within the $CD3^-$ $CD45^+$ populations from either wild-type or Che^- infected mice, suggesting that LTi cells, which lack CD3 (28), were not the source of IL17A production at this time point (Fig. 3.6). Other types of innate lymphoid cells have been shown to drive intestinal pathology in a *Helicobacter hepaticus* model (6); thus it would be interesting to look at earlier time points to see if LTi cells contribute to the initiation of adaptive responses to *H. pylori*. We also performed an immunofluorescence study looking for the co-localization of CD4 and IL17A in gastric tissue slices from two-month infected mice (Fig. 3.5 *C* and *D*). This experiment confirmed the intracellular cytokine staining results, finding that CD4 and IL17A were co-localized to a significant degree in tissue infected with wild-type *H. pylori* (Fig. 3.5 *C* and *D*). We detected a very small percentage of cells that, as would γδ T cells, stained solely with IL17A and not CD4. This finding is consistent with a low number of γδ T cells in wild-type and Che^- infections (Fig. 3.7), and supporting a principal role for Th17 cells. Together the results from the intracellular cytokine staining, the immunofluorescence, and the gastric cytokine analysis strongly indicate that the Th17 subset is elevated significantly in stomachs with wild-type *H. pylori* infection as compared with stomachs with either Che^- *H. pylori* or mock infection. These findings suggest a role for bacterial

chemotaxis in eliciting a Th17 response. Th17 responses have been implicated in *Citrobacter rodentium* (23) and *Salmonella enterica* serovar Typhimurium infections (34), where these responses seem to underlie pathology.

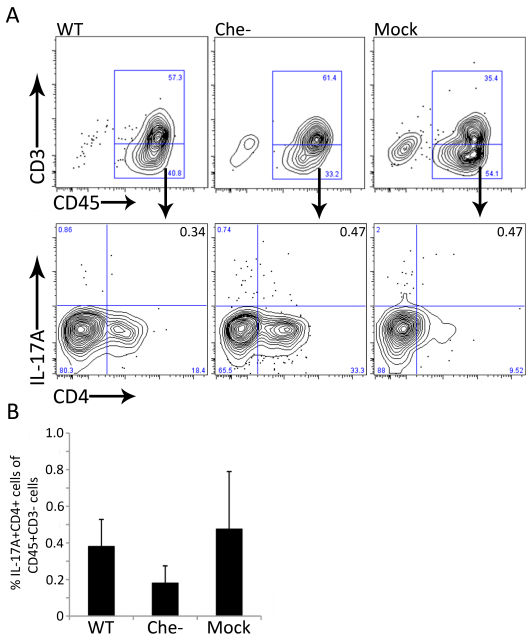

Figure 3.6. IL-17A producing LTi cells do not contribute to differences in IL-17 expression seen in wild-type *H. pylori* infected mice. (*A*) $CD45^{+}PI^{-}$ cells were sorted from the entire stomach of each mouse, which gave different yields depending on infection type and status; therefore, results are presented as percentages of parent populations. Intracellular cytokines were detected 4 h post re-stimulation with PMA/ionomycin. LTi cells are $CD3^{-}$ (1, 2), therefore, flow cytometry plots were gated for $CD3^{-}CD45^{+}$ (top row). The CD3-CD45+ cells were additionally analyzed for CD4 and IL-17A (bottom row). Numbers in quadrants indicate the percentage of positively stained cells in each population. Data shown is one representative from an N=6 from two experiments for WT and Che^{-}, and an N=4 for mock. **(*B*)** Percentage of $CD4^{+}IL\text{-}17A^{+}$ cells from the $CD3^{-}CD45^{+}$ subset. These experiments were the same as seen in Fig. 5A-B, and the mice were colonized with 6.91 ± 0.18 log CFU/g or 6.16 ± 0.18 log CFU/g for wild type and Che^{-}, respectively.



Figure 3.7. IL-17A that is not produced by CD4+ cells is not significantly elevated in wild-type *H. pylori* infected mouse stomachs. Mouse gastric tissue was stained for CD4 (red) and IL-17A (green). This representative image demonstrates non co-localized IL-17A, which would represent γδ T cells. There was not a significant increase of these cells in the wild-type *H. pylori* infected tissue.

3.4.5. Chemotaxis promotes apoptosis in *H. pylori* infection.

Th17 cell differentiation is directed in part when innate immune cells, such as APCs, recognize apoptotic cells combined with bacterial products that activate Toll-like receptors (34). In addition to apoptosis, Th17 development is also associated with IL10 induction (34); we observed high IL10 in the wild-type infection (Fig. 3.4 *A*). Thus one possibility is that wild-type *H. pylori* triggers significant apoptotic cells and in turn Th17 induction. To probe this hypothesis we enumerated apoptotic cells in gastric tissue by TUNEL staining two months post inoculation, when equal numbers of wild-type and Che$^-$ bacteria colonize the stomach and there are differences in the degree of Th17 response (Figs. 3.4-3.5). We found elevated apoptosis in the corpus associated with wild-type *H. pylori* in comparison to Che$^-$ (Fig. 3.8 *A* and *B*). Although apoptosis has

previously been demonstrated in several bacterial infections including *H. pylori* (5), the link to Th17 responses has only been demonstrated in *C. rodentium* infections (34). *C. rodentium* strains are generally non motile (4), and instead use type-three secretion based adherence to deliver pro-apoptotic factors (8). We can now link apoptosis to bacterial chemotaxis and Th17 responses in an *H. pylori* infection.

H. pylori can induce apoptosis in epithelial cells and macrophages via secretion of proapoptotic factors including the VacA cytotoxin (7), urease (12), γ-glutamyl transpeptidase (30), and by up regulating Fas, a TNF receptor that triggers apoptosis of host cells when bound by its ligand FasL (35). Therefore, our results suggest Che$^-$ bacteria express or deliver less pro-apoptotic virulence

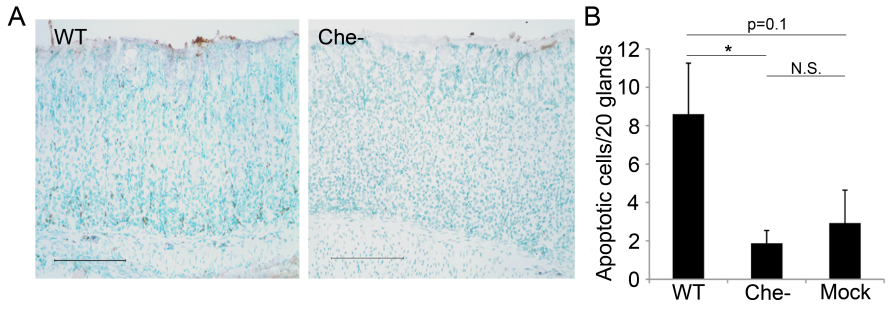

Figure 3.8. *H. pylori* chemotaxis correlates with increased gastric cell apoptosis. (*A*) Representative images taken from the corpus of a mouse infected with wild-type or Che$^-$ *H. pylori* two months post inoculation stained for apoptotic cells (brown) using the TUNEL assay. Size bar=50μm. **(*B*)** Apoptotic cells were counted in 20 randomly selected well-oriented glands of the corpus. Each bar represents the mean ± SEM based on experiments using 6 (WT and Che$^-$) or 3 (mock) mice. These tissue samples were collected two months post inoculation, when the mice were colonized with 6.29 ± 1.1 Log CFU/g for WT and 5.72 ± 0.24 Log CFU/g Che$^-$ *H. pylori*.

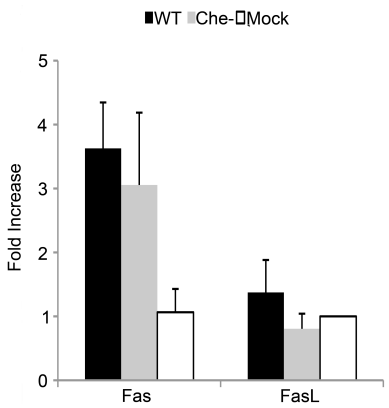

Figure 3.9. Fas/FasL induced cell death does not contribute to increased apoptotic cells in wild-type *H. pylori* infected gastric tissue. Gastric mRNA expression of Fas and FasL in wild-type or Che- *H. pylori*-infected C57Bl/6 mice. RNA was isolated from mouse stomach tissue infected with *H. pylori* for 4 weeks and used for qRT-PCR. mRNA expression levels are presented relative to GAPDH using the ΔΔCt method. Each bar graph represents the mean based on experiments using 4 to 5 (wild type and Che-) or 2 to 4 (mock) mice. All experiments were performed in triplicate.

factors *in vivo.* Che- *H. pylori* localize further away from the gastric epithelial cell surface than does wild type (13, 36) suggesting Che- may be too spatially distant from the target cells for efficient delivery of virulence factors or may experience a different microenvironment that does not trigger appropriate expression of apoptosis-inducing proteins. Supporting this latter idea, chemotaxis regulates virulence factor expression in *Vibrio cholerae* (18).

To investigate if different mechanisms leading to apoptosis vary between wild-type and Che- *H. pylori*, we looked at the gastric mRNA expression of Fas, which is up regulated and contributes to apoptosis in *H. pylori* infection (35), and its ligand, FasL. We found that after two months of infection the expression of Fas in wild-type and Che- *H. pylori* infections is similar to that seen in an uninfected mouse (Fig. 3.9). Additionally, wild-type and Che- infections lead to up regulation of FasL equally (Fig. 3.9) indicating that Fas/FasL-induced cell death does not contribute to apoptotic differences seen in

gastric tissue. We also examined the expression of the *H. pylori* apoptosis-causing virulence factors VacA and UreA in mouse stomachs after two months of infection (Fig. 3.10). We found that on average Che$^-$ bacteria have a somewhat lower expression of VacA but a somewhat higher expression of UreA than wild type bacteria (Fig. 3.10). The expression of UreA is regulated by the ArsRS two component system, which prompts pH-controlled gene expression (20). Therefore, because Che$^-$ bacteria are further from the epithelial cells (13, 36) where they may encounter a more acidic pH, it is not surprising that they have slightly increased expression of UreA. The slightly lower expression of VacA along with a greater delivery distance may contribute to reduced apoptosis through reduced delivery of VacA to the epithelial cells. Interestingly another virulence factor, the cytotoxin-gene associated Pathogenicity Island (*cag*-PAI) has been associated with anti-apoptotic activity (25). The *H. pylori* strain used here, SS1 (17), is *cag*-PAI positive, however for unknown molecular reasons it does not deliver the effector protein CagA and utilizes *cag*-PAI independent mechanisms to evoke immune responses (2, 11), thus we did not examine *cagA* expression.

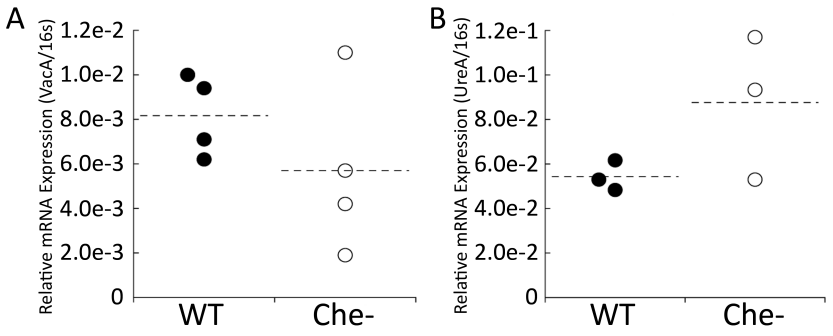

Figure 3.10. Differential expression of VacA may contribute to reduced apoptosis in Che$^-$ infections. Gastric mRNA expression of *vacA* **(*A*)** and *ureA* **(*B*)**, in wild-type or Che$^-$ *H. pylori*-infected C57Bl/6 mouse gastric tissue. RNA was isolated from mouse stomach tissue infected with *H. pylori* for two months and used for qRT-PCR. mRNA expression levels are presented relative to *H. pylori* 16s rRNA. Each dotted line represents the mean based on experiments using 4 mice for VacA or 3 mice for UreA. All experiments were performed in triplicate.

In conclusion, our data suggest a model in which *H. pylori* uses chemotaxis to approach the gastric epithelial cells in such a way as to trigger apoptosis, and the combination of cell death with bacterial products promotes the development of a Th17-skewed immune response, as these same signals do in *C. rodentium* infections (5, 34). Our model fits well with previous *H. pylori* experiments that demonstrated chemotaxis is needed for normal bacterial positioning within the gastric epithelium (13, 36). Here we show that appropriate localization allows *H. pylori* to increase VacA expression (Fig. 3.10) and perhaps promote efficient delivery of this and other pro-apoptotic virulence factors. The simultaneous detection of the apoptotic cells and *H. pylori* bacterial ligands encourages innate immune cells to promote the Th17 cell-dominant

response that we observed in wild-type infections (Figs. 3.4, 3.5). We conclude that one function of the chemotaxis system is to drive *H. pylori* to interact with the host and induce a pathological Th17 immune response that promotes chronic infection.

3.5. Acknowledgements

We thank J. Elliot Carter for his expertise on pathology and scientific contribution to Figure 1. We thank Susan Williams and Victoria Auerbuch Stone for comments on the manuscript. We thank Martha Zuniga for numerous discussions, Holly Scott Algood for advice about gastric sample flow cytometry, and Amber Kofman for assistance with immunohistochemistry. We acknowledge the technical support received from Bari Holm Nazario, CIRM Shared Stem Cell Facility. The described project was supported by Grant Number AI050000 (to K.M.O.) from the National Institutes of Allergy and Infectious Disease (NIAID) at the National Institutes of Health. Its contents are solely the responsibility of the authors and do not necessarily represent the official views of the NIH.

3.6. References

1. **Algood H. M. S., J. Gallo-Romero, K. T. Wilson, R. M. Peek, and T. L. Cover**. 2007. Host response to Helicobacter pylori infection before initiation of the adaptive immune response. FEMS Immunology and Medical Microbiology **51**:577-86.

2. **Arnold I. C., J. Y. Lee, M. R. Amieva, A. Roers, R. a Flavell, T. Sparwasser, and A. Müller**. 2011. Tolerance rather than immunity protects from Helicobacter pylori-induced gastric preneoplasia. Gastroenterology. Elsevier Inc. **140**:199-209.

3. **Beier D., G. Spohn, R. Rappuoli, and V. Scarlato**. 1997. Identification and characterization of an operon of Helicobacter pylori that is involved in motility and stress adaptation. Journal of Bacteriology. Am Soc Microbiol **179**:4676.

4. **Borenshtein D., M. E. McBee, and D. B. Schauer**. 2008. Utility of the Citrobacter rodentium infection model in laboratory mice. Current Opinion in Gastroenterology **24**:32-7.

5. **Brereton C. F., and J. M. Blander**. 2011. The unexpected link between infection-induced apoptosis and a Th17 immune response. J Leukoc Biol **89**:565-576.

6. **Buonocore S., P. P. Ahern, H. H. Uhlig, I. I. Ivanov, D. R. Littman, K. J. Maloy, and F. Powrie**. 2010. Innate lymphoid cells drive interleukin-23-dependent innate intestinal pathology. Nature. Nature Publishing Group **464**:1371-1375.

7. **Cover T. L., and S. R. Blanke**. 2005. Helicobacter pylori VacA, a paradigm for toxin multifunctionality. Nature reviews. Microbiology **3**:320-32.

8. **Deng W., J. L. Puente, S. Gruenheid, Y. Li, B. a Vallance, A. Vázquez, J. Barba, J. A. Ibarra, P. O'Donnell, P. Metalnikov, K. Ashman, S. Lee, D. Goode, T. Pawson, and B. B. Finlay**. 2004. Dissecting virulence: systematic and functional analyses of a pathogenicity island. Proceedings of the National Academy of Sciences **101**:3597-602.

9. **Do J.-su, A. Visperas, C. Dong, W. M. Baldwin, and B. Min**. 2011. Cutting edge: Generation of colitogenic Th17 CD4 T cells is enhanced by IL-17+ γδ T cells. Journal of Immunology **186**:4546-50.

10. **Eaton K. A., M. J. Radin, and S. Krakowka**. 1995. An Animal Model of Gastric Ulcer Due to Bacterial Gastritis in Mice. Veterinary Pathology **32**:489-497.

11. **Eaton K. A., D. Kersulyte, M. Mefford, S. J. Danon, S. Krakowka, and D. E. Berg**. 2001. Role of Helicobacter pylori cag region genes in colonization and gastritis in two animal models. Infection and Immunity. Am Soc Microbiol **69**:2902.

12. **Fan X., H. Gunasena, Z. Cheng, R. Espejo, S. E. Crowe, P. B. Ernst, and V. E. Reyes**. 2000. Helicobacter pylori urease binds to class II MHC on gastric epithelial cells and induces their apoptosis. Journal of Immunology **165**:1918-24.

13. **Howitt M. R., J. Y. Lee, P. Lertsethtakarn, R. Vogelmann, L.-M. Joubert, K. M. Ottemann, and M. R. Amieva**. 2011. ChePep Controls Helicobacter pylori

Infection of the Gastric Glands and Chemotaxis in the Epsilonproteobacteria. mBio **2**:1-10.

14. **Ivanov I. I., K. Atarashi, N. Manel, E. L. Brodie, T. Shima, U. Karaoz, D. Wei, K. C. Goldfarb, C. A. Santee, S. V. Lynch, T. Tanoue, A. Imaoka, K. Itoh, K. Takeda, Y. Umesaki, and D. R. Littman**. 2009. Induction of Intestinal Th17 Cells by Segmented Filamentous Bacteria. Cell. Elsevier Ltd **139**:485-498.

15. **Kao J. Y., M. Zhang, M. J. Miller, J. C. Mills, B. Wang, M. Liu, K. a Eaton, W. Zou, B. E. Berndt, T. S. Cole, T. Takeuchi, S. Y. Owyang, and J. Luther**. 2010. Helicobacter pylori immune escape is mediated by dendritic cell-induced Treg skewing and Th17 suppression in mice. Gastroenterology. Elsevier Inc. **138**:1046-54.

16. **Khamri W., M. M. Walker, P. Clark, J. C. Atherton, M. R. Thursz, K. B. Bamford, R. I. Lechler, and G. Lombardi**. 2010. Helicobacter pylori stimulates dendritic cells to induce interleukin-17 expression from CD4+ T lymphocytes. Infection and Immunity **78**:845-53.

17. **Lee A., J. O'Rourke, M. C. De Ungria, B. Robertson, G. Daskalopoulos, and M. F. Dixon**. 1997. A standardized mouse model of Helicobacter pylori infection: introducing the Sydney strain. Gastroenterology **112**:1386-97.

18. **Lee S., S. Butler, and A. Camilli**. 2001. Selection for in vivo regulators of bacterial virulence. Proceedings of the National Academy of Sciences **98**:6889-6894.

19. **Littman D. R., and A. Y. Rudensky**. 2010. Th17 and regulatory T cells in mediating and restraining inflammation. Cell. Elsevier Inc. **140**:845-58.

20. **Loh J. T., S. S. Gupta, D. B. Friedman, A. M. Krezel, and T. L. Cover**. 2010. Analysis of protein expression regulated by the Helicobacter pylori ArsRS two-component signal transduction system. Journal of Bacteriology **192**:2034-43.

21. **Luzza F., T. Parrello, G. Monteleone, L. Sebkova, M. Romano, R. Zarrilli, M. Imeneo, and F. Pallone**. 2000. Up-regulation of IL-17 is associated with bioactive IL-8 expression in Helicobacter pylori-infected human gastric mucosa. Journal of Immunology **165**:5332-7.

22. **McGeachy M. J., K. S. Bak-Jensen, Y. Chen, C. M. Tato, W. Blumenschein, T. McClanahan, and D. J. Cua**. 2007. TGF-beta and IL-6 drive the production of IL-17 and IL-10 by T cells and restrain T(H)-17 cell-mediated pathology. Nature Immunology **8**:1390-7.

23. **McGee D., M. Langford, E. Watson, and JE**. 2005. Colonization and inflammation deficiencies in Mongolian gerbils infected by Helicobacter pylori chemotaxis mutants. Infection and Immunity **73**:1820-1827.

24. **O'Garra A., and P. Vieira**. 2007. Th1 cells control themselves by producing interleukin-10. Nature Reviews Immunology **7**:425-428.

25. **Peek R. M., C. Fiske, and K. T. Wilson**. 2010. Role of Innate Immunity in Helicobacter pylori-Induced Gastric Malignancy. Physiological Reviews **90**:831-858.

26. **Polk D. B., and R. M. Peek**. 2010. Helicobacter pylori: gastric cancer and beyond. Nature Reviews Cancer. Nature Publishing Group **10**:403-14.

27. **Rugge M., P. Correa, M. F. Dixon, R. Fiocca, T. Hattori, J. Lechago, G. Leandro, a B. Price, P. Sipponen, E. Solcia, H. Watanabe, and R. M. Genta**. 2002. Gastric mucosal atrophy: interobserver consistency using new criteria for classification and grading. Alimentary Pharmacology & Therapeutics **16**:1249-59.

28. **Sawa S., M. Cherrier, M. Lochner, N. Satoh-Takayama, H. J. Fehling, F. Langa, J. P. Di Santo, and G. Eberl**. 2010. Lineage relationship analysis of RORgammat+ innate lymphoid cells. Science (New York, N.Y.) **330**:665-9.

29. **Shi Y., X.-F. Liu, Y. Zhuang, J.-Y. Zhang, T. Liu, Z. Yin, C. Wu, X.-hu Mao, K.-ran Jia, F.-jun Wang, H. Guo, R. A. Flavell, Z. Zhao, K.-Y. Liu, B. Xiao, Y. Guo, W.-J. Zhang, W.-Y. Zhou, G. Guo, and Q.-M. Zou**. 2010. Helicobacter pylori-Induced Th17 Responses Modulate Th1 Cell Responses, Benefit Bacterial Growth, and Contribute to Pathology in Mice. Journal of Immunology **184**:5121-5129.

30. **Shibayama K., K. Kamachi, N. Nagata, T. Yagi, T. Nada, Y. Doi, N. Shibata, K. Yokoyama, K. Yamane, H. Kato, Y. Iinuma, and Y. Arakawa**. 2003. A novel apoptosis-inducing protein from Helicobacter pylori. Molecular Microbiology **47**:443-451.

31. **Soehnlein O., and L. Lindbom**. 2010. Phagocyte partnership during the onset and resolution of inflammation. Nature Reviews Immunology. Nature Publishing Group **10**:427-439.

32. **Symonds E., C. Riedel, D. O'Mahony, S. Lapthorne, L. O'Mahony, and F. Shanahan**. 2009. Involvement of T helper type 17 and regulatory T cell activity in Citrobacter rodentium invasion and inflammatory damage. Clinical and Experimental Immunology **157**:148-54.

33. **Terry K., S. M. Williams, L. Connolly, and K. M. Ottemann**. 2005. Chemotaxis Plays Multiple Roles during Helicobacter pylori Animal Infection. Infection and Immunity **73**:803-811.

34. **Torchinsky M. B., J. Garaude, A. P. Martin, and J. M. Blander**. 2009. Innate immune recognition of infected apoptotic cells directs T(H)17 cell differentiation. Nature. Nature Publishing Group **458**:78-82.

35. **Wang J., X. Fan, C. Lindholm, M. Bennett, J. Connoll, F. Shanahan, E. G. Brooks, V. E. Reyes, and P. B. Ernst**. 2000. Helicobacter pylori Modulates Lymphoepithelial Cell Interactions Leading to Epithelial Cell Damage through Fas / Fas Ligand Interactions. Infection and Immunity **68**:4303-4311.

36. **Williams S. M., Y.-ting Chen, T. M. Andermann, J. E. Carter, D. J. Mcgee, and K. M. Ottemann**. 2007. Helicobacter pylori Chemotaxis Modulates Inflammation and Bacterium-Gastric Epithelium Interactions in Infected Mice. Infection and Immunity **75**:3747-3757.

37. **Wilson K. T., and J. E. Crabtree**. 2007. Immunology of Helicobacter pylori: insights into the failure of the immune response and perspectives on vaccine studies. Gastroenterology **133**:288-308.

CHAPTER 4

The degree of *Helicobacter pylori* inflammation is manipulated by the pre-infection host microbiota

4.1. Abstract

Helicobacter pylori, a significant bacterial pathogen, causes severe disease in only some infected individuals. We demonstrate that one previously unappreciated parameter influencing *H. pylori* disease outcome is variation in pre-infection host microbiota. Utilizing a mouse model, we altered the microbiota by antibiotic treatment and found that microbiota alterations resulted in significantly lowered *H. pylori*-triggered inflammation. Specifically, antibiotic pretreatment reduced $CD4^+$ T-helper cells and *Ifnγ* transcript in gastric tissue after *H. pylori* infection. The bacterial communities in mice with a reduced response to *H. pylori* had significantly more cluster IV and XIVa *Clostridia* spp., bacteria known to increase regulatory T cell populations. Our findings lead to a prediction that microbiota composition, specifically *Clostridium* spp., contribute to the variable disease outcome of *H. pylori* infection by promoting T regulatory cell recruitment or differentiation.

4.2. Introduction

The bacterial gastric pathogen *Helicobacter pylori* colonizes more than half of the world's population (27, 37). Most infected people remain asymptomatic, however ~10% develop either peptic ulcers, gastric adenocarcinoma or mucosa-associated lymphoid tumors (7, 27, 37); it is not yet possible to predict who will develop disease and what form it will take (7). Additionally, *H. pylori* infections are protective against diseases such as esophageal cancer (27). As a result, most *H. pylori* infections are not treated unless the infected individual displays symptoms. However, it would be desirable to cure *H. pylori* infections that will progress to gastric cancer, as this disease has few treatment options and high mortality (26). Several variables that determine *H. pylori*-associated disease outcome have been identified, but they do not fully explain disease risk. These past studies focused on variation in *H. pylori* genetic composition (7, 35, 37), host genetics (7, 27, 37), and environmental factors (37), but there has been no examination of the role played by the host microbiota.

Microbiota have been implicated in aspects of immune system regulation and development (6, 16, 18), and altered microflora communities have been implicated in both ameliorating (16, 25) and enhancing (12, 13, 34) disease symptoms. Specifically, dysbiosis of microbiota have been shown to influence inflammatory bowel disease (IBD) (12), obesity (34), and immune responses to

Citrobacter rodentium (16) and *Helicobacter hepaticus* (36). Gastric microbial communities from people infected with *H. pylori* are somewhat different from uninfected people (3, 24) suggesting an interaction between *H. pylori* and its gastric microbial community. Whether specific communities of microbiota make an individual more susceptible to *H. pylori* infection or disease is unknown.

In this study we investigate how the normal gastric microbiota affects disease that develops from *H. pylori* infection using the well-established *H. pylori* mouse model. Our studies were motivated by initial observations that identical mouse strains from different vendors responded differently to *H. pylori* infection. We report that these mice have variations in their normal gastric flora, akin to what has been seen in mouse intestinal flora (16). Additionally, we found that antibiotic-induced alterations in the mouse normal gastric microflora shaped the immune response to *H. pylori* in a manner that suggested specific microflora members can reduce *H. pylori*-initiated inflammation. Mice that displayed dampened *H. pylori*-initiated inflammation had higher amounts of *Clostridia* species than had been associated with increased inflammation. These data thus suggest that variations in specific microflora members can have a dramatic effect on *H. pylori*-associated disease, and suggest new avenues for curbing *H. pylori* inflammation-related diseases such as ulcers and gastric cancer.

4.3. Experimental procedures

4.3.1. *H. pylori* strains and growth conditions

Helicobacter pylori strain SS1 (19) was used for all studies. SS1 was a gift of Jani O'Rourke (University of New South Wales) and was minimally lab passaged before our experiments. *H. pylori* was cultured on Columbia blood agar (Difco) with 5% difibrinated horse blood (Hemostat Labs, Davis, CA), 50 μg/ml cyclohexamide, 10 μg/ml vancomycin, 5 μg/ml cefsulodin, 2.5 Units/ml polymyxin B, and 0.2% β-cyclodextrin. Mouse stomach samples were plated on the same medium plus 5 μg/ml trimethoprim, 8 μg/ml amphotericin B, 10 μg/ml nalidixic acid and 200 μg/ml bacitracin. To prepare *H. pylori* for mouse infection, we grew the bacteria shaking in brucella broth (Difco) with 10% fetal bovine serum (FBS, Gibco) (BB10). Cultures were incubated at 37°C with 7-10% O_2, 10% CO_2, and 80-83% N_2 over night. For mouse infection, we inoculated animals orally intragastrically via a 20g x 1.5 inch feeding needle with 500 μl containing ~ 1 x 10^7 CFU/mL brucella broth-grown *H. pylori*.

4.3.2. Animal infections

The University of California, Santa Cruz Institutional Animal Care and Use Committee approved all animal protocols and experiments. Female C57Bl/6N mice (*Helicobacter*-free, Taconic Labs, Germantown, NY or Charles River Laboratories) were housed at the animal facility of the U.C. Santa Cruz under standard conditions with a microisolator cage top. Mice were housed in sterile

cages, with sterile bedding and water. Cages were changed under laminar flow sterile conditions to minimize environmental exposure. For the experiments, 0.6 g/L of Penicillin/Streptomycin (Omega Scientific) was administered *ad libitum* in the water bottle for eight days; the antibiotic was replenished every two days. Two days after completing the antibiotic treatment, reconstituted mice were orally intragastrically fed 200 μl stomach homogenates from non-antibiotic treated C57Bl/6N mice. Ten days after receiving the stomach homogenates, mice were inoculated intragastrically with *H. pylori*. Mice were seven weeks old at the time of *H. pylori* infection and age-matched uninfected mice were included in all experiments. Four weeks post inoculation the animals were sacrificed via CO_2 narcosis, the stomach dissected, opened along the lesser curvature and divided into longitudinal strips for preservation and analysis. The tissue pieces were either, (1) homogenized using the Bullet Blender (Next Advance) with 1.0mm Zirconium Silicate beads and plated to determine the number of *H. pylori* CFU/gram of stomach or used for DNA isolation for determining microbial profiles; (2) frozen in liquid nitrogen and stored at -80°C for quantitative RT PCR of cytokines (see below); (3) stored in cold Hanks Balanced Salt Solution (HBSS, Lonza) to be used in flow cytometry experiments (see below).

4.3.3. Flow cytometry

For flow cytometry, T cells were examined by expression of the CD3 T cell co-receptor and CD45 protein tyrosine phosphatase. T-helper or T-cytotoxic cell subsets were identified by their expression of CD4 or CD8 receptors, respectively. To prepare single cell suspensions, mice stomachs were dissected, opened longitudinally along the lesser curvature and placed in cold HBSS (Lonza). The stomach was cut with a razor blade into approximately 2 cm slices and incubated for 45 minutes at 37ºC in an HBSS solution supplemented with 10% FBS, 15mM HEPES, 5mM EDTA and 0.014% DTT (HED solution). Subsequently the tissue was rinsed once with cold HBSS and incubated for 1 hour at 37ºC in 10 mL RPMI media with 10% FBS plus 1 mg/mL Dispase (Roche) and 0.25 mg/mL collagenase (Roche). The tissue was then vortexed, and gently massaged through a 40μm cell strainer (BD Biosciences), followed by rinsing of the strainer with 10mL cold HBSS. After filtering, the cells were collected by centrifugation and washed two times in cold PBS. The cells were then incubated on ice with IgG (US Biological) for 10 minutes to block non-specific binding, followed by incubation with the test antibody for 20 minutes in the dark. The optimal concentrations for the antibodies were determined in prior experiments to be 2 μg/mL for AlexaFlour488-CD3 (eBioscience), PeCy7-CD4 (eBioscience), APC/Cy-7-CD8 (Biolegend), and for AlexaFluor647-CD45 (Biolegend). An isotype control was included. Subsequently, the cells were centrifuged and washed twice in PBS plus 2.0% FBS then fixed in 2% paraformaldehyde for 10 minutes on ice.

50,000 cells were counted on a BD LSR II (BD Biosciences) and analyzed using FlowJo (BD Biosciences) software, results are presented as a percentage of the 50,000 cells counted. Student T test was used for statistical analysis.

4.3.4. Quantitative PCR

Quantitative analysis of *Ifnγ, Il17, Il4, Foxp3* and *Il10* in the mouse stomach was performed by real-time PCR. RNA was isolated from mouse stomach samples using TRIzol (Gibco). Briefly, stomachs were homogenized with a Polytron (Kinematica, Switzerland) in 1 mL TRIzol per 100 mg of stomach tissue. Following homogenization, the mixture was centrifuged (12000g, 10 minutes 4 ºC), the supernatant extracted with chloroform and the RNA precipitated with isopropyl alcohol. 1-3 μg of RNA was converted to cDNA using RT^2 First Strand Kit (Superarray Bioscience Corporation). The cDNA was subsequently measured in a qPCR reaction with SYBR green master mix (Bioline). The data was normalized to the housekeeping gene GAPDH, and is presented as fold increased over mock using the ΔΔCt method (22). All samples were analyzed in triplicate, along with no reverse transcriptase controls. The Student T test was used for statistical analysis. qPCR for bacterial species in the mouse stomach was performed on DNA samples isolated from homogenized mouse stomach using the DNEasy Kit (Qiagen), and quantified using a standard curve of plasmids containing the bacterial 16s rRNA gene.

4.3.5. Pathology

Gastric tissue preserved in OCT was sectioned, stained with hematoxylin and eosin and evaluated in a blind fashion by a pathologist (J.E. Carter). Each slide was evaluated twice. Lymphocytic infiltration was scored as outlined by Eaton et al (11). The scores are 0, no infiltrate; 1, mild, multifocal infiltration; 2 mild, widespread infiltration; 3, mild widespread and moderate multifocal infiltration; 4, moderate, widespread infiltration; and 5, moderate, widespread and severe multifocal infiltration.

4.3.6. PhyloChip analysis

Bacterial DNA was isolated using Dneasy Blood and Tissue kit (Qiagen), including the pre-treatment for gram-positive bacteria. The isolated DNA was sent to Second Genome (San Francisco, CA) for bacterial 16s DNA amplification. Microbial profiles for each sample were generated by hybridizing the bacterial 16S rDNA amplicons to the Phylochip (Second Genome). The Phylochip has been validated to detect 90% of cloned subfamilies at a 2.5-fold higher diversity than cloning (10). The Phylochip array contains 1,016,064 probes. For analysis, the probe gene sequences are clustered into groups known as operational taxomonic units (OTUs). Each OTU summarizes an average of 0.5% sequence divergence between probes and includes an average of 37 probe pairs, which

include a perfectly matching probe and a control, mismatching probe. In total, the Phylochip array contains 59,959 OTUs, which represent 147 phyla, 1,123 classes, and 1,219 orders within the archaea and bacteria (10, 14).

4.4. Results and Discussion

4.4.1. Mice from Taconic and Charles River have different inflammatory responses to *H. pylori*.

While studying the mouse inflammatory response to *H. pylori* infection, we noted significant differences in the degree of inflammation that *H. pylori* strain SS1 triggered in C57Bl/6N mice from Charles River Labs (CRL) or Taconic

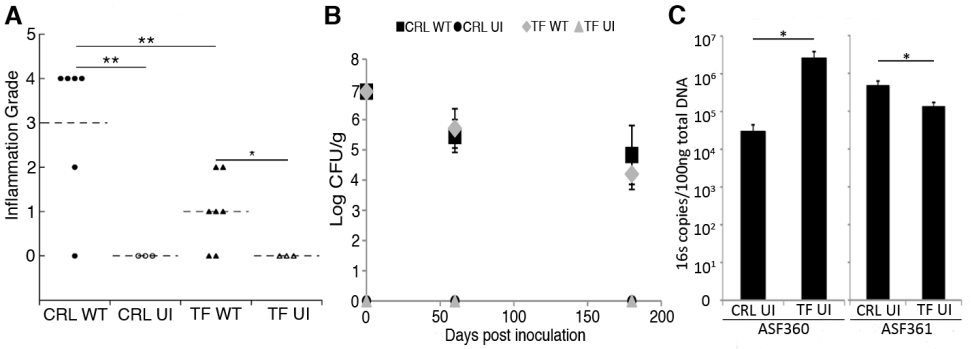

Figure 4.1. C57Bl/6N mice from different vendors mount different inflammatory responses to *H. pylori* and possess varying amounts of key *Lactobacillus* spp. (*A*) Inflammation grade given to gastric tissue from C57Bl/6N mice from either Charles River Laboratories (CRL) or Taconic Farms (TF) infected with wild-type *H. pylori* strain SS1 (WT) for six months compared to uninfected (UI) controls. **(*B*)** *H. pylori* colonization load in colony forming units (CFU) per gram stomach at two and six months post inoculation; the CFU on day 0 is the inoculating dose. **(*C*)** Quantitative PCR on the 16s gene for *Lactobacillus* species ASF360 and ASF361 in 2-month-old uninfected mice from CRL and TF. N ≥ 6 mice per group infected with *H. pylori*, N = 3 for uninfected groups. For (B) and (C) data are presented as averages ± SEM. *P<0.05; **P<0.01, Student T test.

Farms, Inc. (TF) (Fig. 4.1 *A*). Mice from both vendors reacted with an increase in inflammation grade compared to the uninfected controls, however, the CRL mice had significantly higher inflammation grades than the mice from TF (Fig. 4.1 *A*), even though *H. pylori* colonizes mice from each group equally (Fig. 4.1 *B*). This outcome suggested a difference between CRL and TF mice that could not be attributed to *H. pylori* genetics, length of infection, bacterial load, or mouse husbandry, gender or age at infection. Studies have found differences in intestinal microbiota in C57Bl/6 mice from different vendors (16), so we compared *Lactobacillus* species ASF360 and ASF361, two resident bacteria of the gastric microbiota (29). We noticed a significant difference in the copies of each *Lactobacillus* type, with ASF360 significantly higher in the TF mice and ASF361 significantly higher in the CRL mice (Fig. 4.1 *C*). These data suggest that the divergent starting stomach microbial populations may be responsible for different inflammatory reactions against *H. pylori* observed in C57Bl/6N mice from different distributors.

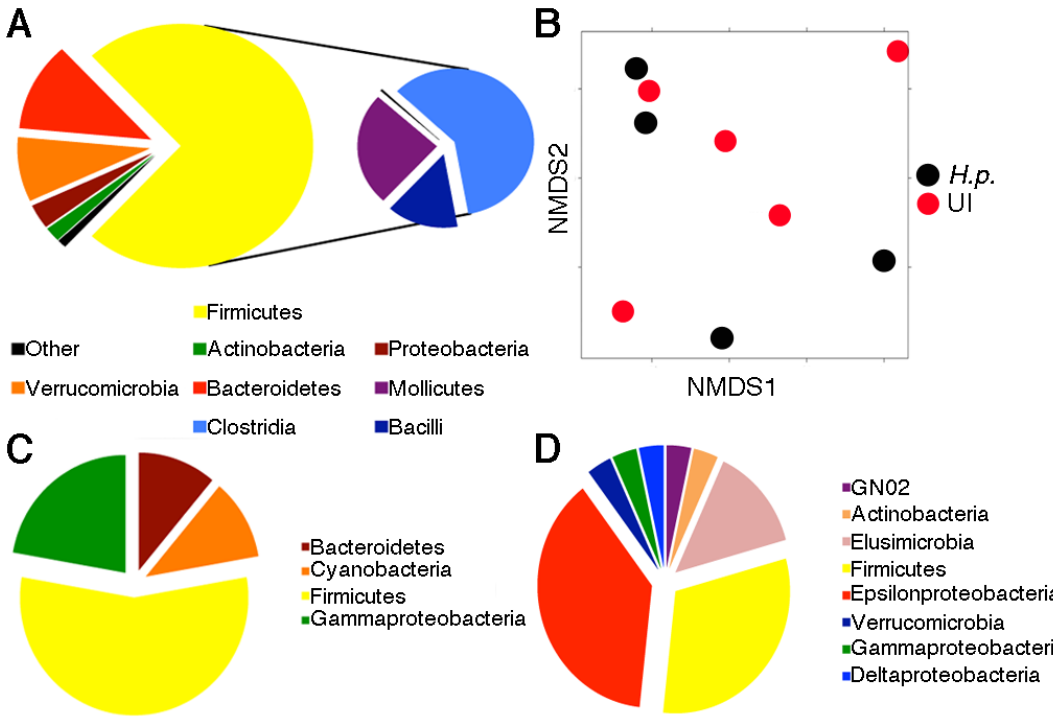

Figure 4.2. The murine stomach microbiota is refractory to *H. pylori*-triggered perturbations and similar to the human stomach microbiota. **(*A*)** The diversity of the 2056 taxa that were present in all non-infected Taconic mice; 74% of them are *Firmicutes*, specifically, 44% of the total are *Clostridia*. 12032 taxa were present in at least one of five mouse stomachs. **(*B*)** Significant differences in microbiota are not apparent between *H. pylori* infected and non-infected samples, as indicated by non-metric multidimensional scaling (NMDS) based on Bray-Curtis distance between samples given the presence/absence of 12032 taxa present in at least one of nine mouse samples; each dot represents one mouse in the study. *H.p.*=4 week *H. pylori* infection; UI=uninfected. **(*C*)** The diversity of the 19 taxa that were significantly decreased in *H. pylori* infected compared to the uninfected control. **(*D*)** The diversity of the 29 taxa that were significantly increased in *H. pylori* infected compared to the uninfected control.

4.4.2. The murine stomach microbiota is refractory to *H. pylori*-triggered perturbations and similar to the human stomach microbiota.

The differing levels of *Lactobacillus* ASF360 and ASF361 in CRL and TF mice suggest that different gastric microbial constituents might influence the

degree of *H. pylori*-induced inflammation in the mouse model. We thus undertook two analyses of the mouse gastric microbiota—the effect of *H. pylori* infection on the existing microbiota and the effect of pre-infection microbiota on *H. pylori* infection and disease outcome. We isolated total DNA from the stomachs of five specific pathogen free C57Bl/6N mice (TF) and amplified the 16S rRNA genes. We used this DNA in hybridization studies with the Phylochip microbial profiling system, a microarray-based method that identifies and measures the relative abundance of more than 59,000 individual microbial taxa (10). This analysis found that all mouse stomachs contained 2056 core groups of closely related species, termed operational taxonomic units (OTU) (Excel File S1.1). The majority of these isolates came from members of the *Firmicutes* phylum with members from the order *Clostridia* being the most common (Fig. 4.2 *A*). Members of the *Bacteroidetes* and *Verrucomicrobia* phyla were the second and third most highly represented phyla. The 2056 OTUs represented 110 different families (Figs. 4.2, 4.3). The stomach phylotypes with the most members were the *Bacteroidetes*, *Firmicutes*, *Proteobacteria* and *Actinobacteria*, which is similar to what has been observed in humans except in human samples *Fusobacteria* are also dominant (3, 9, 24).

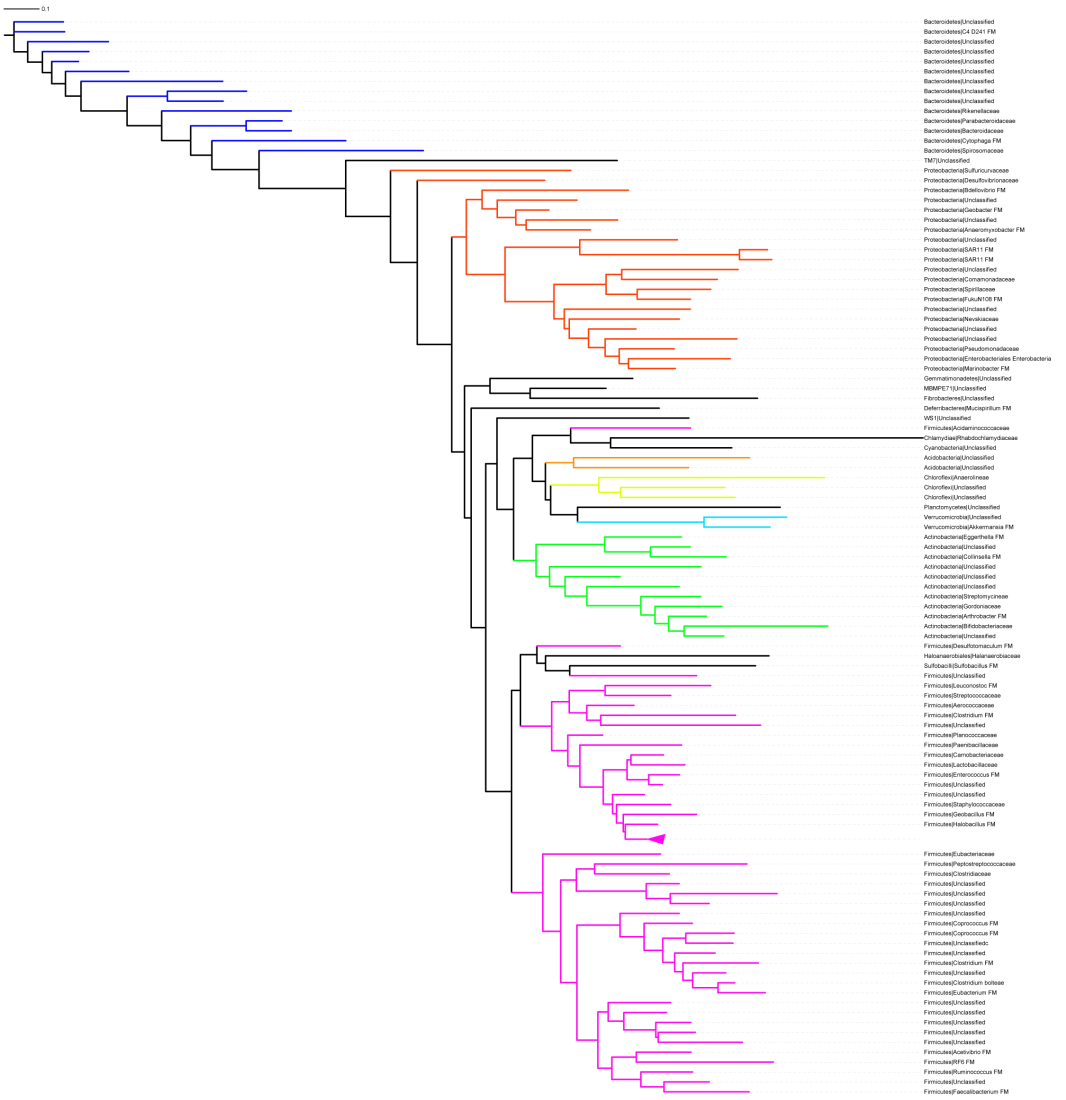

Figure 4.3. A phylogenetic tree displaying the 109 families present in all five of the uninfected mice demonstrates the diversity of the microbiota in the mouse stomach. Clades are color-coded based on the phylum and collapsed branches had branch lengths < 0.05. The leaf labels indicate the phylum and the family of the identified bacteria. Blue, *Bacteroidetes*; Red, *Proteobacteria*; Pink, *Firmicutes*; Orange, *Acidobacteria*; Yellow, *Chloroflexi*; Light blue, *Verrucomicrobia*; Green, *Actinobacteria*.

We next determined how the normal mouse stomach microbiota responds to the presence of *H. pylori* strain SS1 for four weeks of infection, using Phylochip analysis as described above. While we observed changes in a small number of OTUs (Excel File S1.2), overall, the microbiota communities from each group were not significantly different from each other when we examined the difference in the presence/absence of bacterial species or their abundance (Figs. 4.2 *B*, 4.4) demonstrating that *H. pylori* infection does not alter the stomach microbiota, as supported by the previous limited analysis in mice (33). Despite not observing overall community changes upon *H. pylori* infection, there were a few significant differences in specific taxa. Upon examination of the OTUs affected by *H. pylori* colonization, we noticed many similarities to what has been reported for changes upon *H. pylori* colonization in humans (24). For example, we observed a decrease in *Firmicutes (Bacilli)*, *Bacteroidetes* and *Proteobacteria* (Fig. 4.2 *C;* Excel File S1.2), and an increase in *Firmicutes (Clostridia)*, *Proteobacteria (Helicobacter)*, and *Verrucomicrobia* (Fig. 4.2 *D;* Excel File S1.2); all of these changes also occurred in human infections (24). Mouse studies thus show that *H. pylori* infection only modestly changes the microbiota (33) while human studies show slightly more significant changes in microbiota (3, 9, 24) suggesting that long-term infections may lead to temporal changes in microbiota. To address whether we observe temporal changes in the microbiota

in mice, we tracked the populations of *Lactobacillus* spp. ASF360 and ASF361 (2, 29) in *H. pylori* infected stomachs as infection progressed from one day to four weeks post inoculation (Fig. 4.5). We did not observe any significant differences in the copies of ASF360 and ASF361 between the *H. pylori* infected stomachs and the uninfected stomachs at any time point (Fig. 4.5), however overtime the population of ASF361 seems to be changing over time. This finding suggests that *H. pylori* does not impact the microbiota directly, but that accompanying immune or physiological changes, such as loss of parietal cells, may drive more substantial changes over time. Furthermore, these data suggest that microbiota changes post *H. pylori* infection would have only a limited effect on the immune response to *H. pylori*.

4.4.3. Fewer CD4+ T cells infiltrate into the stomach in response to *H. pylori* when mice have been pre-treated with antibiotics.

We hypothesized that different pre-infection stomach microbial populations might affect the inflammatory response to *H. pylori* infection based on the inflammatory differences between the TF and CRL C57Bl6/N mice (Fig. 4.1). To address this hypothesis, we performed an experiment in which we

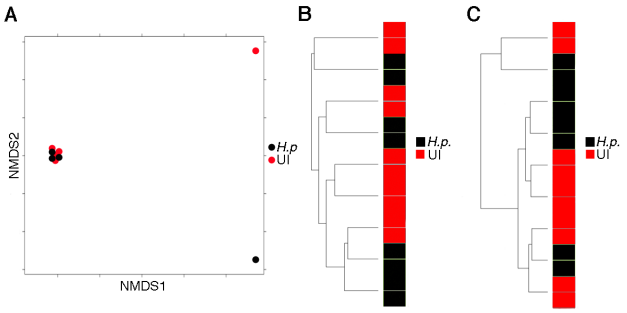

Figure 4.4. *H. pylori* infection for four weeks does not alter the gastric microbiota. (*A*) Non-metric multidimensional scaling (NMDS) based on Bray-Curtis distance between samples given the abundance of 12032 taxa present in at least one sample; each dot represents one mouse in the study. *H. p.*=4 week *H. pylori* infection; UI=uninfected. **(*B and C*)** Hierarchical clustering (average linkage) based on Bray-Curtis distance between samples given the presence/absence **(*B*)** or abundance **(*C*)** of 12032 taxa present in at least one sample.

altered the starting microbial populations by antibiotic treatment of mice from a common source, TF. We included three treatment groups in this analysis: the first group was normal (not antibiotic treated), the second group received antibiotics for eight days, and the third group received antibiotics for eight days followed by gavage with stomach homogenates from normal mice. The last group was thus reconstituted with normal mouse stomach microbiota (Fig. 4.6

A). For each treatment group, five mice were infected with *H. pylori* and five were left uninfected. Four weeks post *H. pylori* inoculation we examined the

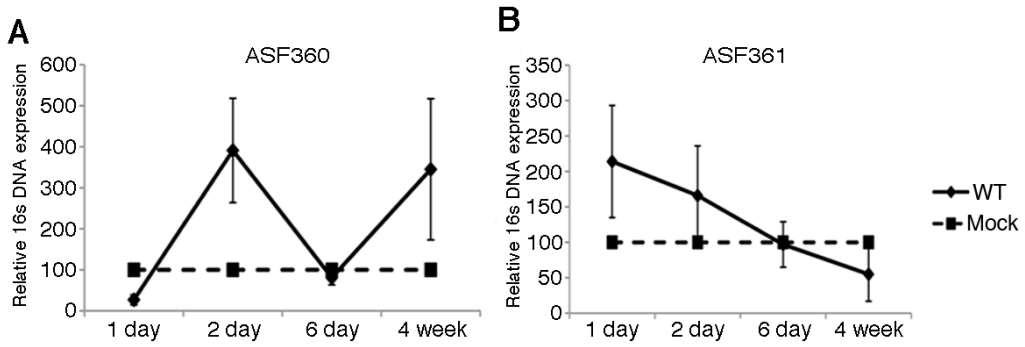

Figure 4.5. Components of microbiota change overtime after *H. pylori* infection. Mouse stomachs infected with *H. pylori* for 1 day, 2 days, 6 days or 4 weeks were subjected to quantitative PCR for the bacterial 16s rRNA gene of *Lactobacillus* species ASF360 **(*A*)** and ASF361 **(*B*)**. ASF361 changes size from 1 day to 4 weeks post *H. pylori* inoculation N ≥ 5 for wild-type infections at each time point; n ≥ 2 for mock infections at each time point. Data are presented as averages ± SEM. There were no significant differences between *H. pylori* infected and mock at any time point.

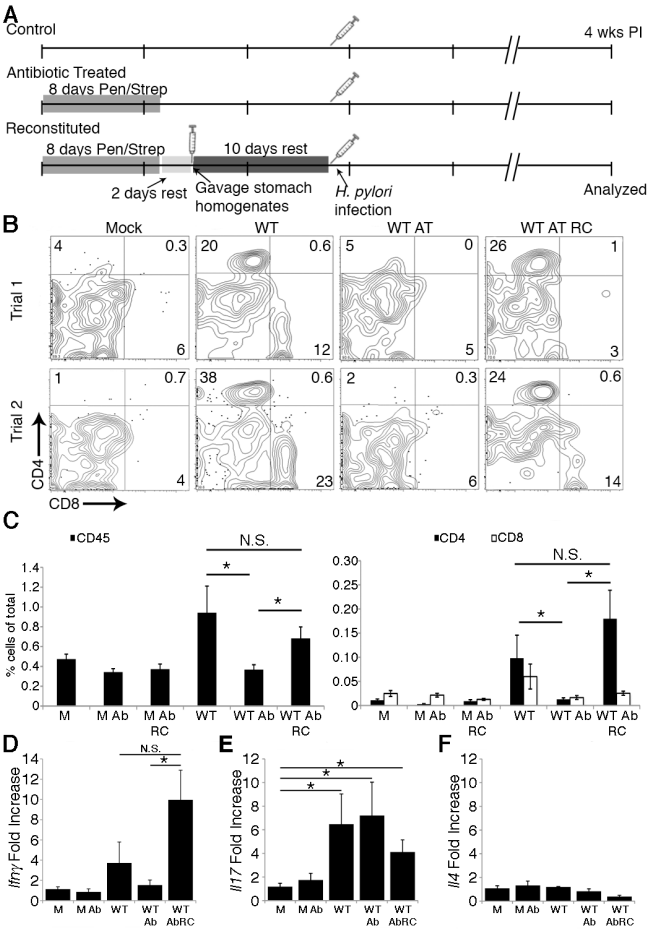

Figure 4.6. Fewer CD4⁺ T cells infiltrate the stomach in response to *H. pylori* when mice have been pre-treated with antibiotics. **(*A*)** Experimental set up for altering the microbiota and infecting with *H. pylori*. **(*B*)** Representative flow cytometry plots showing the percentage of CD4⁺ and CD8⁺ cells of the CD45⁺CD3⁺ gastric lymphocytes from tissue four weeks post inoculation. Numbers in quadrants indicate the percentage of positively stained cells. Quadrants determined by isotype control. **(*C*)** CD45⁺ cell percentage is presented as the percent of CD45⁺ stained cells out of 50,000 cells counted (left panel). CD4⁺ (black bars) and CD8⁺ (white bars) cell percentages are presented as the percent of positively stained cells out of 50,000 cells counted (right panel). Data were obtained from two independent experiments with similar results. N ≥ 7 mice for each group. Total gastric mRNA expression of **(*D*)** *Ifnγ,* **(*E*)** *Il17,* and **(*F*)** *Il4.* mRNA expression levels are normalized to the housekeeping gene, *Gapdh*, and expressed as fold increase over mock, using the ΔΔCt method (22). Non-treated uninfected mice (M), antibiotic treated uninfected mice (M Ab), non-treated *H. pylori* infected mice (WT), antibiotic treated *H. pylori* infected mice (WT Ab), and gastric flora reconstituted mice (WT Ab RC). Data in (C - F) are presented as averages ± SEM. N.S.= not significant. *P<0.05, Student T test.

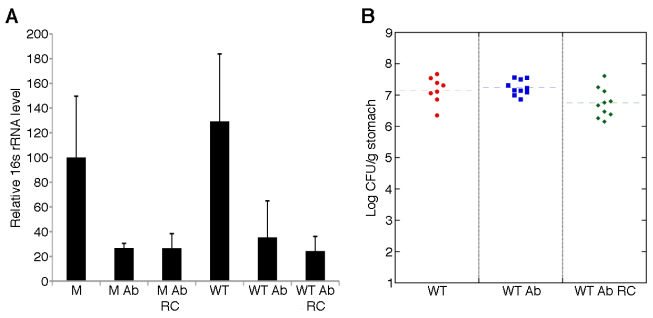

Figure 4.7. Antibiotic treatment does not significantly change the numbers of total bacteria or *H. pylori* present in the stomach. (*A*) DNA was isolated from total mouse stomach tissue and used for qPCR of the bacterial 16s rRNA gene. N ≥ 6 for M, M Ab, M Ab RC, and WT. N = 4 for WT Ab and WT Ab RC. No significant differences were found between groups by Mann Whitney U test. Data is presented as averages ± SEM. **(*B*)** Colonization level of *H. pylori* in the three infected groups was determined by plating and is presented as Log CFU/g stomach tissue. *H. pylori* was not detected in any uninfected groups. Non-treated uninfected mice (M), antibiotic treated uninfected mice (M Ab), non-treated *H. pylori* infected mice (WT), antibiotic treated *H. pylori* infected mice (WT Ab), and gastric flora reconstituted mice (WT Ab RC).

abundance of total microbiota members and the abundance of *H. pylori* and found that neither parameter were different between the groups (Fig. 4.7). To determine whether there were inflammatory differences between the groups, we analyzed the mouse stomachs by flow cytometry for $CD45^+CD3^+CD4^+$ T helper cells and $CD45^+CD3^+CD8^+$ T cytotoxic cells (Fig. 4.6 *B, C*). Interestingly, mice treated with antibiotics did not respond immunologically to an *H. pylori* infection, displaying levels of $CD4^+$ T helper cells that were comparable to uninfected controls (Fig. 4.6 *B, C*). In contrast, mice with reconstituted microbiota had a robust influx of gastric T lymphocytes that was comparable to the *H. pylori* response of normal mice (Fig. 4.6 *B, C*). To determine what type of immune response was inhibited in the antibiotic-treated mice we examined transcripts encoding inflammatory cytokines for T-helper Type 1

(Th1) (*Ifnγ),* T-helper Type 17 (Th17) (*Il17),* and T-helper Type 2 (Th2) (*IL4)* responses in the mouse stomach (Fig. 4.6 *D-F*). We found that *Ifnγ* was elevated in the *H. pylori*-infected normal mice and in the *H. pylori*-infected reconstituted mice (Fig. 4.6 *D*), similar to the pattern we observed with the infiltrating $CD4^+$ T cells (Fig. 4.6 *C*). *Il17* and *Il4* were not different between the three *H. pylori* infected groups (Fig. 4.6 *E, F*). This outcome suggests that changes in microbiota that occurred in the antibiotic-treated mice specifically inhibited Th1 inflammatory responses four-weeks post *H. pylori* inoculation. We were surprised not to see a reduction in *Il17.* However, the kinetics of Th1 and Th17 responses are different (30) suggesting that differences in Th17 responses may not be observed until later post-infection. These results demonstrate that the pre-infection microbial populations affect the extent of *H. pylori*-triggered immune cell infiltration. Other researchers have noted that *H. pylori* disease does not develop in germ-free animals (23), or in the presence of *Helicobacter bilis* co-infection (20), suggesting that normal flora influences *H. pylori* disease outcome. Since our antibiotic treated mice have normal numbers of microbiota in their stomach (Fig. 4.7), we hypothesized that there were differences in members of the microbiota between antibiotic-treated versus normal mice. We thus compared the stomach microbiome of these two groups using PhyloChip microbial profiling system. We found that the microbial populations were

significantly different from each other; specifically, over 4,400 OTUs were different between

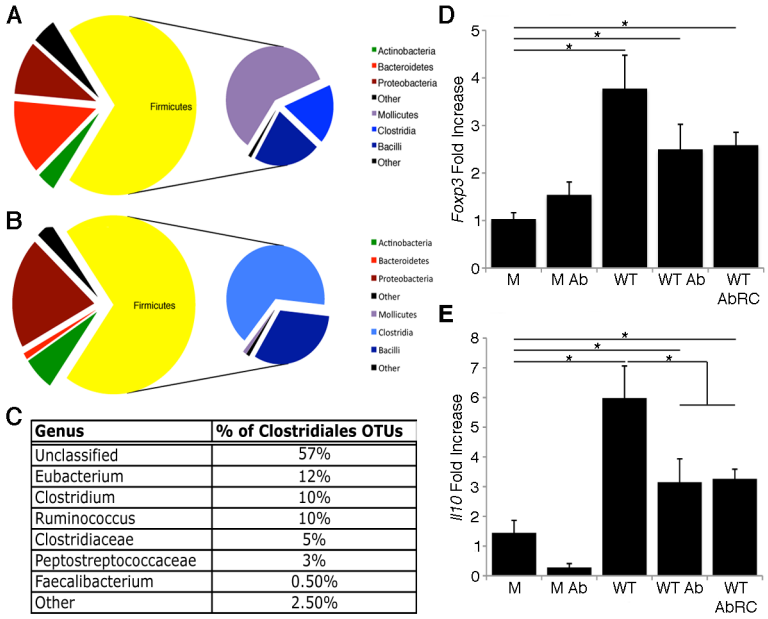

C

Genus	% of Clostridiales OTUs
Unclassified	57%
Eubacterium	12%
Clostridium	10%
Ruminococcus	10%
Clostridiaceae	5%
Peptostreptococcaceae	3%
Faecalibacterium	0.50%
Other	2.50%

Figure 4.8. The antibiotic-treated mice are dominated by Clostridiales, yet all *H. pylori* infections have increased *Foxp3* and *Il10* transcripts. 4,400 OTUs were different between the antibiotic-treated *H. pylori*-infected mice and the *H. pylori*-infected untreated mice. Of those OTUs, 55% were significantly decreased **(*A*)** in the and 45% were significantly increased **(*B*)** antibiotic-treated mice compared to the untreated mice. Each pie chart (A and B) represents the diversity of taxa that changed in the antibiotic-treated mice compared to the non-treated mice. The majority of the taxa that were increased in the antibiotic treated mice were the *Clostridia.* **(*C*)** 94% of the *Clostridia* OTUs that were increased in the antibiotic treated mice were in the order *Clostridiales;* the chart details those *Clostridiales* at the genus level. Total gastric mRNA expression of *Foxp3* **(*D*)** and *Il10* **(*E*)** in non-treated uninfected mice (M), antibiotic-treated uninfected mice (M Ab), non-treated *H. pylori* infected mice (WT), antibiotic treated *H. pylori* infected mice (WT Ab), and gastric flora reconstituted mice (WT Ab RC). mRNA expression levels are normalized to the housekeeping gene, *Gapdh*, and expressed as fold increase over mock, using the ΔΔCt method. N = 5 for each group. For (D) and (E) data is displayed as average ± SEM. *P<0.05; Student T test.

the two groups. Of those OTUs 55% were significantly decreased (Fig. 4.8 *A*; Excel File S1.3) in the antibiotic-treated mice and 45% were significantly increased (Fig. 4.8 *B*; Excel File S1.4), as compared to normal mice. Members of the *Firmicutes* phylum of gram-positive bacteria stood out as having substantial changes between the antibiotic-treated versus normal mice. Some *Firmicutes* were decreased in the antibiotic-treated group, mainly members of the *Mollicutes* class (41% of all the decreased OTUs) (Fig. 4.8 *A*). Other *Firmicutes* were increased in the antibiotic-treated group, including members of the class *Clostridia* (46% of all the increased OTUs) (Fig. 4.8 *B*)—most of these fell within the order *Clostridiales*. Two genera within this order have been found to affect immune responses: *Faecalibacterium* spp. (32) and *Clostridium* spp. (6, 16) (Fig. 4.8 *C*). We focused on the *Clostridium* genus because a larger number of these species were increased in antibiotic-treated mice (Fig. 4.8 *C*), and additionally, one *Clostridium* OTU was the sixth most increased of all the 4,400 OTUs (Table 4.1). We analyzed the phylogeny of all the *Clostridium* spp. that increased in the antibiotic-treated mice, and found that they all group within to two clusters of species within this genus, clusters IV and XIVa (Fig. 4.9). The genus *Clostridium* is subdivided into 19 clusters, but members of clusters IV and XIVa have been found to specifically induce regulatory T cells (T regs) in the colon (6). These T

reg-inducing *Clostridium* spp. have been narrowed down to a group of 46 species (6). Furthermore, the *Clostridium* in clusters IV and XIVa mediate a dampened inflammatory response to a chemical inflammatory agent (6). Similarly, these species constitute a smaller portion of the fecal microbial community in patients with IBD than in normal patients (12). These studies thus correlate well with ours in finding that elevated *Clostridium* spp. in clusters IV and XIVa correlate with a dampened immune response.

To determine whether the antibiotic-treated mice had elevated T regs, we examined transcripts encoding the key T reg transcription factor *Foxp3* and the regulatory cytokine *Il10* in the mouse stomachs. We observed that both *Il10* and *Foxp3* were elevated in all *H. pylori*-infection groups as compared to mock-infected mice (Fig. 4.8 *D, E*). However, the antibiotic-treated mice have many fewer total $CD4^+$ T cells (Fig. 4.6 *C*) and thus a greater percentage of them may be T reg in character. Thus, an increased percentage of T regs may underlie the reduced pathology.

A precedent already exists for T regs to influence *H. pylori* pathogenesis; specifically, an influx of T regs associated with *H. bilis* infection reduces pathology in response to *H. pylori* (23) and neonatal mice infected with *H. pylori* develop a regulatory T cell response that is protective against *H. pylori* disease (30). However, the T reg cell response is not seen in adult mice infected with *H. pylori* (31–33). In addition, regulation of Th1 and Th17 responses by the

cytokine IL-10 has been shown to occur both through T regs (25) and through APCs (26, 27). Thus examining IL-10 production by specific subsets of immune cells may illuminate the mechanism by which $CD4^+$ cell infiltration is regulated by the endogenous microbiota in *H. pylori* infection.

Additionally, specific components of the intestinal microbiota have been shown to affect the propensity of hosts to develop a pro-inflammatory Th17 response (6, 29), which changes how mice respond to subsequent challenge by bacterial pathogens. In this study, we demonstrated that antibiotic-induced alterations in the microbiota reduce the number of $CD4^+$ T cells and *Ifnγ* transcript that develop in response to *H. pylori* infection. While it is not known if there are specific bacteria that promote Th1 responses, it is possible that the microbiota of the antibiotic-treated mice had less of a Th1-promoting bacteria, thus reducing the Th1 response to *H. pylori.*

One intriguing difference we observed between the microbiota of the untreated and antibiotic-treated mice was the increase in cluster IV and XIVa *Clostridium* spp.. Bacteria in these Clostridial groups have been shown to increase T regulatory cells in the intestine, by an as-yet-unknown mechanism (8). Our results suggest these same types of bacteria may operate in the stomach as well as the intestine.

We suggest that in adults, differing pre-infection gastric microbial populations affect the subsequent immune response to *H. pylori,* thus

contributing to the diverse outcomes of *H. pylori* infection. Our work also suggests that microbial composition could be used as a marker to predict the disease outcome of *H. pylori* infection, and that manipulating the stomach microbial populations may be an avenue to pursue to prevent disease in response to *H. pylori* infection.

Phylum	Class	Order	Family	Genera	Log Ratio
Firmicutes	Clostridia	Clostridiales	Unclassified	Unclassified	1.775
Firmicutes	Clostridia	Clostridiales	Unclassified	Unclassified	1.718
Firmicutes	Clostridia	Clostridiales	Unclassified	Unclassified	1.682
Firmicutes	Bacilli	Bacillales	Staphylococcaceae	Unclassified	1.663
Firmicutes	Bacilli	Bacillales	Staphylococcaceae	Unclassified	1.655
Firmicutes	**Clostridia**	**Clostridiales**	**Clostridiaceae**	**Clostridium**	**1.619**
Firmicutes	Clostridia	Clostridiales	Unclassified	Unclassified	1.61
Firmicutes	Clostridia	Clostridiales	Unclassified	Unclassified	1.592
Firmicutes	Clostridia	Clostridiales	Ruminococcaceae	Ruminococcus	1.588
Firmicutes	Clostridia	Clostridiales	Unclassified	Unclassified	1.572

Table 4.1. The top ten most enriched OTUs in the antibiotic treated mice within two clusters of species within this genus, clusters IV and XIVa (Fig. 4.9).

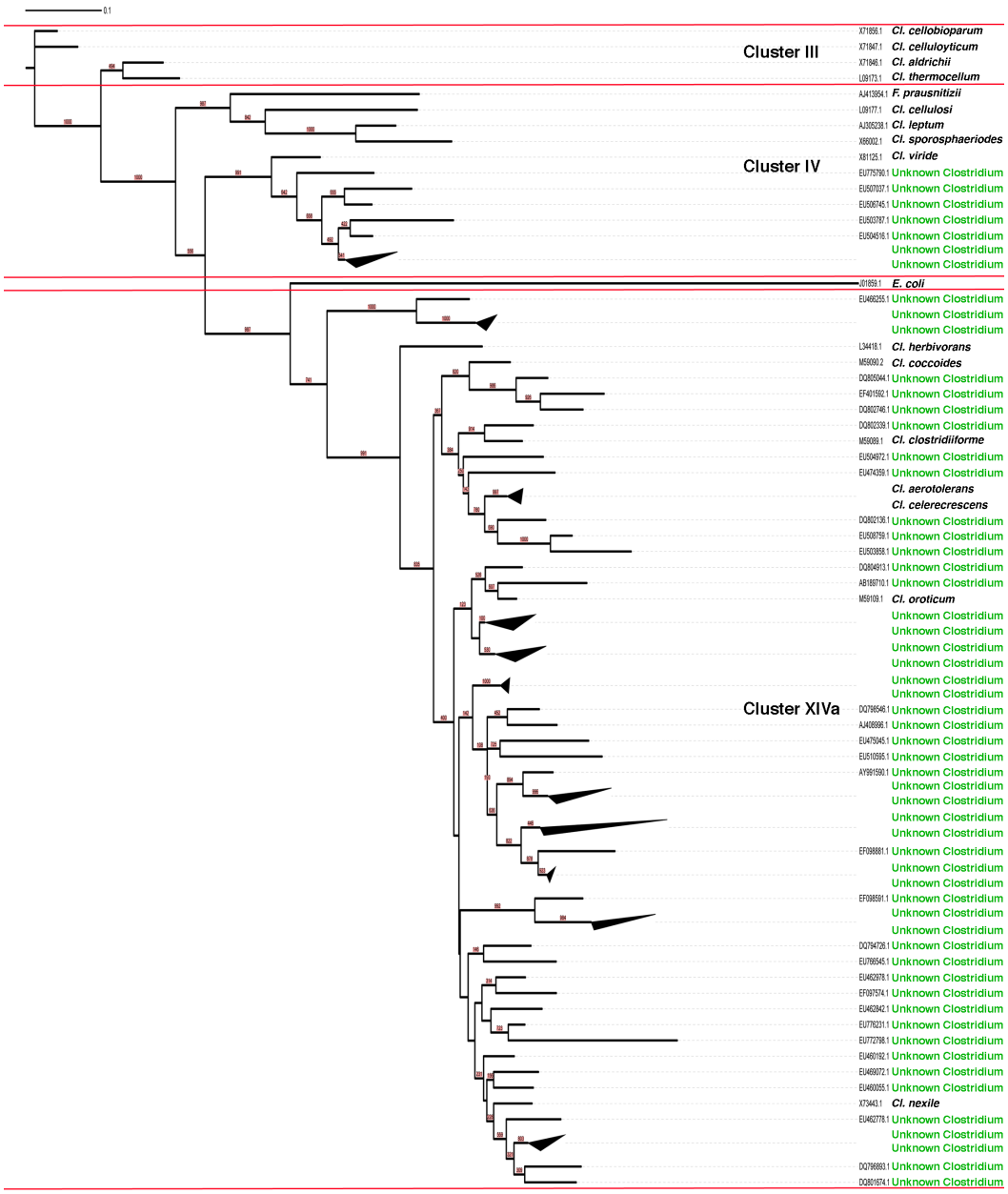

Figure 4.9. *Clostridium* increased in the antibiotic treated mice all map to Cluster IV and XIVa. The phylogenetic tree displays all the unknown *Clostridium* increased in the antibiotic treated mice (green labels) with some known *Clostridium* species (black labels) to anchor the tree. Collapsed branches had branch lengths < 0.05 and bootstrap values are displayed at branch junctions.

4.5. Acknowledgements

I thank and acknowledge two outstanding undergraduate students that assisted me with this project, Ethan Ahler and Cynthia Cech. I also acknowledge the expertise of our pathologist, Dr. Elliot Carter, and thank him for his contribution to figure 4.1. We acknowledge the technical support received from Bari Holm Nazario, UC Santa Cruz California Institute for Regenerative Medicine Shared Stem Cell Facility and Martin Polz (M.I.T.) for supplying the p360 and p361 plasmids for *Lactobacillus* quantification. We thank Fitnat Yildiz and Martha Zuniga for their comments on the manuscript. We are also grateful to the late David Schauer (M.I.T) for several informative and encouraging discussions about stomach microflora. The described project was supported by Grant Number AI050000 (to K.M.O.) from the National Institutes of Allergy and Infectious Disease (NIAID) at the National Institutes of Health and the University of California Cancer Research Coordinating Committee (to K.M.O.). Its contents are solely the responsibility of the authors and do not necessarily represent the official views of the NIH.

4.6. References

1. **Albright C. a, R. B. Sartor, and S. L. Tonkonogy**. 2009. Endogenous antigen presenting cell-derived IL-10 inhibits T lymphocyte responses to commensal enteric bacteria. Immunology Letters **123**:77-87.

2. **Alexander A. D., R. P. Orcutt, J. C. Henry, J. Baker, A. C. Bissahoyo, and D. W. Threadgill**. 2006. Quantitative PCR assays for mouse enteric flora reveal strain-dependent differences in composition that are influenced by the microenvironment. Mammalian Genome **17**:1093-104.

3. **Andersson A. F., M. Lindberg, H. Jakobsson, F. Bäckhed, P. Nyrén, and L. Engstrand**. 2008. Comparative analysis of human gut microbiota by barcoded pyrosequencing. PloS One **3**:e2836.

4. **Arnold I. C., N. Dehzad, S. Reuter, H. Martin, B. Becher, C. Taube, and A. Müller**. 2011. Helicobacter pylori infection prevents allergic asthma in mouse models through the induction of regulatory T cells. The Journal of Clinical Investigation **121**:3088-3093.

5. **Arnold I. C., J. Y. Lee, M. R. Amieva, A. Roers, R. a Flavell, T. Sparwasser, and A. Müller**. 2011. Tolerance rather than immunity protects from Helicobacter pylori-induced gastric preneoplasia. Gastroenterology. Elsevier Inc. **140**:199-209.

6. **Atarashi K., T. Tanoue, T. Shima, A. Imaoka, T. Kuwahara, Y. Momose, G. Cheng, S. Yamasaki, T. Saito, Y. Ohba, T. Taniguchi, K. Takeda, S. Hori, I. I.**

Ivanov, Y. Umesaki, K. Itoh, and K. Honda. 2010. Induction of Colonic Regulatory T Cells by Indigenous Clostridium Species. Science **331**:337-341.

7. **Atherton J. C.** 2006. The pathogenesis of Helicobacter pylori-induced gastro-duodenal diseases. Annual Review of Pathology **1**:63-96.

8. **Bamford K., X. Fan, S. Crowe, J. Leary, and W. Gourley**. 1998. Lymphocytes in the human gastric mucosa during Helicobacter pylori have a T helper cell 1 phenotype. Gastroenterology **114**:482-92.

9. **Bik E. M., P. B. Eckburg, S. R. Gill, K. E. Nelson, E. A. Purdom, F. Francois, G. Perez-Perez, M. J. Blaser, and D. A. Relman**. 2006. Molecular analysis of the bacterial microbiota in the human stomach. Proceedings of the National Academy of Sciences of the United States of America. National Acad Sciences **103**:732.

10. **DeSantis T. Z., E. L. Brodie, J. P. Moberg, I. X. Zubieta, Y. M. Piceno, and G. L. Andersen**. 2007. High-density universal 16S rRNA microarray analysis reveals broader diversity than typical clone library when sampling the environment. Microbial Ecology **53**:371-83.

11. **Eaton K. A., M. J. Radin, and S. Krakowka**. 1995. An Animal Model of Gastric Ulcer Due to Bacterial Gastritis in Mice. Veterinary Pathology **32**:489-497.

12. **Frank D. N., A. L. St Amand, R. a Feldman, E. C. Boedeker, N. Harpaz, and N. R. Pace**. 2007. Molecular-phylogenetic characterization of microbial

community imbalances in human inflammatory bowel diseases. Proceedings of the National Academy of Sciences **104**:13780-5.

13. **Garrett W. S., C. a Gallini, T. Yatsunenko, M. Michaud, A. DuBois, M. L. Delaney, S. Punit, M. Karlsson, L. Bry, J. N. Glickman, J. I. Gordon, A. B. Onderdonk, and L. H. Glimcher**. 2010. Enterobacteriaceae act in concert with the gut microbiota to induce spontaneous and maternally transmitted colitis. Cell Host & Microbe. Elsevier Inc. **8**:292-300.

14. **Hazen T. C., E. a Dubinsky, T. Z. DeSantis, G. L. Andersen, Y. M. Piceno, N. Singh, J. K. Jansson, A. Probst, S. E. Borglin, J. L. Fortney, W. T. Stringfellow, M. Bill, M. E. Conrad, L. M. Tom, K. L. Chavarria, T. R. Alusi, R. Lamendella, D. C. Joyner, C. Spier, J. Baelum, M. Auer, M. L. Zemla, R. Chakraborty, E. L. Sonnenthal, P. D'haeseleer, H.-Y. N. Holman, S. Osman, Z. Lu, J. D. Van Nostrand, Y. Deng, J. Zhou, and O. U. Mason**. 2010. Deep-sea oil plume enriches indigenous oil-degrading bacteria. Science **330**:204-8.

15. **Huber S., N. Gagliani, E. Esplugues, W. O'Connor, F. J. Huber, A. Chaudhry, M. Kamanaka, Y. Kobayashi, C. J. Booth, A. Y. Rudensky, M. G. Roncarolo, M. Battaglia, and R. a Flavell**. 2011. Th17 cells express interleukin-10 receptor and are controlled by Foxp3$^-$ and Foxp3+ regulatory CD4+ T cells in an interleukin-10-dependent manner. Immunity. Elsevier Inc. **34**:554-65.

16. **Ivanov I. I., K. Atarashi, N. Manel, E. L. Brodie, T. Shima, U. Karaoz, D. Wei, K. C. Goldfarb, C. A. Santee, S. V. Lynch, T. Tanoue, A. Imaoka, K. Itoh, K.**

Takeda, Y. Umesaki, and D. R. Littman. 2009. Induction of Intestinal Th17 Cells by Segmented Filamentous Bacteria. Cell. Elsevier Ltd **139**:485-498.

17. **Ivanov I. I., R. D. L. Frutos, N. Manel, K. Yoshinaga, D. B. Rifkin, R. B. Sartor, B. B. Finlay, and D. R. Littman**. 2008. Specific microbiota direct the differentiation of IL-17-producing T-helper cells in the mucosa of the small intestine. Cell Host & Microbe **4**:337-49.

18. **Lathrop S. K., S. M. Bloom, S. M. Rao, K. Nutsch, C.-W. Lio, N. Santacruz, D. a. Peterson, T. S. Stappenbeck, and C.-S. Hsieh**. 2011. Peripheral education of the immune system by colonic commensal microbiota. Nature. Nature Publishing Group 1-6.

19. **Lee A., J. O'Rourke, M. C. De Ungria, B. Robertson, G. Daskalopoulos, and M. F. Dixon**. 1997. A standardized mouse model of Helicobacter pylori infection: introducing the Sydney strain. Gastroenterology **112**:1386-97.

20. **Lemke L. B., Z. Ge, M. T. Whary, Y. Feng, A. B. Rogers, S. Muthupalani, and J. G. Fox**. 2009. Concurrent Helicobacter bilis infection in C57BL/6 mice attenuates pro-inflammatory H. pylori induced gastric pathology. Infection and Immunity **77**:2147-58.

21. **Liu B., S. L. Tonkonogy, and R. B. Sartor**. 2011. Antigen-Presenting Cell Production of IL-10 Inhibits T-Helper 1 and 17 Cell Responses and Suppresses Colitis in Mice. Gastroenterology. Elsevier Inc. **141**:653-662.

22. **Livak K. J., and T. D. Schmittgen**. 2001. Analysis of relative gene expression data using real-time quantitative PCR and the 2(-Delta Delta C(T)) Method. Methods **25**:402-8.

23. **Lofgren J. L., M. T. Whary, Z. Ge, S. Muthupalani, N. S. Taylor, M. Mobley, A. Potter, A. Varro, D. Eibach, S. Suerbaum, T. C. Wang, and J. G. Fox**. 2011. Lack of commensal flora in Helicobacter pylori-infected INS-GAS mice reduces gastritis and delays intraepithelial neoplasia. Gastroenterology **140**:210-20.

24. **Maldonado-Contreras A., K. C. Goldfarb, F. Godoy-Vitorino, U. Karaoz, M. Contreras, M. J. Blaser, E. L. Brodie, and M. G. Dominguez-Bello**. 2010. Structure of the human gastric bacterial community in relation to Helicobacter pylori status. The ISME journal 1-6.

25. **Mazmanian S. K., J. L. Round, and D. L. Kasper**. 2008. A microbial symbiosis factor prevents intestinal inflammatory disease. Nature **453**:620-5.

26. **Peek R. M., Jr, and M. J. Blaser**. 2002. Helicobacter pylori and gastrointestinal tract adenocarcinomas. Nat. Rev. Cancer **2**:28-37.

27. **Polk D. B., and R. M. Peek**. 2010. Helicobacter pylori: gastric cancer and beyond. Nature Reviews Cancer. Nature Publishing Group **10**:403-14.

28. **Rolig A. S., J. E. Carter, and K. M. Ottemann**. 2011. Bacterial chemotaxis modulates host cell apoptosis to establish a T-helper cell, type 17 (Th17)-dominant immune response in Helicobacter pylori infection. Proceedings of the National Academy of Sciences of the United States of America **108**:19749-19754.

29. **Sarma-Rupavtarm R. B., Z. Ge, D. B. Schauer, J. G. Fox, and M. F. Polz**. 2004. Spatial Distribution and Stability of the Eight Microbial Species of the Altered Schaedler Flora in the Mouse Gastrointestinal Tract. Applied and Environmental Microbiology **70**:2791-2800.

30. **Shi G., M. Ramaswamy, B. P. Vistica, C. A. Cox, C. Tan, E. F. Wawrousek, R. M. Siegel, and I. Gery**. 2009. Unlike Th1, Th17 cells mediate sustained autoimmune inflammation and are highly resistant to restimulation-induced cell death. Journal of Immunology **183**:7547-56.

31. **Shi Y., X.-F. Liu, Y. Zhuang, J.-Y. Zhang, T. Liu, Z. Yin, C. Wu, X.-hu Mao, K.-ran Jia, F.-jun Wang, H. Guo, R. A. Flavell, Z. Zhao, K.-Y. Liu, B. Xiao, Y. Guo, W.-J. Zhang, W.-Y. Zhou, G. Guo, and Q.-M. Zou**. 2010. Helicobacter pylori-Induced Th17 Responses Modulate Th1 Cell Responses, Benefit Bacterial Growth, and Contribute to Pathology in Mice. Journal of Immunology **184**:5121-5129.

32. **Sokol H., B. Pigneur, L. Watterlot, O. Lakhdari, L. G. Bermúdez-Humarán, J.-J. Gratadoux, S. Blugeon, C. Bridonneau, J.-P. Furet, G. Corthier, C. Grangette, N. Vasquez, P. Pochart, G. Trugnan, G. Thomas, H. M. Blottière, J. Doré, P. Marteau, P. Seksik, and P. Langella**. 2008. Faecalibacterium prausnitzii is an anti-inflammatory commensal bacterium identified by gut microbiota analysis of Crohn disease patients. Proceedings of the National Academy of Sciences **105**:16731-6.

33. **Tan M. P., M. Kaparakis, M. Galic, J. Pedersen, M. Pearse, O. L. C. Wijburg, P. H. Janssen, and R. A. Strugnell**. 2007. Chronic Helicobacter pylori infection does not significantly alter the microbiota of the murine stomach. Applied and Environmental Microbiology **73**:1010-3.

34. **Turnbaugh P. J., M. Hamady, T. Yatsunenko, B. L. Cantarel, A. Duncan, R. E. Ley, M. L. Sogin, W. J. Jones, B. a Roe, J. P. Affourtit, M. Egholm, B. Henrissat, A. C. Heath, R. Knight, and J. I. Gordon**. 2009. A core gut microbiome in obese and lean twins. Nature. Nature Publishing Group **457**:480-4.

35. **Weel J. F., R. W. van der Hulst, Y. Gerrits, P. Roorda, M. Feller, J. Dankert, G. N. Tytgat, and A. van der Ende**. 1996. The interrelationship between cytotoxin-associated gene A, vacuolating cytotoxin, and Helicobacter pylori-related diseases. The Journal of Infectious Diseases **173**:1171-5.

36. **Whary M. T., N. S. Taylor, Y. Feng, Z. Ge, S. Muthupalani, J. Versalovic, and J. G. Fox**. 2011. Lactobacillus reuteri promotes Helicobacter hepaticus-associated typhlocolitis in gnotobiotic B6.129P2-IL-10(tm1Cgn) (IL-10(-/-)) mice. Immunology 1-14.

37. **Wroblewski L. E., R. M. Peek, and K. T. Wilson**. 2010. Helicobacter pylori and gastric cancer: factors that modulate disease risk. Clinical Microbiology Reviews **23**:713-39.

CHAPTER 5

Conclusions and future directions

5.1. Summary

This thesis presents results on the roles *H. pylori* chemotaxis and the endogenous microbiota play in the inflammatory response to *H. pylori* infection. These results contribute information to a fundamental question in *H. pylori* pathogenesis: why do some patients develop severe disease while others remain asymptomatic?

The ability to chemotax influences *H. pylori* infection in multiple ways; it promotes stomach sub-region localization and it initiates contact with host epithelial cells. Specifically, chemotaxis drives *H. pylori* strain SS1 to the antrum where *H. pylori* colonizes more densely and causes increased inflammation compared to the corpus. Survival and growth in the antrum depends on the cytoplasmic chemoreceptor TlpD. We propose that TlpD is necessary for *H. pylori* to find a nutrient or avoid the heightened inflammatory response in the antrum. In addition to localizing *H. pylori* in specific regions of the stomach, chemotaxis also drives *H. pylori* closer to the epithelial cell layer (12), a position that we have shown directs virulence factor expression, increases host cell apoptosis, and promotes host-pathogen contact that encourages the development of proinflammatory Th17 cell responses.

A host's development of specific immune responses, such as Th17 (6, 7) or T reg (3) have been shown to be influenced by specific components of the gut microbiota. The propensity to develop Th17 or T reg responses changes how mice respond to challenge by bacterial pathogens (6, 7) or chemically induced inflammation (3). Similarly, we have shown that antibiotic-induced alterations in the microbiota reduce the number of $CD4^+$ T cells and *Ifnγ* transcript in the stomachs of *H. pylori* infected mice. Alterations made in the microbiota included an increase in cluster IV and XIVa *Clostridium* spp., bacteria previously shown to increase T regulatory cells (3). These results suggest that the pre-infection microbiota influence the inflammatory response, and by extension, the disease outcome of *H. pylori* infection.

Results discussed in this thesis have advanced the field of *H. pylori* pathogenesis, however they have also led to more questions regarding the signals detected by chemoreceptors that promote survival in an inflammatory environment and drive virulence factor expression, and which species in the normal gut bacteria encourage low inflammation in response to *H. pylori* infection.

5.2. Future directions

5.2.1. Does TlpD promote growth or survival in the antrum?

We demonstrated that the chemoreceptor TlpD is necessary for antral colonization after three days of infection. One of the big questions remaining in regards to *H. pylori* antral colonization is whether TlpD directed chemotaxis is necessary for growth or survival. Similar questions have been addressed in the past with the use of a temperature sensitive plasmid that does not replicate at 37°C (9). This plasmid can be introduced into *H. pylori* to distinguish between slow growth or increased in wild-type versus Che$^-$ *H. pylori.* The presence of the plasmid within the bacterial population can be compared between bacteria grown at the non-permissive temperature *in vivo* and at the permissive temperature *in vitro.* In this experiment, different stomach regions could be plated separately to compare growth rates in the corpus and the antrum. We would expect nearly 100% of bacteria grown *in vitro* to contain the plasmid, while wild-type *H. pylori* grown *in vivo* would lose 50% of plasmid containing bacteria every division. A higher percentage of plasmid-containing bacteria but fewer colonies would demonstrate slow growth of Che$^-$, while fewer colonies with a similar percentage of plasmid-containing bacteria to wild-type *H. pylori* would indicate more bacteria were dying, perhaps as a result of increased sensitivity or increased exposure to an immune component.

To confirm the contribution of the inflammatory component in the observed reduced growth or survival of Che$^-$, transgenic mice with reduced or no inflammatory response to *H .pylori,* such as IFN$\gamma^{-/-}$ (1, 5) or IL-12$^{-/-}$ (1) mice

could be used. Colonization levels of wild-type, Che$^-$ and ΔTlpD *H. pylori* in the corpus and the antrum could be compared in these low inflammation models. We would predict that Che$^-$ and ΔTlpD *H. pylori* would no longer have a growth or survival defect in the low inflammatory environment.

5.2.2. Chemotaxis driven interactions that promote specific immune responses

Wild-type *H. pylori* localizes closer to the epithelial cell layer than the Che$^-$ mutants (12); we showed that wild-type *H. pylori* also induces more host cell apoptosis and brings in more Th17 cells to the stomach than Che$^-$ *H. pylori*. Based on this information we suggested that APC interact with apoptosing host cells in combination with *H. pylori* bacterial products and thus direct the differentiation of Th17 cells, as has been seen in a *Citrobacter rodentium* infection (4, 11). However, we did not specifically demonstrate the connection between increased apoptosis and Th17 cells. To solidify this association we could chemically induce apoptosis during a Che$^-$ infection and examine the cytokine secretion from $CD3^+CD4^+$ T helper cells. We predict that this treatment would shift the immune response toward Th17. However, the distance of the Che$^-$ bacteria from the epithelial cells may complicate this experiment by reducing APC contact with bacterial products, which could result in the immune response shifting toward more regulatory, IL-10 secreting cells.

Another experiment that could help connect increased apoptosis with Th17 cells would be the examination of the immune response to non-apoptosis-inducing *H. pylori* mutants. Because *H. pylori* has many apoptosis-inducing genes and some are necessary for mouse colonization, making infectious non-apoptosis-inducing *H. pylori* mutants is impossible. However, we observed increased transcription of *vacA* in the wild type compared to Che$^-$, therefore, a *vacA* mutant might be a good place to start. We would observe the induction of apoptosis by the *vacA* mutant, and subsequently examine the cytokine secretion from the $CD3^+CD4^+$ T cells infiltrating into the gastric mucosa. In this case we would predict that reduced apoptosis in a *vacA* mutant infection would lead to a Th1 dominant immune response.

We have also shown that the Che$^-$ mutant somewhat differentially transcribes *vacA* and *ureA*, and we hypothesize that the Che$^-$ mutants are in an environment that does not trigger the correct expression of these and other virulence factors, resulting in reduced host cell apoptosis. To test this hypothesis we need to analyze the transcription of other virulence genes *in vivo* Che$^-$ infections, such as *cagA* in a *cag*-PAI positive strain. Additionally, we need to address, perhaps *in vitro,* if increased delivery distance of apoptosis inducing virulence factors decreases the number of apoptosing cells.

5.2.3. Which endogenous microbiota affect the immune response to *H. pylori?*

We demonstrated that altering the gut microbiota reduces the numbers of $CD4^+$ T cells and *Ifnγ* transcripts in the stomach in response to *H. pylori.* These results can potentially have great impact on the treatment of *H. pylori* infection and disease. Some questions remaining to be answered include: does changing the intestinal microflora affect gastric immune responses, which species of the microbiota reduce the immune response, can treating an *H. pylori* infection with microbiota change the course of the immune response, can the constituents of the gut microbiota serve as a predictive tool for the disease severity of *H. pylori* infection?

Because we treated our mice with broad-spectrum antibiotics the microbiota was altered in both the stomach and in the intestines, thus it would be interesting to monitor the immune cells in the intestine prior to and after an *H. pylori* inoculation to ensure that alterations specifically in the stomach microbiota impact the immune cells infiltrating into the stomach. Additionally, we hypothesize a role for the cluster IV and XIVa *Clostridium* spp., which were increased in the antibiotic treated mice. To confirm the role of the regulatory T cell inducing *Clostridium* spp., gnotobiotic mice colonized solely with the 46 *Clostridium* spp. that induce regulatory T cells (3) could be infected with *H. pylori* and monitored for their immune responses. Other experiments that could help confirm the role of cluster IV and XIVa *Clostridium* spp. include examining the $CD4^+CD25^+Foxp3^+$ regulatory T cell populations and checking their function by

production of the regulatory cytokine IL-10 and their origin by examining the presence of the transcription factor Helios, which is reported to be expressed in thymus-derived natural T regs (10). We would expect T regs induced by microbiota to be IL-10 positive and Helios negative.

Thus far, our experiments show that pre-existing microflora influences the immune response to *H. pylori*, however in order to address the treatment of *H. pylori* we would need to prove that introducing altered microbiota after *H. pylori* inoculation changed the course of the inflammatory response. To do so we could orally-gavage stomach homogenates of antibiotic-treated mice, or suspensions of cluster IV and XIVa *Clostrida* spp. into *H. pylori* infected mice and monitor immune responses before and after the introduction of new bacteria.

5.3. Conclusions

H. pylori infects 50% of the worlds population. It is the primary risk factor for gastric cancer, which is the second leading cause of cancer related death in males and the fourth in females. The five-year survival rate for gastric cancer is about 25%, thus understanding the host-pathogen interactions that lead to gastric cancer contributes knowledge that improves *H. pylori* treatment and addresses a global health concern.

As mentioned, one mystery surrounding *H. pylori* pathogenesis is that infection can result in a range of diseases from asymptomatic gastritis to gastric

cancer. *H. pylori* infection can also have some beneficial outcomes, such as reduced esophageal cancer (8) and early infection is protective against asthma (2). These complicated interactions between the bacteria and its host suggest that eradicating *H. pylori* with antibiotics might not always be the best treatment. Therefore, identifying and treating only those patients who are prone to develop severe disease or treating *H. pylori* infection in order to reduce inflammation and retain colonization may allow us to preserve the beneficial aspects of *H. pylori* infection while reducing the occurrence of diseases caused by *H. pylori*.

The work described in this thesis provides evidence that targeting the chemotaxis pathway would reduce inflammation by reducing virulence factor expression and thus, the Th17 proinflammatory immune response, but allow *H. pylori* to continue to colonize. We do not yet know if Che$^-$ *H. pylori* would provide the same protective benefits as early infection with wild-type *H. pylori.* Work described herein also suggests that knowledge of pre-infection gastric microbiota constituents may be a new way to identify which patients will develop disease and require antibiotic treatment to eradicate *H. pylori.* Further characterization of the affects of specific microbiota on the immune response against *H. pylori* might expose new treatment and disease prediction tools to help treat and prevent *H. pylori* disease.

5.4. References

1. **Akhiani A. a, J. Pappo, Z. Kabok, K. Schön, W. Gao, L. E. Franzén, and N. Lycke**. 2002. Protection against Helicobacter pylori infection following immunization is IL-12-dependent and mediated by Th1 cells. Journal of Immunology **169**:6977-84.

2. **Arnold I. C., N. Dehzad, S. Reuter, H. Martin, B. Becher, C. Taube, and A. Müller**. 2011. Helicobacter pylori infection prevents allergic asthma in mouse models through the induction of regulatory T cells. The Journal of Clinical Investigation **121**:3088-3093.

3. **Atarashi K., T. Tanoue, T. Shima, A. Imaoka, T. Kuwahara, Y. Momose, G. Cheng, S. Yamasaki, T. Saito, Y. Ohba, T. Taniguchi, K. Takeda, S. Hori, I. I. Ivanov, Y. Umesaki, K. Itoh, and K. Honda**. 2010. Induction of Colonic Regulatory T Cells by Indigenous Clostridium Species. Science **331**:337-341.

4. **Brereton C. F., and J. M. Blander**. 2011. The unexpected link between infection-induced apoptosis and a Th17 immune response. J Leukoc Biol **89**:565-576.

5. **Eaton K. A., M. Mefford, and T. Thevenot**. 2001. The role of T cell subsets and cytokines in the pathogenesis of Helicobacter pylori gastritis in mice. The Journal of Immunology. Am Assoc Immnol **166**:7456.

6. **Ivanov I. I., K. Atarashi, N. Manel, E. L. Brodie, T. Shima, U. Karaoz, D. Wei, K. C. Goldfarb, C. A. Santee, S. V. Lynch, T. Tanoue, A. Imaoka, K. Itoh, K.**

Takeda, Y. Umesaki, and D. R. Littman. 2009. Induction of Intestinal Th17 Cells by Segmented Filamentous Bacteria. Cell. Elsevier Ltd **139**:485-498.

7. **Ivanov I. I., R. D. L. Frutos, N. Manel, K. Yoshinaga, D. B. Rifkin, R. B. Sartor, B. B. Finlay, and D. R. Littman**. 2008. Specific microbiota direct the differentiation of IL-17-producing T-helper cells in the mucosa of the small intestine. Cell Host & Microbe **4**:337-49.

8. **Peek R. M., Jr, and M. J. Blaser**. 2002. Helicobacter pylori and gastrointestinal tract adenocarcinomas. Nat. Rev. Cancer **2**:28-37.

9. **Stecher B., M. Barthel, M. C. Schlumberger, L. Haberli, W. Rabsch, M. Kremer, and W.-D. Hardt**. 2008. Motility allows S. Typhimurium to benefit from the mucosal defence. Cellular Microbiology **10**:1166-80.

10. **Thornton A. M., P. E. Korty, D. Q. Tran, E. a Wohlfert, P. E. Murray, Y. Belkaid, and E. M. Shevach**. 2010. Expression of Helios, an Ikaros transcription factor family member, differentiates thymic-derived from peripherally induced Foxp3+ T regulatory cells. Journal of Immunology **184**:3433-41.

11. **Torchinsky M. B., J. Garaude, A. P. Martin, and J. M. Blander**. 2009. Innate immune recognition of infected apoptotic cells directs T(H)17 cell differentiation. Nature. Nature Publishing Group **458**:78-82.

12. **Williams S. M., Y.-ting Chen, T. M. Andermann, J. E. Carter, D. J. Mcgee, and K. M. Ottemann**. 2007. Helicobacter pylori Chemotaxis Modulates

Inflammation and Bacterium-Gastric Epithelium Interactions in Infected Mice. Infection and Immunity **75**:3747-3757.

APPENDIX 1

Primer Name	Sequence 5'-> 3'	Amplicon size (bp)	Anneal. Temp. (C)	Source
IL-4 F	ACAGGAGAAGGGACGCCAT	95 bp	62	(2)
IL-4 R	GAAGCCCTACAGACGAGCTCA			
IL-6 F	GAGGATACCACTCCCAACAGACC	141 bp	63	(2)
IL-6 R	AAGTGCATCATCGTTGTTCATACA			
TGFb1 F	TGACGTCACTGGAGTTGTACGG	170 bp	63	(2)
TGFb1 R	GGTTCATGTCATGGATGGTGC			
GAPDH F	CGTCCCGTAGACAAAATG	110 bp	62	Kathryn A. Eaton, Department of Microbiology and Immunology, University of Michigan.
GAPDH R	TGGCAACAATCTCCACCT			
IL-17a F	CTCCAGAAGGCCCTCAGACTAC	101 bp	61	Kathryn A. Eaton, Department of Microbiology and Immunology, University of Michigan.
IL-17a R	GAGCTTCCCAGATCACAGAGG			
FoxP3 F	TTCGAGGAGCCAGAAGAGTTTC	70 bp	62	(5)
FoxP3 R	GGGCCTTGCCTTTCTCATC			
IFNg F	CAGCAACAGCAAGGCGAAA	73 bp	63	(5)
IFNg R	CTGGACCTGTGGGTTGTTGAC			
IL-2 F	CCTGAGCAGGATGCAGAATTACA	141 bp	62	(2)
IL-2 R	TCCAGAACATGCCGCAGAG			
CCL2 F2	CTTCTGGGCCTGCTGTTCA	126 bp	64	(2)
CCL2 R2	CCAGCCTACTCATTGGGATCA			
IL-10 F	GGTTGCCAAGCCTTATCGGA	191 bp	60	(2)
IL-10 R	ACCTGCTCCACTGCCTTGCT			
CCL12F	GGAGGATCACAAGCAGCCAGT	79 bp	64	(1)
CCL12R	TCAGCACAGATCTCCTTATCCAGTAT			
GAPDH64 F	CGTCCCGTAGACAAAATGGTG	132 bp	64	This study
GAPDH64 R	GTGGAGGTCAATGAAGGGGTCG			
Rorc F	GGAGGACAGGGAGCCAAGTT	95 bp	60	(3)
Rorc R	CCGTAGTGGATCCCAGATGACT			
Fas F	TGGGCTGTCCTGCCTCTG	102 bp	64	This study
Fas R	ACGAACCCGCCTCCTCAGCT			
FasL F	AGCCGAGGAGTGTGGCCCAT	186 bp	64	This study
FasL R	TGTTCGAAGACTGACCCCGGA			
VacA F1	CGCTATCAATCAGCATGATTTTG	147 bp	60	(4)
VacA R1	CCCGCATCATGGCTATCAAT			
UreA F1	TATGGAAGAAGCGAGAGCTGGTA	62 bp	60	(4)
UreA R1	GAGTGCGCCCTTCTTGCAT			

Table A1.1. Primers used for qRT-PCR in Chapter 3

References

1. **Algood H. M. S., J. Gallo-Romero, K. T. Wilson, R. M. Peek, and T. L. Cover**. 2007. Host response to Helicobacter pylori infection before initiation of the adaptive immune response. FEMS Immunology and Medical Microbiology **51**:577-86.

2. **Giulietti a, L. Overbergh, D. Valckx, B. Decallonne, R. Bouillon, and C. Mathieu**. 2001. An overview of real-time quantitative PCR: applications to quantify cytokine gene expression. Methods **25**:386-401.

3. **Ivanov I. I., K. Atarashi, N. Manel, E. L. Brodie, T. Shima, U. Karaoz, D. Wei, K. C. Goldfarb, C. A. Santee, S. V. Lynch, T. Tanoue, A. Imaoka, K. Itoh, K. Takeda, Y. Umesaki, and D. R. Littman**. 2009. Induction of Intestinal Th17 Cells by Segmented Filamentous Bacteria. Cell. Elsevier Ltd **139**:485-498.

4. **Janzon A., T. Bhuiyan, A. Lundgren, F. Qadri, A.-M. Svennerholm, and A. Sjöling**. 2009. Presence of high numbers of transcriptionally active Helicobacter pylori in vomitus from Bangladeshi patients suffering from acute gastroenteritis. Helicobacter **14**:237-47.

5. **Quiding-Järbrink M., B. Lundin, H. Lonroth, and A. Svennerholm**. 2001. CD4 + and CD8 + T cell responses in Helicobacter pylori-infected individuals. Clinical and Experimental Immunology **123**:81-87.

APPENDIX 2

List of supplementary files

Excel File S1.1. ..... 2056 OTUs present in all 5 uninfected mice

Excel File S1.2. ..... 47 OTUs found to be different by abundance comparing 5 uninfected samples to 4 infected samples

Excel File S1.3. ..... 2424 OTUs found to be decreased in antibiotic treated mice by abundance comparison with 10 non-antibiotic pretreated samples

Excel File S1.4. ..... 1984 OTUs found to be increased in antibiotic treated mice by abundance comparison with 10 non-antibiotic pretreatment samples